TECHNICAL REPORT RL-80-10

A METHODOLOGY FOR MODELING CONFINED, TEMPERATURE SENSITIVE CUSHIONING SYSTEMS

Virginia P. Kobler
US Army Missile Command

June 1980

U.S. ARMY MISSILE COMMAND
Redstone Arsenal, Alabama 35809

Approved for public release;
distribution unlimited.

DISPOSITION INSTRUCTIONS

DESTROY THIS REPORT WHEN IT IS NO LONGER NEEDED. DO NOT RETURN IT TO THE ORIGINATOR.

DISCLAIMER

THE FINDINGS IN THIS REPORT ARE NOT TO BE CONSTRUED AS AN OFFICIAL DEPARTMENT OF THE ARMY POSITION UNLESS SO DESIGNATED BY OTHER AUTHORIZED DOCUMENTS.

TRADE NAMES

USE OF TRADE NAMES OR MANUFACTURERS IN THIS REPORT DOES NOT CONSTITUTE AN OFFICIAL INDORSEMENT OR APPROVAL OF THE USE OF SUCH COMMERCIAL HARDWARE OR SOFTWARE.

DISCLAIMER NOTICE

THIS DOCUMENT IS BEST QUALITY PRACTICABLE. THE COPY FURNISHED TO DTIC CONTAINED A SIGNIFICANT NUMBER OF PAGES WHICH DO NOT REPRODUCE LEGIBLY.

UNCLASSIFIED

SECURITY CLASSIFICATION OF THIS PAGE *(When Data Entered)*

REPORT DOCUMENTATION PAGE		READ INSTRUCTIONS BEFORE COMPLETING FORM
1. REPORT NUMBER Technical Report RL-80-10 ✓	2. GOVT ACCESSION NO. AD-A087351	3. RECIPIENT'S CATALOG NUMBER
4. TITLE *(and Subtitle)* A METHODOLOGY FOR MODELING CONFINED, TEMPERATURE SENSITIVE CUSHIONING SYSTEMS		5. TYPE OF REPORT & PERIOD COVERED Technical Report 6. PERFORMING ORG. REPORT NUMBER
7. AUTHOR(s) Virginia P. Kobler		8. CONTRACT OR GRANT NUMBER(s)
9. PERFORMING ORGANIZATION NAME AND ADDRESS Commander, US Army Missile Command ✓ Attn: DRSMI-RL Redstone Arsenal, AL 35809		10. PROGRAM ELEMENT, PROJECT, TASK AREA & WORK UNIT NUMBERS
11. CONTROLLING OFFICE NAME AND ADDRESS Commander, US Army Missile Command Attn: DRSMI-RPT Redstone Arsenal, AL 35809		12. REPORT DATE June 1980 13. NUMBER OF PAGES 152
14. MONITORING AGENCY NAME & ADDRESS*(if different from Controlling Office)*		15. SECURITY CLASS. *(of this report)* UNCLASSIFIED 15a. DECLASSIFICATION/DOWNGRADING SCHEDULE

16. DISTRIBUTION STATEMENT *(of this Report)*

Approved for public release; distribution unlimited.

17. DISTRIBUTION STATEMENT *(of the abstract entered in Block 20, if different from Report)*

18. SUPPLEMENTARY NOTES

19. KEY WORDS *(Continue on reverse side if necessary and identify by block number)*

Containers
Bulk cushioning
Mathematical modeling

20. ABSTRACT *(Continue on reverse side if necessary and identify by block number)*

A methodology for modeling the impact response of a confined cushioning system has been demonstrated. Data for modeling were acquired from test drops made with a test specimen comprised of a plywood cube (protected item) within a cleated plywood shipping container, under controlled environmental conditions, utilizing 2-inch Minicel as the cushioning system. Individual curves were developed for each temperature and drop height for both the

(Continued)

DD FORM 1 JAN 73 1473 EDITION OF 1 NOV 65 IS OBSOLETE

UNCLASSIFIED

SECURITY CLASSIFICATION OF THIS PAGE *(When Data Entered)*

20. ABSTRACT (Continued)

interior box and total container system. Utilizing a stepwise regression procedure, a general model was developed for the interior box and also for the total container system. The general model permits the cushion designer to predict the impact response of a container system within drop heights of 12 to 30 inches, a temperature range of -65°F to 160°F, and a static stress range of 0.088 to 1.255 psi.

ACKNOWLEDGEMENTS

There are a number of people whose contributions to this effort I would like to acknowledge:

Dr. R. M. Wyskida, University of Alabama-Huntsville, for his ideas, stimulating discussions, and encouragement. His assistance encompassed the entire effort, from problem formulation to final edit.

Drs. Robert Shannon, C. Dennis Pegden, Norman Bucher, and Merle Roach, University of Alabama-Huntsville, for their support and encouragement.

Dr. Don McDaniel, Martin-Marietta Corporation, Orlando, Florida, for his suggestions and guidance in the initial stages of this research effort.

Dr. James D. Johannes, University of Alabama-Huntsville, who rendered support with his computer science expertise and penetrating evaluations.

TABLE OF CONTENTS

LIST OF TABLES

LIST OF FIGURES

CHAPTER I. INTRODUCTION

The scientific and technological developments in all fields tend toward equipment of ever-increasing complexity. This complexity brings with it the inescapable concomitant — delicacy. In addition, the multinational posture of many of the leading corporations demand that this delicate equipment be transported to virtually every corner of the globe. Consequently, extremely sophisticated container systems are required to protect this delicate equipment during its journey throughout the world.

Many items come adequately packaged by nature. Consider the grapefruit with its outside protective shield which protects it from damage on the tree and in transit to the consumer's table. Unfortunately, many of man's physical creations do not possess a protective shield, since to provide one would be economically infeasible. If a protective shield capable of preventing any damage to a missile system were incorporated into the basic structure of the missile, the missile would be incapable of flight due to the weight burden. Consequently, missile systems are designed with only an in-flight protective shield incorporated. The container designer is then assigned the task of designing a protective shield, for the various segments of the missile system, to be utilized for ground handling protection. The fundamental product of the design effort is identified as a container system. The container system is the

dev : utilized to protect the item during transit to its destination point, hopefuliy without damage and at a minimum cost.

In an attempt to satisfy the demand for unique container systems, the container designer is confronted with a three faceted problem. He is expected to protect items of greater and greater fragility against greater and greater environmental shock hazards, at lower and lower values of weight, volume, and cost. In response, the container designer has turned to a variety of bulk cushioning materials, primarily because of the rapidly mounting costs for the design of special shock-isolation systems. However, to provide protection against the anticipated hazards encountered in transit, the container designer requires information on the physical properties of cushioning materials, and the methods of configurations available for the most economical use of the cushioning materials.

The Container Cushioning Concept

Cushioning systems are incorporated into container systems to protect fragile items. The degree of fragility of the item determines the amount of cushioning required to protect it from damage during handling and shipment. Some items are inherently strong and rugged except for one or more exceedingly fragile components. When the fragile components cannot be removed for separate cushioning, the entire item must be treated as fragile, even though the result may be an unavoidably large, cumbersome container.

A basic container cushioning problem is shown in Figure 1 which utilizes a foamed material as the cushioning system. The item which is to be

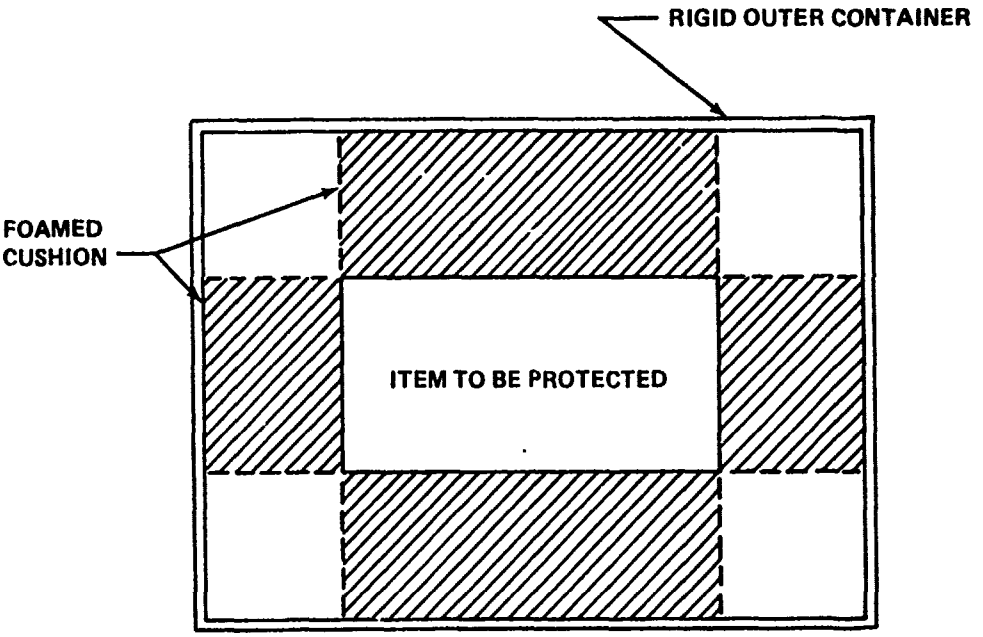

Figure 1. Container cushioning system.

protected from damage is located in the center. A rigid, wooden outside container encases the protected item and the foamed cushion. The thickness of the cushioning material is apparent. In this simplified sketch, when the container is accidentally dropped, it falls freely until a rigid surface of some type is encountered. Assuming a nonresilient rigid surface which the container strikes in a flat fashion, it is noted that the container, being rigid, impacts with considerable force. However, if the proper foamed cushion has been provided, the item to be protected does not stop as quickly as the outside container (from a time point of view) since the protected item compresses into the foamed cushioning material. If the cushion is thick enough and of proper density for the ensuing impact, the protected item will not be damaged.

The challenge then is to determine the proper size and density of a foamed cushioning material to utilize as a shock mitigation system.

The container system includes the container and the cushioning system, regardless of the cushioning material utilized. The cushioning system relates to the cushioning material itself, together with the cushioning configuration utilized. In Figure 1 the cushioning configuration shown utilizes side pads. Since various outer containers can be devised to encase almost any size of item, the crucial determination reduces to cushion thickness and cushion configuration.

Research Objective

The objective of this research effort is to develop the methodology for confined, temperature sensitive, cushioning system modeling. These models should be capable of predicting the dynamic cushioning performance of the Minicel cushioning material in the confined state. A secondary objective is to assess the relationship between unconfined drop test results on the Minicel material.

In response to this research objective, a systematic study of background material was conducted. The evolution of cushion design is discussed in Chapter II. The experimental design necessary for drop test data acquisition is given in Chapter III. The parameters of the overall impact response model are identified, together with the viscoelastic theory upon which the model is predicated, in Chapter IV.

The development of the interior box model, together with the total box model, is presented in Chapter V. This includes the individual dynamic cushioning equations for the interior box, the general model for the interior box, the individual total box equations, and the general model for the total box. Chapter VI contains the results of the validation of the two general models. Chapter VII combines the two models for an analysis of the temperature effects upon the cushioning material. Chapter VIII contains the conclusions and recommendations resulting from the research effort.

It is anticipated that the development of the overall container impact response mathematical model will result in a more realistic predictor of cushioning response within the container and, in turn, will prove to be more cost effective to cushioning designers.

CHAPTER II. THE EVOLUTION OF CUSHION DESIGN

Prior to the 1940's, proper cushioning was determined via the "cut and try" method. One used his judgment in selecting the optimum cushioning material, the cushion configuration, and the material thickness. If it provided the required protection it was deemed adequate.

Early scientific investigation took the classic stress-strain approach. By slowly applying a load to a specimen and measuring the resulting deflection, data were collected for the plotting of strain curves for various cushioning materials. These curves provided information pertaining to the amount of energy stored by the specimen and the point at which resilient properties were lost by the specimen.

Prompted by the increased sophistication of equipment and the advances in cushioning material fabrication, serious scientific research into cushioning design was begun. R. D. Mindlin of Columbia University is credited with having made the first scientific effort in this field in 1945.

Mindlin [1] first derived equations of motion by treating the cushion as a linear spring. Then, assuming a linear load-displacement, he used the equations of motion to find the maximum displacement of the packaged item within the container to insure the item does not attain a critical acceleration.

Since in practice a container system rarely has linear spring characteristics, Mindlin developed equations to describe the maximum displacement for non-linear springs.

In determining the optimum cushion thickness, Mindlin used the maximum allowable acceleration, the predicted drop height, and the weight of the item to find the necessary displacement of the cushion. The displacement distance can be compared with the load-displacement data for the various cushioning materials from which a selection can be made.

In this approach, load-displacement data were acquired by applying successively increasing loads, with weights or in a load testing machine, and measuring the corresponding displacements. This type of testing is categorized as static because of the low loading rate.

Mindlin's development of the mathematical equations describing the maximum acceleration and displacement of the protected item is considered classical and his approach to cushion design was not significantly changed for over a decade.

Although information on the static properties of cushioning materials is helpful, it does not permit the cushioning designer to predict the expected limit of protection for an item under severe handling conditions. Protective cushioning must be capable of responding to a sharp force of short duration if adequate item protection is to be provided.

Figure 2, taken from Mindlin's paper, depicts an idealized mechanical system representing an item during a drop test. The outer container is

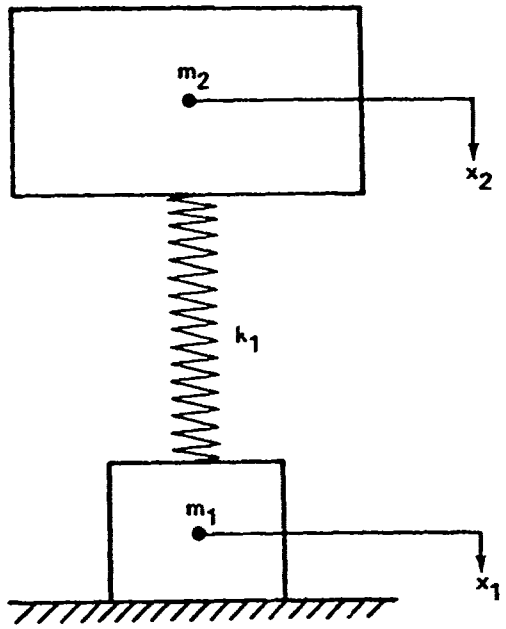

Figure 2. Idealized mechanical system representing item during a drop test [1].

represented by m_1, and m_2 is the protected item. The cushion between the item and the outer container is represented by a spring, k_1.

In addition to Mindlin, extensive research effort was conducted by K. Q. Kellicutt, R. E. Jones, and D. L. Hunzicker at the Forest Products Laboratory of the U. Department of Agriculture. Another active researcher was A. M. Underhill of the General Electric Company. Most of these efforts were directed toward collection of load-displacement data on the various materials available at that time for application to the cushion design methods of Mindlin [1] and Masel [2].

Gretz [3] extended the force-displacement approach to derive an efficiency factor for the cushioning material. The efficiency factor was

then used in the following equation to arrive at the necessary cushion thickness:

$$\text{Cushion Thickness} = \frac{(\text{Drop Height})\ (\text{Cushion Deflection})\ (\text{Efficiency})}{(\text{Maximum G's})}$$

Janssen [4] utilized the applied load to the cushion and the energy absorbing capacity of the cushion (defined as the area under the load-displacement curve) to form a dimensionless ratio which he called the cushion factor or "J" factor. The cushion factor was the ratio of optimum stress to optimum strain and was used to calculate the cushion thickness.

These cushion design methods were adequate for most of the cushioning materials available during the 1940's and early 1950's. However, with the development and proliferation of a myriad of foam materials in the late 1950's, it became apparent to cushion designers that the load-displacement curves produced through static testing did not reflect the true nature of viscoelastic materials.

Consequently, it was necessary to perform dynamic tests to investigate foamed material performance. A dynamic test is performed by having a plate, whose weight may be varied to achieve different static stresses, drop onto the cushioning material. The plate is instrumented to sense the peak acceleration it attains. Figure 3 shows the apparatus used in this type of test. This type of testing is referred to as flat pad or unconfined dynamic testing.

Kerstner [5] pointed out the inconsistencies found in the dynamic testing of only one thickness of cushion and then utilizing that data to predict the

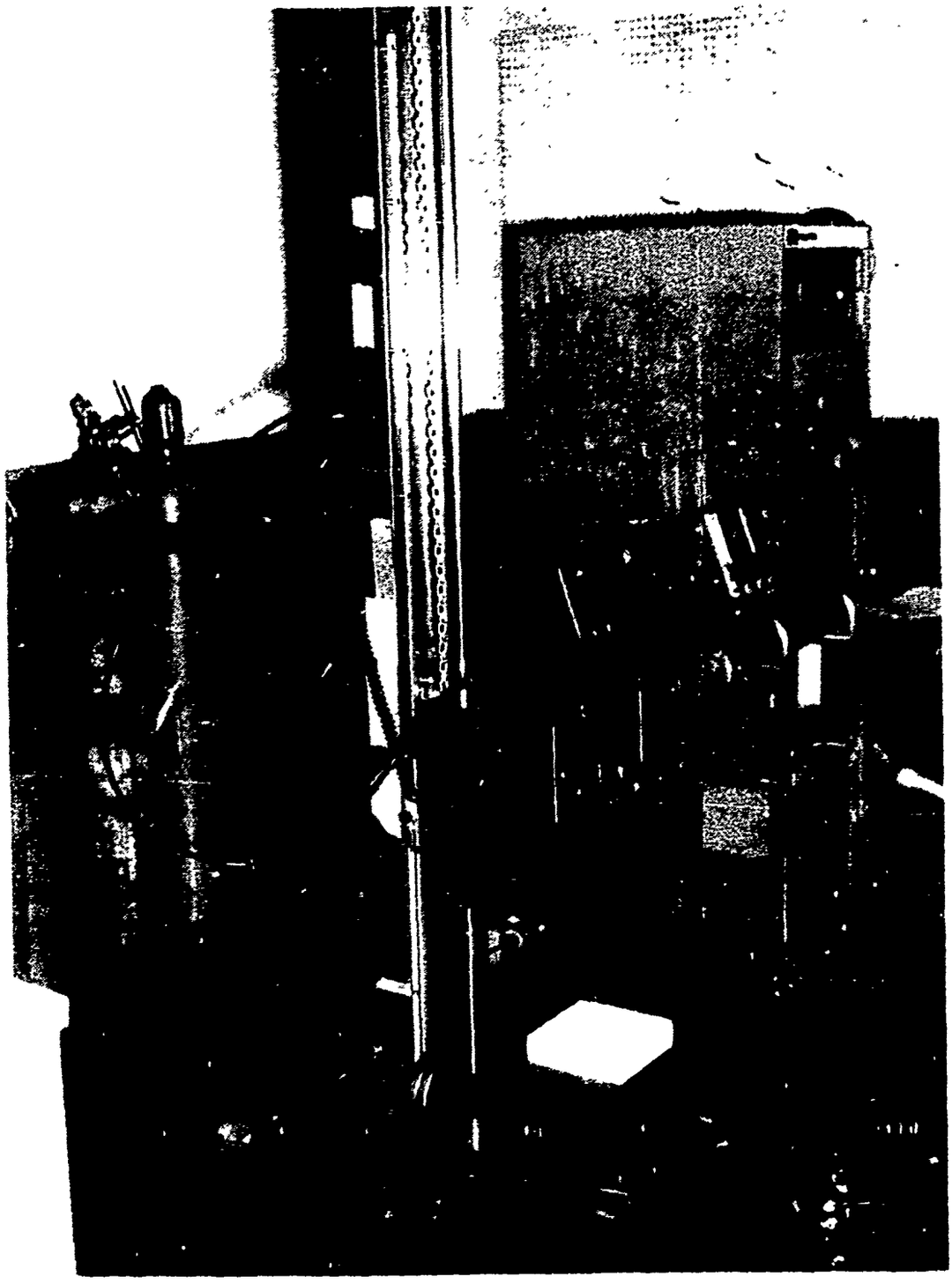

Figure 3. Drop test apparatus.

behavior of other thicknesses. He also stated that the cushion factors would vary according to the area of the cushion specimen tested. He attributed this to materials which had a relatively high pneumatic characteristic.

Stern [6] described the phenomenon of the drastic difference between the response of some materials to dynamic loading and that of static loading. He attributed this to the pneumatic effect of the partially entrapped air in the material. The effect was found to be most pronounced in interconnected cellular materials and varied with the dimensions of the material. In a static test the air had sufficient time to escape without absorbing energy. In a dynamic test the load approached that of a free falling object and the rate of loading upon the cushion was much more rapid. As the cushion was compressed, the entrapped air in the cellular material was not able to escape as the cells suddenly collapsed.

Figure 4 shows the difference in energy absorption ability during static and impact loading. E_d is the energy dissipated, E_s is the energy stored in the cushion, and e_m is the maximum strain the cushion encounters [7]. The open circles represent static loading while the solid circles depict the ratio of dissipated energy to stored energy of a cushion under impact loading conditions.

Kerstner's solution to the dilemma of static versus dynamic data was to use peak acceleration versus static stress graphs. The peak accelerations obtained during dynamic testing were plotted against the change in load or static stress. This resulted in the graphs shown in Figure 5 [8]. Peak acceleration-static stress graphs were developed for various cushioning

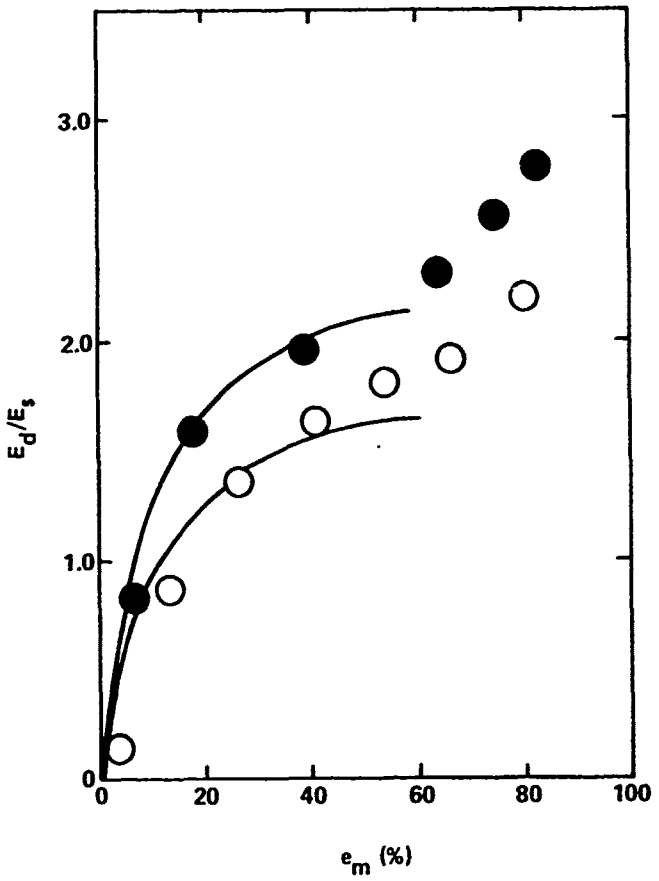

Figure 4. The ratio of dissipated energy to stored energy during static and impact loading [7].

materials at various drop heights. The fragility level of the item to be protected was determined by anticipating the maximum acceleration the item could undergo without being damaged or destroyed. The graphs are read by finding the fragility level on the vertical axis and drawing a horizontal line from that point, intersecting the dynamic cushioning curves. The cushion thickness associated with the first curve which falls below the line, within the expected stress levels the item will encounter, is the proper cushion amount to utilize.

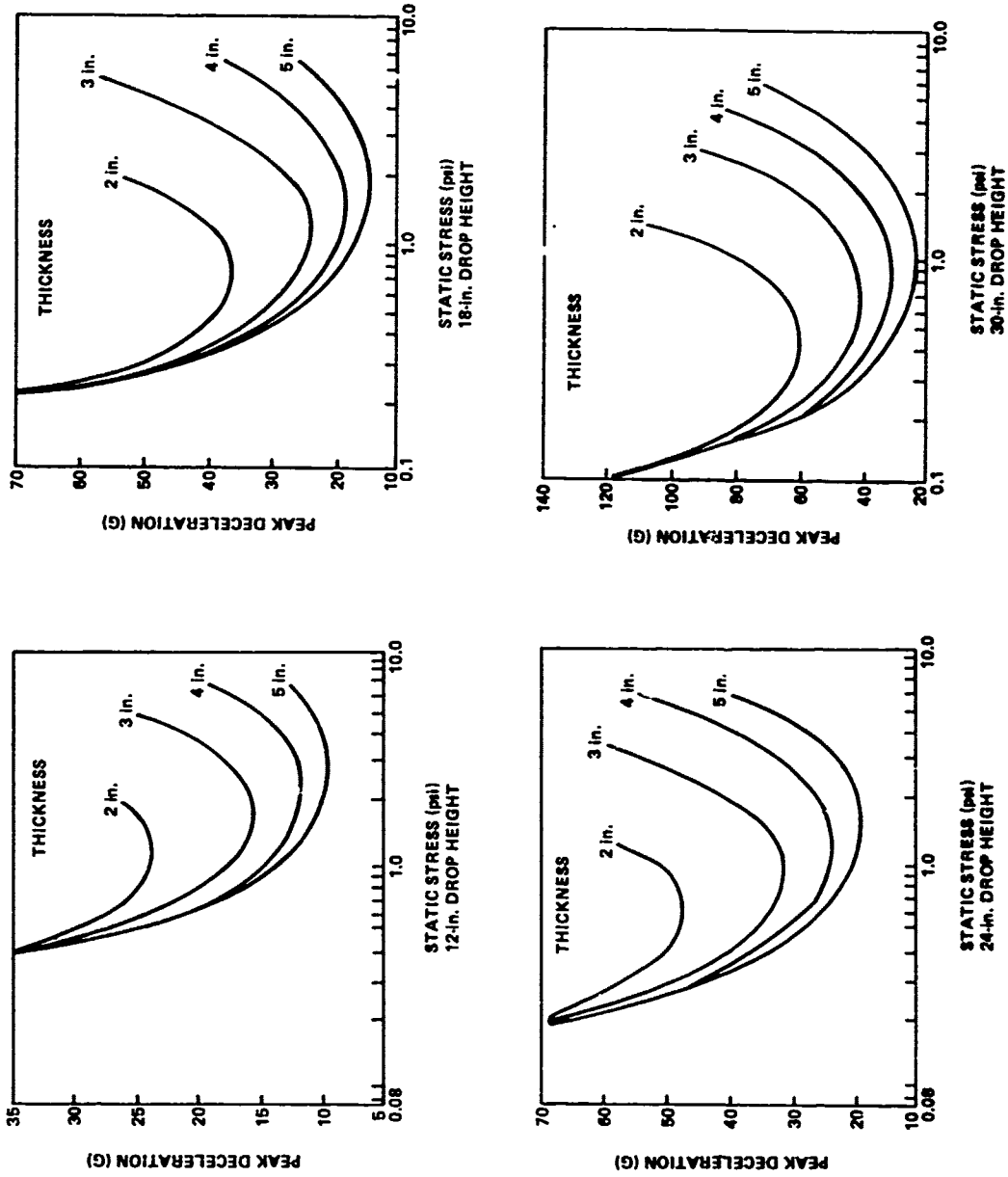

Figure 5. Peak acceleration versus static stress curves for polyethylene foam [8].

Although Kerstner indicated that his method could also be utilized to produce the cushion efficiency factor, the dynamic cushioning curves gained lone acceptance and are still utilized today.

Extensive research work has been underway over the past two decades resulting in the development of dynamic cushioning curves for various cushioning materials. However, many of these early curves were derived from data collected at ambient temperature.

McDaniel and Wyskida [9] were the first to conduct extensive research on the effects of temperature upon cushioning materials. It was demonstrated conclusively that the temperature effects were significant. In 1975, McDaniel [10] derived the first general mathematical model to predict peak acceleration for flat pad drops at different temperatures. He generated, via drop tests, dynamic test data on Minicel, the commercial name for a closed cell, cross-linked polyethylene foam material. Using a stepwise regression procedure he was able to develop the general mathematical model from the experimental data. McDaniel's general model has been used to develop specific mathematical models for polyester and polyether types of polyurethane, and Dow Ethafoam polyethylene.

Figure 6 is a typical set of dynamic cushioning curves used by modern package designers. The three curves represent three different temperatures. Points on the curves correspond to the peak acceleration (given in G's) experienced by the cusnioned item at the corresponding static stresses. The horizontal line depicts the fragility level to which the item under consideration

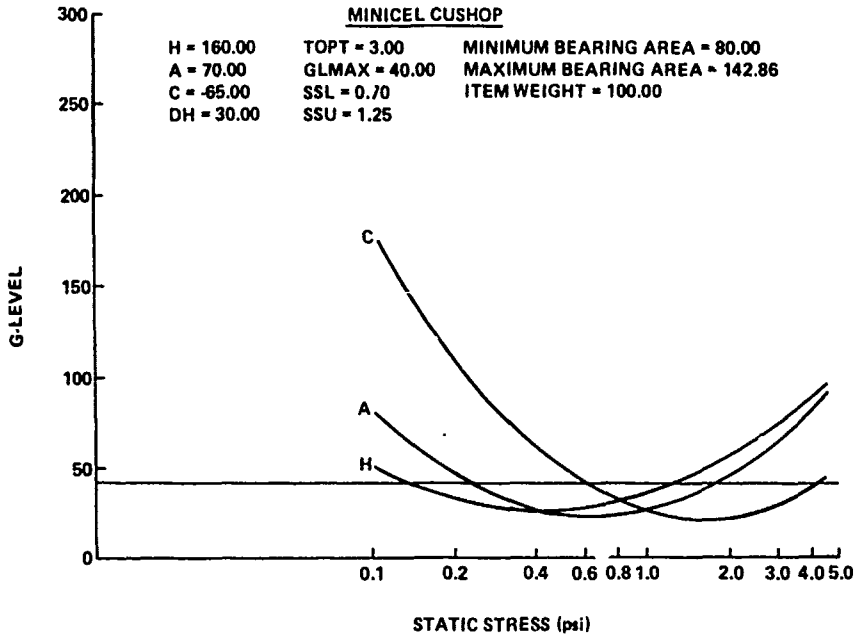

Figure 6. Typical dynamic cushioning curves at selected temperatures derived from unconfined test data.

must be protected. The package designer must choose a material with a material thickness which possesses dynamic cushioning curves for the temperature range for which he is designing and, furthermore, a portion of the curves must be below the specified fragility level. A separate set of curves is necessary for each unique set of parameters (i.e., drop height, cushion thickness, and material).

Wyskida, Johannes, and Wilhelm [11] also devised a cushion optimization program on the Hewlett-Packard (HP) 9815A with a plotting capability. The modern design engineer has access to this program which includes five cushioning materials.

As stated previously, the dynamic cushioning curves used by cushion designers are derived from data obtained when drop tests are made on a flat pad (unconfined testing). Even the impact response model developed by McDaniel [10] was derived from flat pad drops. The cushion itself is not enclosed in any way. In spite of this advancement of the state-of-the-art, many items must be placed within a container for shipment purposes. McDaniel did not consider the effects of a container in his model development. This lack of data on container effects and inability to predict them has been a major concern to cushion designers.

Since the flat pad impact response has been modeled, it is now possible to extend it to the response within a container. Although there have been very few direct comparisons in this area, the assumption has been that the flat-pad data result in conservative designs. Grabowski [12], using foamed polystyrene and flat drops in a corrugated board container, wood crate, and steel cylinder at 30-in. drop heights, found that the peak accelerations were lower than those for corresponding static stresses and thicknesses of the flat pad test. If the impact response of the overall container system (i.e., the container together with the cushioning material as one unit) could be modeled, it would undoubtedly result in substantial savings to the cushion design.

Prior to modeling the overall container system, it is necessary to develop an experimental design which is capable of acquiring the experimental data for modeling purposes. This is the topic of Chapter III.

CHAPTER III. EXPERIMENTAL CONSIDERATIONS

Dynamic cushioning curves are derived from data obtained when drop tests are conducted on a flat pad cushion. This method of obtaining impact response was not designed to take into consideration the effects of an outside container upon the impact response. Mazzei [13] found that there was a definite difference in confined (outside container) and unconfined (no container) test results. He attributed this difference to pneumatic effects within the container. Since there are known to be container effects, the lack of data on container effects and the inability to predict them has been a major concern to cushion system designers. Consequently, the immediate objective is tc determine whether the methodology, developed by McDaniel in constructing a mathematical model for impact response from unconfined data, could be extended to the development of a general model for data collected from drop tests of an overall container. Consequently, a drop test experiment was designed from which data were available to apply these mathematical modeling techniques.

McDaniel [10] developed a specific model for the impact response of the Hercules Minicel cushioning material based upon flat pad cushion data. Minicel possesses the ability to withstand extreme temperatures, without a degradation in cushioning ability. Consequently, a 2-in. thick Minicel

cushion was selected as the bulk cushioning material for use in the overall container experimental model.

Physical Description

Twenty-five complete container systems were prepared for experimental testing. A complete container system is shown in Figure 7. The two major components are the outside container and the interior box. The interior box is a 19-in. plywood cube protected by a 2-in. thickness of Minicel cushioning material configured as corner void pads. This interior box was enclosed in a military standard cleated plywood shipping container as shown in Figure 7.

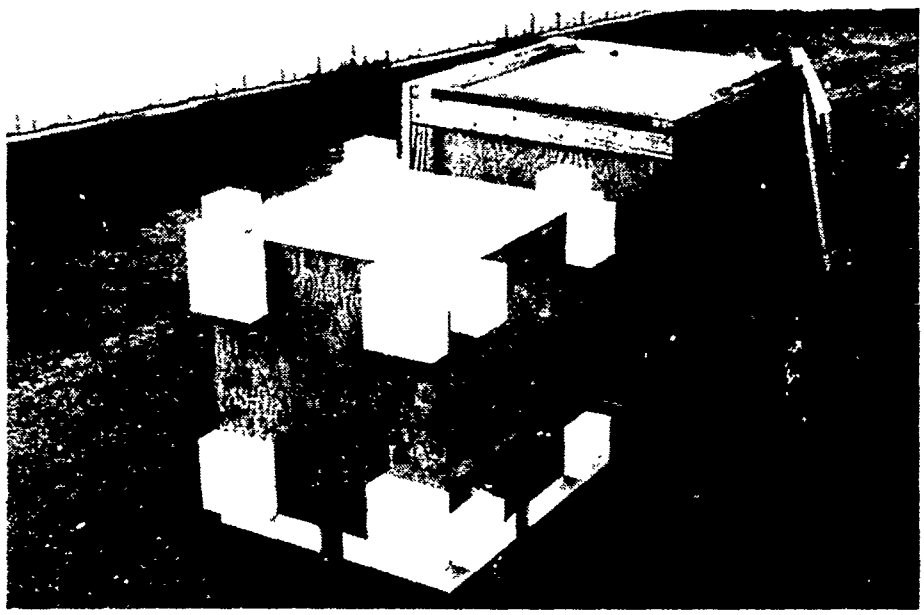

Figure 7. Interior box and outside container.

Six different static stress levels were obtained by varying the total area of the cushioning material on the six faces of the interior box so that each face of the box represents a different stress level. The relationship between static stress σ, weight W, and total cushion area A, was used to determine the size of the corner pads in the following equation:

$$\sigma = \frac{W}{A} \quad .$$

Using the average weight of the interior boxes, 25.5 lb, and the following cushion pad dimensions, the resulting static stress levels are:

Cushion Pad Side (in.)	Total Area ($in.^2$)	Static Stress Levels (psi)
8.50	289.00	0.088
5.00	100.00	0.255
3.50	49.00	0.520
3.00	36.00	0.708
2.75	30.25	0.843
2.25	20.25	1.255

It should be noted that the actual size of the corner void pads was determined prior to calculating the static stress levels, due to the physical dimension constraint on the surface of the interior box. Should lower stress levels be desired, the dimensions of the interior box must be increased accordingly to accommodate the larger cushions which would be required.

The six temperatures at which drops were considered desirable were -65, -20, 20, 70, 110, and 160°F. These are the temperatures specified by the U. S. Army Natick Laboratories for use in testing bulk cushioning materials. The -20°F temperature is especially important since this is the region where some bulk cushions crystallize. The four standard drop heights utilized were 12, 18, 24, and 30 in. Three replicates were performed for each set of experimental conditions with four containers for each replicate.

One set of 12 containers was utilized for temperatures -20, 70, and 160°F, and the other 12 containers for 20, 110, and -65°F. This prevents any one container system from experiencing the entire temperature range of 225°F, which is unlikely to occur in an actual situation. The remaining container system was utilized as the prototype in the development of the container design.

Prior to conditioning, the container systems were instrumented with three accelerometers in the interior box, and three in the outer container. The complete container systems were conditioned in environmental chambers (Figure 8) at the required temperature for 24 hours prior to testing.

All tests were conducted at the U. S. Army Missile Research and Development Command's Dynamic Test Facility. Figure 9 shows the drop tester and the container positioned ready to drop. Figure 10 shows the test apparatus after a drop. Note that the outer container is almost as wide as the drop tester platform. Therefore, the choice of size for the outer container

Figure 8. Container systems in environmental chambers.

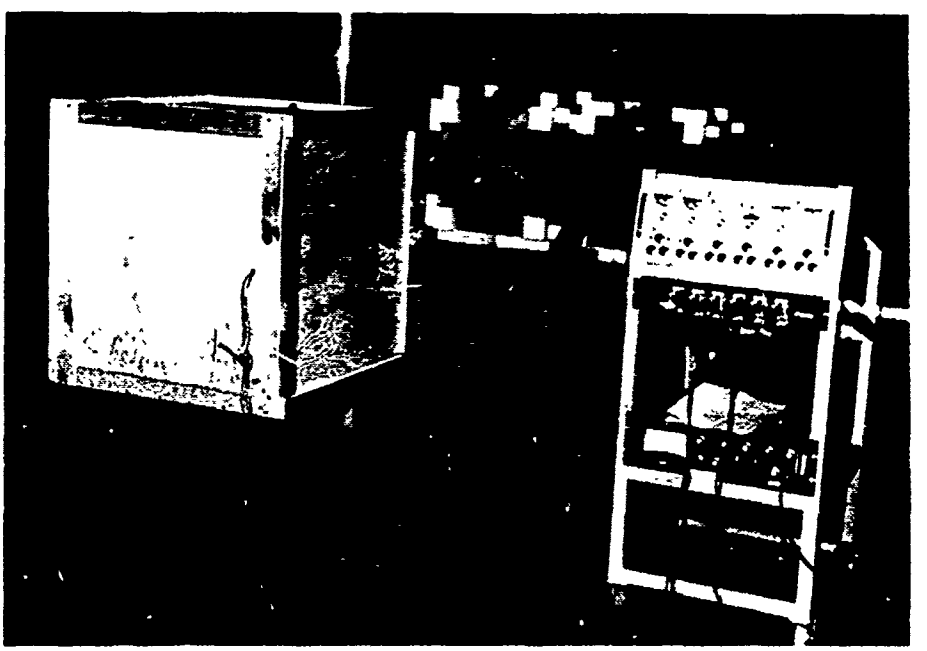

Figure 9. Drop tester and container system prior to drop.

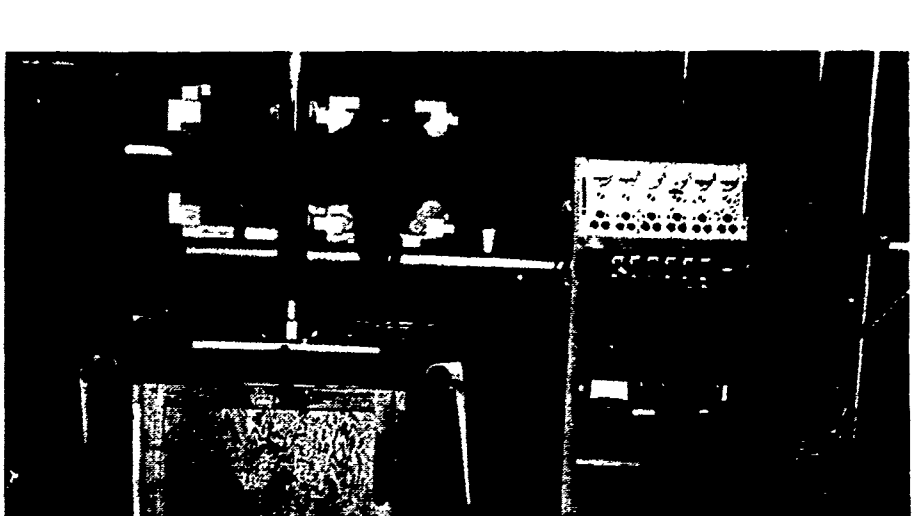

Figure 10. Test apparatus after drop.

was constrained. This, in turn, limited the choice of cushion thicknesses and and the ability to test various thicknesses.

Experimental Design

The order of the drops was randomized as much as physically possible. One constraint on randomization was the use of the environmental chambers for temperature conditioning. Chamber space necessitated the drop test procedure to consider all of one temperature simultaneously. That is, all three replicates for one temperature were conditioned as a group. Since each box required a cable to be attached, just prior to testing but after removal from the chamber, it was not feasible to randomize the boxes within the replicate. However, the static stresses and drop heights were randomized within each replicate. The randomized order of the drops was determined by the computer

generated form shown in Figure 11. One page of this form gives the order of drops for one replicate at a particular temperature on each of four boxes. The order of drops for each box is given in the column under the box number. The letter for each drop indicates the face (or stress level) on which the box is being dropped, while the inches following the letter indicate the drop height.

The time required to perform the necessary drops on all six surfaces of one box was less than 2 minutes. Since temperature is involved, experimentation was performed to determine if a significant change in temperature occurred prior to completion of the sequence of six drops on one container. Fortunately, the change in temperature was not significant in the required 2-minute interval.

The peak accelerations encountered by the interior box and the total box during the 432 drops were compiled. The peak accelerations (in G's) for the interior box are given in Appendix A. Appendix B contains the peak accelerations for the total box. It is these basic test data which will now be utilized in the development of a mathematical model for the confined cushioning material situation. However, prior to model development initiation, it is necessary to consider the theoretical aspects of the situation which is to be modeled.

MATERIAL: MINICEL THICKNESS:

TEMPERATURE: REPLICATION:

DROP HEIGHT

BOX-1	BOX-2	BOX-3	BOX-4
C-12"	F-18"	B-18"	E-24"
F-12"	D-18"	A-18"	D-12"
E-30"	B-12"	F-30"	F-24"
B-24"	E-12"	D-24"	A-12"
D-30"	C-30"	E-18"	B-30"
A-30"	A-24"	C-18"	C-24"

Figure 11. Randomized drop test sequence.

CHAPTER IV. THEORETICAL CONSIDERATIONS

A container system is composed of three elements; the exterior shipping container, the cushioning material, and the protected item. Figure 12A depicts the system with the three elements. By substituting springs for the cushioning material, the system may be represented as in Figure 12B. To study the reaction in only one direction, all the springs may be represented as one as in Figure 12C. When a container is dropped, it obeys the laws of Galileo and Newton by uniformly increasing its speed of descent under the pull of gravity until it strikes whatever floor or platform intervenes at a speed

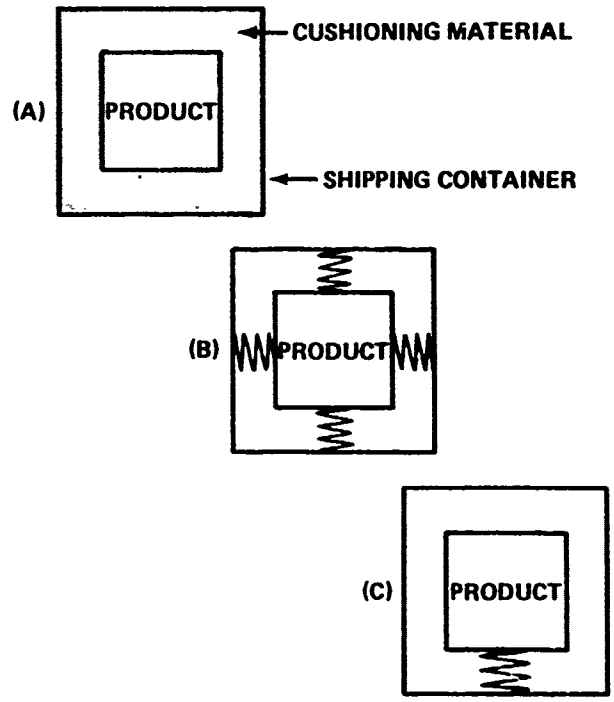

Figure 12. Schematics of standard container system [3].

dependent upon the drop height (8.5 mph for a 30-in. drop height). As shown in Figure 13, the container stops but the protected item, also moving at 8.5 mph, pushes into the cushioning until the resistance of the compressed cushioning is equal to the force of the moving item. The protected item, slowed to a stop after expending its energy of motion (derived from the free fall) in compressing the cushioning, is returned to its original position by the energy stored in the compressed cushion.

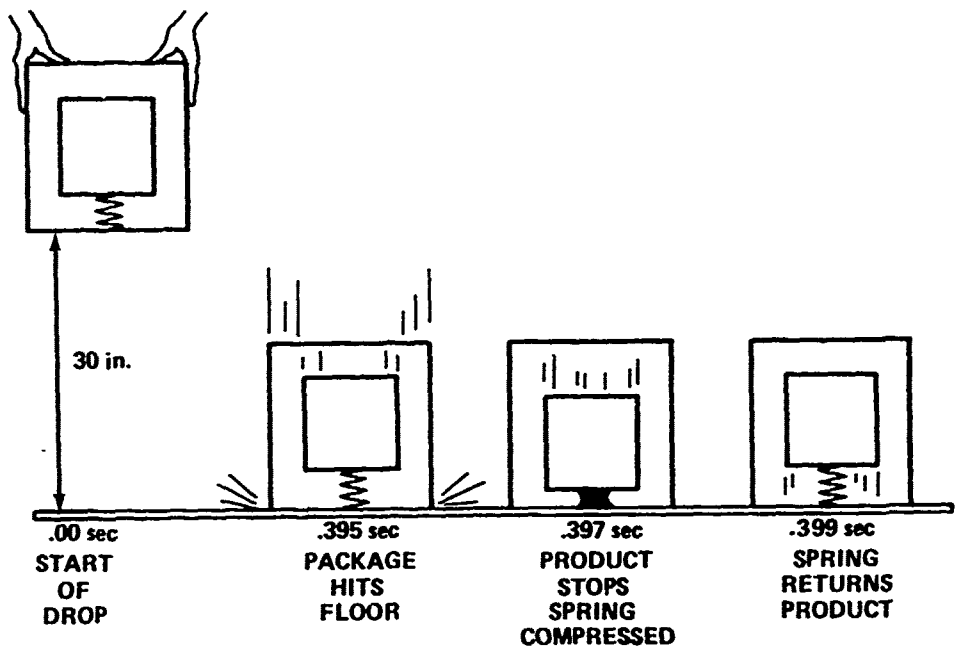

Figure 13. Free fall of container system shown in various stages [3].

The cushion's function is to decelerate the protected item in a few inches which is a fraction of the drop height originally available for the package to accelerate to its impact velocity. Since the initial acceleration was due to the force of gravity, the deceleration must be proportionately greater, since the distance available is much less.

The protected item, during its deceleration, experiences the same pressure as the cushion which is resisting the downward pressure of the descending protected item. This force starts at zero at the time contact and initial compression are made and increases to a maximum when the protected item is stopped and returns to zero as the compressed cushioning material returns the product to its original position.

In developing the impact response of the protected item several parameters were considered. From previous research, the peak acceleration is related to other parameters as

$$G = f(\sigma_s, T, \theta, h)$$

where

G = acceleration (G's)

σ_s = static stress (psi)

T = thickness of cushion (in.)

θ = cushion temperature (°F)

h = drop height (in.).

The objective of the derivation which follows is to determine the relationship of the previously mentioned parameters in the impact response model for the interior box. However, some basic concepts will be discussed first.

The theoretical model to predict impact response is developed from the constitutive relationships taken from viscoelastic theory. The approach is to

consider the viscoelastic cushioning material as a standard linear solid, defined as a material in which the stress-strain behavior can be represented by linear relations involving not only stress and strain but also their time derivatives of all orders. An elastic material represents the special case of a linear material in which the time derivatives can be neglected for the range of frequencies involved. Materials which are time dependent in their response are called viscoelastic.

In past studies when a falling body was dropped directly onto the cushion placed on a rigid base, a Kelvin viscoelastic model was utilized to depict this situation. The present research is more complicated in that the falling body and the cushion are packed together in a wooden box which is dropped onto the rigid base. The box provides shock absorbing or cushioning capacity, as does the cushioning material. The mechanical model used to describe this behavior is shown in Figure 14. The cushioning material is represented by a Kelvin model. The wooden box is represented by a group of springs in parallel in which the springs impact the rigid plane. The shock is

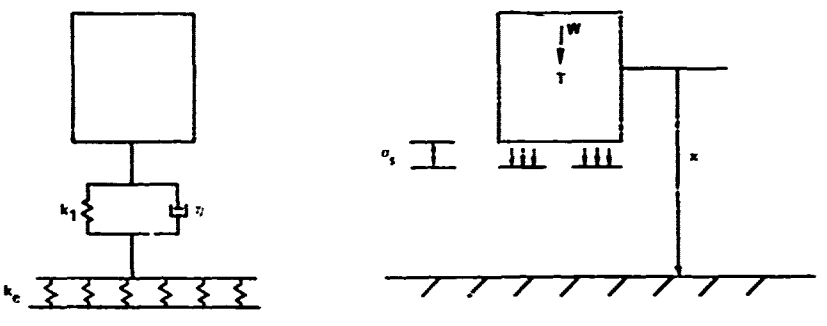

Figure 14. Interior box cushioned under impact loads.

transmitted through the springs representing the box into the Kelvin model representing the foamed cushion material and finally into the protected item.

Consider a container system which is dropped a distance h. Inside the container is another box with weight W and mass m. The interior box is cushioned by the cushioning material which is in a tailored corner void configuration of thickness T. The static stress between the cushion, with total area per side, A, and the interior box, is represented by σ_s.

The spring and dashpot configuration on the left in Figure 14 represents a standard linear solid. The stiffness of the outer box is represented by parallel springs whose sum is k_e. The relaxation modulus according to Flugge [14] for the standard linear solid may be expressed as

$$E_r(t) = \left(\frac{k_e k_1}{k_e + k_1}\right)\left[1 + \frac{k_e}{k_1} e^{-t(k_e+k_1)/\eta}\right] \qquad \text{(IV-1)}$$

where t represents time and η represents the viscosity of the cushioning material.

The equation of motion of the interior box after contact with the cushion may be expressed as

$$m\ddot{x} = W - \sigma_s A \qquad \text{(IV-2)}$$

where x is the position of the interior box with respect to the top of the cushioning material.

If the model used is that of a linear viscoelastic solid, then

$$\sigma_s = E_r(t)\epsilon \quad .$$

The strain ϵ is defined as the ratio of displacement x to thickness T of the cushioning material so that the static stress may be expressed as

$$\sigma_s = \frac{E_r(t)x}{T}$$

and the equation of motion becomes

$$m\ddot{x} = W - \frac{AE_r(t)x}{T} \quad . \tag{IV-3}$$

The correspondence principle described by Flugge [14] states that under impact conditions, the modulus of elasticity (which is not time dependent) may be substituted for the viscoelastic relaxation modulus in linear solids, giving

$$m\ddot{x} = W - \frac{AEx}{T} \quad , \tag{IV-4}$$

where E is the elastic counterpart corresponding to $E_r(t)$.

The general solution of Equation (IV-4) may be expressed as

$$x(t) = \frac{WT}{AE} + A \sin \omega t + B \cos \omega t$$

where $\omega^2 = \frac{AE}{Tm}$ is the square of the undamped natural frequency of the system. Using the initial conditions $x(0) = 0$ and $\dot{x}(0) = \sqrt{2gh}$ where g is the gravitational constant, the constants A and B are evaluated and the solution of $x(t)$ is

$$x(t) = \frac{WT}{AE} + \sqrt{\frac{2TWh}{AE}} \sin \omega t - \frac{WT}{AE} \cos \omega t \quad . \tag{IV-5}$$

Using

$$\phi = \tan^{-1} \frac{\left(\frac{WT}{AE}\right)}{\sqrt{\frac{2TWh}{AE}}} \quad ,$$

Equation (IV-5) becomes

$$x(t) = \frac{WT}{AE} + \sqrt{\frac{2TWh}{AE} + \left(\frac{WT}{AE}\right)^2} \sin (\omega t - \phi) \quad . \tag{IV-6}$$

According to Fowles [15], the amplitude of the oscillations or maximum value of x is $\frac{WT}{AE} + \sqrt{\frac{2TWh}{AE} + \left(\frac{WT}{AE}\right)^2}$. Differentiating Equation (IV-6) twice with respect to time to obtain the acceleration yields

$$\ddot{x}(t) = -g \sqrt{1 + \frac{2AEh}{WT}} \sin (\omega t - \phi) \quad .$$

Using Schapery's approximation method for obtaining viscoelastic solutions [16], the relaxation modulus may be substituted for the modulus of elasticity so that

$$\ddot{x}(t) = -g\sqrt{1 + \frac{2AE_r(t)\,h}{WT}}\,\sin(\omega t - \phi) \quad .$$

Since only the peak accelerations are of interest in this research, the oscillatory component may be ignored. Using the series approximation

$$\sqrt{1+x} = 1 + \frac{1}{2}x - \frac{1}{8}x^2 + \frac{1}{16}x^3 + \ldots$$

the peak acceleration may be expressed as

$$\ddot{x}(t) = -g\left[1 + \frac{hAE_r(t)}{WT} - \frac{1}{2}\left(\frac{hAE_r(t)}{WT}\right)^2 + \ldots\right] \quad . \qquad \text{(IV-7)}$$

Past research [10, 17] has shown that only the quadratic terms are significant. The stiffness factor k_e in the relaxation modulus $E_r(t)$ should be many times greater than the stiffness factor k_1. Then, for impact loads, the magnitude of $E_r(t)$ may be approximated as

$$|E_r| \approx k_e e^{c/\eta}$$

where c is a constant. Equation (IV-7) may then be expressed as

$$\ddot{x}(t) = -g\left[1 + \frac{hAk_e e^{c/\eta}}{WT} - \frac{1}{2}\left(\frac{hAk_e e^{c/\eta}}{WT}\right)^2 + \ldots\right] \quad . \qquad \text{(IV-8)}$$

The quantity W/A is the static stress σ_s. If the stiffness factor k_2 is assumed to be approximately equal to the square of the intensity of the load

as measured by the static stress, Equation (IV-8) may be expressed as

$$\ddot{x}(t) = -g\left[1 + \frac{h\sigma_s e^{c/\eta}}{T} - \frac{1}{2}\left(\frac{h\sigma_s e^{c/\eta}}{T}\right)^2 + \ldots\right] \quad . \qquad \text{(IV-9)}$$

For values of σ_s less than approximately 1.5, a transformation function of the form $(1 - \cos \sigma_s)$ permits Equation (IV-9) to be expressed approximately as

$$\ddot{x}(t) \approx -g\left[1 + \frac{he^{c/\eta}}{T}(1 - \cos \sigma_s) - \frac{1}{2}\frac{h^2}{T^2}(1 - \cos \sigma_s)^2 \cdot e^{2c/\eta} + \ldots\right] \quad . \qquad \text{(IV-10)}$$

If a series approximation is used for $e^{c/\eta}$ in the form

$$e^x = 1 + x + \frac{x^2}{2} + \ldots$$

and the viscosity η is inversely proportional to the temperature θ, then

$$\ddot{x}(t) = -g\left[1 + \frac{h(1 - \cos \sigma_s)}{T}(C_1 + C_2\theta + C_3\theta^2 + \ldots) - \frac{h^2}{T^2}(1 - \cos \sigma_s)^2 (C_1 + C_2\theta + C_3\theta^2 + \ldots)^2 + \ldots\right] \quad .$$

If only arbitrary constants are used, selected terms from the following general form may be used to approximate the peak acceleration:

$$G = C + \sum_{i=1}^{n} C_i \left(\frac{h}{T}\right)^i (1 - \cos \sigma_s)^i \left[\sum_{j=1}^{m} D_{ij} \theta^j\right] \quad . \qquad \text{(IV-11)}$$

Previous studies [10, 17] on the impact response of unconfined cushioning materials predicted an expression of the form

$$G = C + \sum_{i=1}^{n} \frac{C_i h^{1/2}}{(\sigma_s T)^{1/2}} \sum_{j=1}^{m} k_{ij} \theta^j \quad . \qquad \text{(IV-12)}$$

Expressions of the form given in Equations (IV-11) and (IV-12) are likely candidates for empirically curve-fitting cushioning system experimental data. Chapter V will utilize the previous expressions as a framework from which to develop a general model for the conditions under study.

CHAPTER V. MODEL DEVELOPMENT

As stated previously in Chapter IV, the relationship of static stress to weight of a cushioned item and total cushioned area is given by the equation

$$\sigma_s = \frac{W}{A} \quad .$$

Although the 19-in. plywood cubes utilized as the dummy items within the containers were constructed according to government specifications, their individual weights varied enough to cause the static stresses to vary among the 24 samples. Table I lists the weights of the protected interior box, the exterior box, and the total box. The resulting variation in the respective static stresses for each of the six surfaces of each cube are given in Table II.

The data analysis procedure was determined prior to the experimentation. This procedure requires the experimental data to be in replicates of three for each surface of the experimental boxes, as outlined in the experimental considerations chapter. Consequently, it was necessary to devise a method to transform the experimental data for the interior box to reflect a common static stress level for each respective side. This was accomplished through the use of the following linear transformation. If the adjusted acceleration is denoted by G, the uniform static stress by σ_s, the measured peak

Table I. Weights of Test Specimens

Box No.	Interior Box Weight (lb)	Exterior Box Weight (lb)	Total Box Weight (lb)
1	24.50	32.25	56.75
2	26.31	34.56	60.88
3	26.06	34.25	60.31
4	25.00	32.88	57.88
5	26.50	34.81	61.31
6	25.81	33.94	59.75
7	25.19	33.13	58.32
8	26.19	34.44	60.63
9	24.75	32.56	57.31
10	25.44	33.44	58.88
11	25.69	33.75	59.44
12	26.13	34.38	60.50
13	24.56	32.31	56.88
14	24.75	34.50	59.25
15	26.25	34.50	60.75
16	23.81	31.31	55.13
17	25.44	33.44	58.88
18	26.38	33.81	60.19
19	25.38	33.38	58.75
20	24.88	31.88	56.75
21	25.50	33.25	58.75
22	26.50	34.81	61.31
23	24.63	32.38	57.00
24	25.13	33.00	58.13

Table II. Shear Stresses for Each Surface of Each Interior Box

Box No.	Surface					
	A	B	C	D	E	F
1	0.082	0.245	0.500	0.681	0.810	1.210
2	0.088	0.263	0.537	0.731	0.870	1.299
3	0.088	0.261	0.532	0.724	0.862	1.287
4	0.084	0.250	0.510	0.694	0.826	1.235
5	0.089	0.265	0.541	0.736	0.876	1.309
6	0.087	0.258	0.527	0.717	0.853	1.275
7	0.085	0.252	0.514	0.700	0.833	1.244
8	0.088	0.262	0.534	0.727	0.866	1.293
9	0.083	0.248	0.505	0.688	0.818	1.222
10	0.085	0.254	0.519	0.707	0.841	1.256
11	0.086	0.257	0.524	0.714	0.849	1.269
12	0.088	0.261	0.533	0.726	0.864	1.290
13	0.083	0.246	0.501	0.682	0.812	1.213
14	0.083	0.248	0.505	0.688	0.818	1.222
15	0.088	0.263	0.536	0.729	0.868	1.296
16	0.080	0.238	0.486	0.661	0.787	1.176
17	0.085	0.254	0.519	0.707	0.841	1.256
18	0.088	0.264	0.538	0.733	0.872	1.302
19	0.085	0.254	0.518	0.705	0.839	1.253
20	0.084	0.249	0.508	0.691	0.822	1.228
21	0.086	0.255	0.520	0.708	0.843	1.259
22	0.089	0.265	0.541	0.736	0.876	1.309
23	0.083	0.246	0.503	0.684	0.814	1.216
24	0.084	0.251	0.513	0.198	0.831	1.241

acceleration by A, and the actual static stress by S, then the following relationship may be used to obtain the adjusted peak acceleration:

$$G = \sigma_s \left(\frac{A}{S}\right) .$$

The original data with the associated static stresses are given in Appendix A. The adjusted accelerations are given in Appendix C.

Preliminary Data Analysis

With any experimental effort, a set of observations, assumed to be taken under the same conditions, may vary widely from other observations or be what is known as an outlier. The experimenter must decide whether to retain the outlier observation in his computations or to discard it as a faulty measurement. Even though the data point is discarded from computation, it is still recorded.

The argument for exclusion of outlying data is that if the data are good one simply loses some of the relevant information; in this research effort, it means discarding one of the three replicated observations. If the discarded observation is truly inaccurate, then its inclusion would bias the results and the estimate of precision by an unknown, and generally unknowable, amount.

Consequently, it was determined that a test for outliers would be performed. The first step in the outlier test is to compute the sample variance, while holding static stress constant, for each set of three replications of peak accelerations to find which set has the maximum sample variance. For the

set of observations having the largest variance, each observation of the set is then tested individually as a candidate for rejection as an outlier by using the statistic

$$t = \frac{\left| x_e - \bar{x} \right|}{s_\nu}$$

where

x_e = an individual observation in a set of three replications

$\bar{x}$ = the sample mean of the three observations

s_ν = an independent external estimate of the standard deviation from concurrent data.

This statistic is based upon an extension of the extreme studentized deviate from the sample mean (Nair Criterion).

The set of replications of G's having the maximum sample variance corresponding to a particular stress level is eliminated from the calculation of s_ν. From the remaining sets of replications of G's, s_ν is calculated with the expression

$$s_\nu = \sqrt{\frac{\sum_{i=1}^{n-1} s_i^2}{n-1}}$$

where s_i^2 is the sample variance of the i^{th} set of replications of G's and n is the number of stress levels.

The values of the statistic for each observation in the set of replicates being tested are compared with the appropriate value from a table of percentage points of the extreme studentized deviate from the sample mean, and a point is rejected as an outlier if $t_{(\text{calculated})} > t_{(\text{table})}$.

If an observation is rejected in the first iteration of the outlier test, the set of replicates to which it belonged is no longer considered in further calculations, but the procedure then moves to the set of replicates with the next highest sample variance to check for outliers. Iteration is continued until a set of replications is checked and no points are rejected. Those data points determined to be outliers are marked with an asterisk in Appendix B. Also, a computer code for determining outliers as described is contained in Appendix D.

Interior Box Model Development

With the outlying data points determined and isolated from the computations, development was initiated on the polynomial regression model which would predict the maximum acceleration the interior box undergoes upon impact (inside a container) for a given temperature and drop height. Initial attempts to acquire a meaningful model with the experimental data in its original form proved fruitless. Consequently, a search was initiated for a data transformation for the static stress variable. If y_i is the predicted acceleration and x_i represents the static stress, the general form of the p-order polynomial regression equation is:

$$y_i = b_0 + b_2 x_i^2 + \ldots + b_p x_i^p \quad .$$

Many relationships of peak acceleration versus static stress were investigated. It was found that the best agreement was obtained when the transformation was $(1-\cos x)$. As a statistical test of this agreement, first, second, third, and fourth order regression equations were developed for each temperature and drop height combination. An ANOVA was compiled for each order, with a comparison of

$$F = \frac{MS_{DUE\ TO}}{MS_{ABOUT}}$$

with $F_{table} = 3.0$ and $\alpha = 0.10$ for each order indicating that the second order regression was the only order not rejected. The correlation coefficients for the individual dynamic cushioning curves (IDCC) were in the 0.70 to 0.96 range.

Consequently, the IDCCs took the general form:

$$y_i = b_0 + b_1\left(1 - \cos \sigma_{s_i}\right) + b_2\left(1 - \cos \sigma_{s_i}\right)^2 \quad .$$

The resulting IDCC equations for predicting the maximum acceleration as seen by the interior box are given in Table III. These equations may be utilized over the specific data range which was identified by the experimental data. They represent the specific mathematical model given for each temperature.

Table III. Interior Box IDCC Equations

Temperature (°F)	Drop Height (in.)	Box Equation
-65	12	$y = 34.56 - 40.75(1 - \cos x) + 24.83(1 - \cos x)^2$
	18	$y = 43.13 - 45.38(1 - \cos x) + 29.40(1 - \cos x)^2$
	24	$y = 32.15 \quad 2.97(1 - \cos x) + 9.08(1 - \cos x)^2$
	30	$y = 46.90 - 58.71(1 - \cos x) + 60.42(1 - \cos x)^2$
-20	12	$y = 42.26 - 110.62(1 - \cos x) + 118.69(1 - \cos x)^2$
	18	$y = 43.43 - 74.75(1 - \cos x) + 68.70(1 - \cos x)^2$
	24	$y = 64.63 - 170.13(1 - \cos x) + 164.84(1 - \cos x)^2$
	30	$y = 62.51 - 123.09(1 - \cos x) + 120.88(1 - \cos x)^2$
20	12	$y = 42.18 - 109.62(1 - \cos x) + 108.26(1 - \cos x)^2$
	18	$y = 41.70 - 55.87(1 - \cos x) + 48.88(1 - \cos x)^2$
	24	$y = 43.74 - 49.24(1 - \cos x) + 36.23(1 - \cos x)^2$
	30	$y = 57.55 - 130.25(1 - \cos x) + 151.13(1 - \cos x)^2$
70	12	$y = 32.07 - 58.67(1 - \cos x) + 61.64(1 - \cos x)^2$
	18	$y = 38.33 - 43.61(1 - \cos x) + 30.49(1 - \cos x)^2$
	24	$y = 36.04 - 9.38(1 - \cos x) + 0.09(1 - \cos x)^2$
	30	$y = 60.49 - 145.11(1 - \cos x) + 160.52(1 - \cos x)^2$
110	12	$y = 27.03 - 49.05(1 - \cos x) + 47.24(1 - \cos x)^2$
	18	$y = 28.47 - 13.52(1 - \cos x) + 7.67(1 - \cos x)^2$
	24	$y = 46.28 - 73.39(1 - \cos x) + 65.84(1 - \cos x)^2$
	30	$y = 36.47 - 45.93(1 - \cos x) + 64.80(1 - \cos x)^2$
150	12	$y = 31.97 - 86.81(1 - \cos x) + 96.25(1 - \cos x)^2$
	18	$y = 32.30 - 50.53(1 - \cos x) + 53.23(1 - \cos x)^2$
	24	$y = 31.17 - 46.78(1 - \cos x) + 63.77(1 - \cos x)^2$
	30	$y = 45.80 - 54.76(1 - \cos x) + 51.37(1 - \cos x)^2$

Figure 15 provides a representative sample of an IDCC plotted from an equation from Table III.

The IDCC's developed are applicable only to a specific temperature and drop height with 2-in. Minicel bulk cushioning. The next step is the

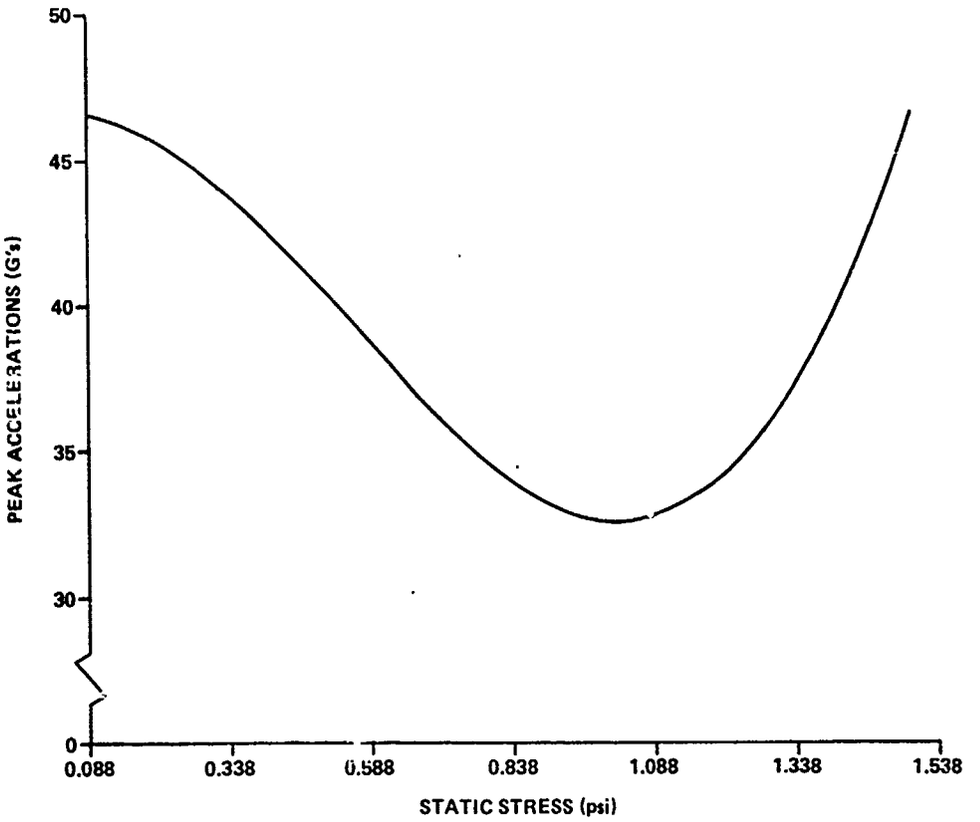

Figure 15. Interior box IDCC prediction at -65°F and a 30-in. drop height.

development of the general model for 2-in. Minicel which has as independent variables, drop height h, static stress σ_s, thickness of cushion T, and temperature θ, and as a dependent variable, G, the peak acceleration.

The initial model, Equation (IV-11), proved deficient in representing the nonlinear characteristics of cushion response for the interior box. Consequently, a modular modeling technique was utilized in which each independent variable was studied with its effect upon the dependent variable. Previous research efforts [10] have shown that the peak acceleration is related to an exponential form of temperature θ. Similarly, the drop height h has been

found to enter the mathematical model as the square root of that value, while thickness T is a negative exponential. Note that the data transformation $(1-\cos \sigma_s)$ used for static stress in the IDCC equations, is also utilized here for static stress.

A stepwise regression procedure was utilized in acquiring the general model expression. Draper and Smith [18] offer this procedure as an improved version of the forward selection process for variable selection. In the stepwise regression procedure, the variables already in the equation are reevaluated at each stage. A total of 45 terms were examined in the stepwise regressior. procedure. These terms were various combinations of variables found by previous research [9, 10, 11] to describe the behavior of bulk cushioning. Table IV lists the 45 terms. The variable combinations are identified by an x in the appropriate column. A zero value in the coefficient column indicates a variable combination which is not in the developed model.

The interior box general model may be stated as:

$$G = C_0 + \sum_{\ell=0}^{1} h^{\ell/2} \sum_{k=0}^{1} \frac{1}{T^{(1/2+k)}} \sum_{j=1}^{3} \theta^j \sum_{i=0}^{2} C_{ijk\ell} (1 - \cos \sigma_s)^i + \sum_{n=1}^{3} \theta^n \sum_{m=0}^{2} c_{mn} (1 - \cos \sigma_s)^m \quad .$$

From this general model it is necessary to select the combination of terms which best describes the situation to be modeled. Each time a variable is added to the interior box general model, it is necessary to evaluate the

Table IV. General Model for Interior Box

Terms	Coefficient	Variables							
		θ	θ^2	θ^3	$h^{1/2}$	$\tau^{-1/2}$	$\tau^{-3/2}$	$(1 - \cos \sigma_s)$	$(1 - \cos \sigma_s)^2$
0	-14.475703								
1	0.0	x				x			
2	0.0	x				x		x	
3	0.0	x				x			x
4	7.1865626	x			x		x		
5	0.0	x			x		x	x	
6	0.0	x			x		x		x
7	0.0	x			x	x			
8	0.0	x			x	x		x	
9	0.0	x			x	x			x
10	0.0		x			x			
11	0.0		x			x		x	
12	0.0		x			x			x
13	-0.57911897		x		x		x		
14	0.0		x		x		x	x	
15	0.0		x		x		x		x
16	0.0		x		x	x			
17	0.0		x		x	x		x	
18	0.0		x		x		x		x
19	0.0			x		x			
20	0.0			x		x		x	
21	-0.53894447			x		x			x
22	0.0			x	x		x		
23	0.0			x	x		x	x	
24	0.0			x	x		x		x
25	0.0			x	x	x			
26	0.0			x	x	x		x	
27	0.0			x	x		x		x
28	30.088255	x					x		
29	0.0	x					x	x	
30	66.557902	x					x		x
31	0.0		x				x		
32	0.0		x				x	x	
33	0.0		x				x		x
34	0.0			x			x		
35	4.1031526			x			x	x	
36	0.0			x			x		x
37	0.0	x							
38	0.0	x						x	
39	0.0	x							x
40	0.0		x						
41	-10.219992		x					x	
42	0.0		x						x
43	-0 22965288			x					
44	0.0			x				x	
45	0.0			x					x

NOTE: $\theta = \frac{°F + 460}{100}$

resultant dynamic cushioning curves to assure the proposed model is providing the hypothesized U-shaped curves of unconfined testing which do not possess negative peak accelerations and the curves are distinct. Obviously, many of the proposed models are similar in their predictive ability. However, based upon first-hand observations during the experimental phase, and supported by statistical evaluations at each step of the model development effort, it was determined that the best interior box general model to describe the confined situation for the cushioning material under consideration was a constant and eight independent variables. The resulting nine term interior box general model is:

$$G = -14.88 + 7.19\,\frac{\theta h^{1/2}}{T^{3/2}} - 0.58\,\frac{\theta^2 h^{1/2}}{T^{3/2}} - 0.54\,\frac{\theta^3\,(1-\cos\sigma_s)^2}{T^{1/2}}$$

$$+ 30.99\,\frac{\theta}{T^{3/2}} + 66.56\,\frac{\theta(1-\cos\sigma_s)^2}{T^{3/2}} + 4.10\,\frac{\theta^3\,(1-\cos\sigma_s)}{T^{3/2}}$$

$$- 10.22\,\theta^2\,(1-\cos\sigma_s) - 0.23\,\theta^3$$

where

$$\theta = \frac{°F + 460}{100} \quad .$$

The confined general model has a 0.806 correlation coefficient. All statistical tests have been performed at an alpha level of 0.10. The model should be used only within the ranges of the following independent variables:

h = drop height from 12 to 30 in.

σ_s = static stress range from 0.088 to 1.255 psi

θ = temperature from -65 to 160°F.

The model will predict accurately within the ranges given for the previously mentioned variables. Since data were not available outside the ranges of the independent variables, the accuracy of the model to predict in those ranges is unknown.

Figure 16 is a typical example of the predictive ability of the interior box general model. It is noted that the curve is U-shaped and possesses characteristics similar to the unconfined situation. Further comparisons between the confined and unconfined models will be presented in Chapter VII.

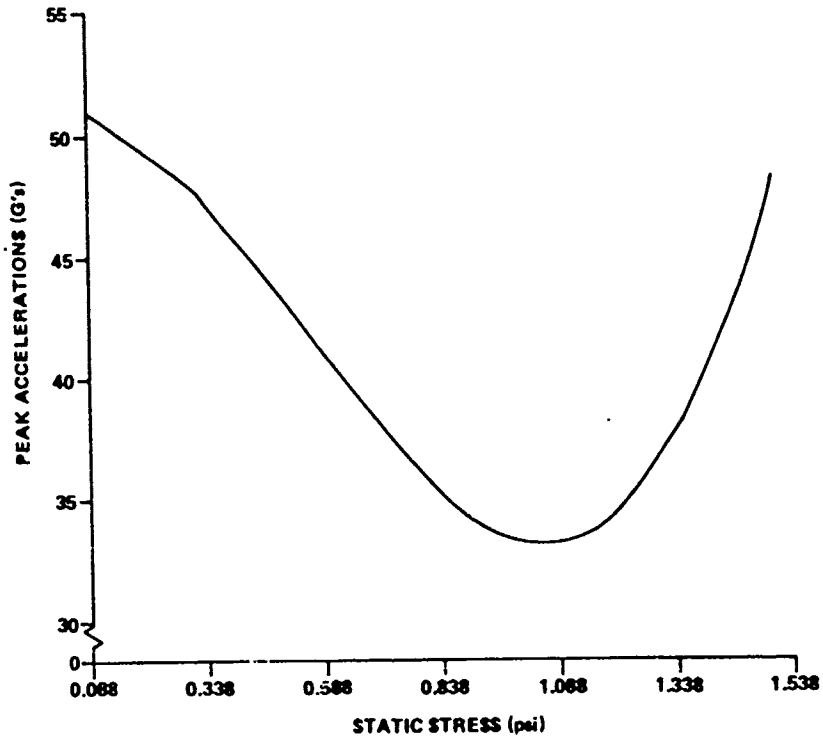

Figure 16. Interior box general model prediction at -65°F and a 30-in. drop height.

Total Box Model Development

The manner in which the experimental design acquired experimental data permitted the acquisition of total box peak acceleration observations at no additional testing cost. Consequently, three accelerometers were attached on an internal surface of the exterior box to acquire these peak accelerations.

Since the interior box varied in weight, the total weight of the interior and exterior box combined also varied. This total weight variation was also affected by the moderately varying weight between each of the individual outside boxes. A summary of the individual box weights, both interior and exterior, is given in Table I.

Since the total box weights did vary, it was hypothesized that a total box model could be developed that could predict the peak accelerations which the exterior box encounters as a function of total box weight. Furthermore, it is intuitive that as box weight increases, the G-level will also increase. What is not known is the effect of temperature upon the exterior box and the increased total box weight. It is anticipated, however, that the total box model will be linear in nature.

The total box experimental data are given in Appendix B, with truly anomalous readings identified with an asterisk, based upon an outlier procedure. The best fitting equation for a particular drop height and temperature situation was determined in the same manner as that utilized for the interior box. The correlation coefficients for the individual box equations were in the 0.65 to 0.80 range. A complete set of individual total box equations is given

in Table V. The computer program used to obtain the individual total box equations is given in Appendix E. It is significant to note that 22 of the 24 developed individual total box equations possess a positive slope, verifying the earlier conjecture of increasing peak acceleration as a function of increasing weight.

These equations will predict total box peak accelerations for a particular drop height, temperature, and total box weight. However, the predictive range is limited to the values of the basic experimental data. Figure 17 is a typical plot of a total box individual equation.

To provide further compatibility between the interior and exterior boxes, a general model is desirable which depicts the peak acceleration anticipated by the total box. Consequently, the data utilized to develop the individual total box equations is combined to provide an experimental basis for a general total box model. The total box model development modifies the procedure utilized in the development of the interior box general model. In particular, weight (W) is substituted for the term $(1 - \cos x)$.

The total box model may be stated as:

$$G = C_0 + \sum_{\ell=0}^{1} h^{\ell/2} \sum_{j=1}^{3} \theta^j \sum_{i=0}^{1} C_{ij\ell}(W)^i \quad .$$

From this general model it is possible to identify the combination of terms which best describes the situation to be modeled. Each time a variable is added to the total box general model, it is necessary to evaluate the

Table V. Individual Total Box Equations

Temperature (°F)	Drop Height (in.)	Box Equation
-65	12	y = -239.44 + 5.78 W
	18	y = -281.00 + 7.29 W
	24	y = 103.33 + 1.24 W
	30	y = -122.48 + 4.58 W
-20	12	y = -551.45 +11.04 W
	18	y = 92.67 + 1.06 W
	24	y = -409.48 + 9.23 W
	30	y = -36.99 + 3.52 W
20	12	y = 30.66 + 2.21 W
	18	y = -145.90 + 4.98 W
	24	y = 94.72 + 1.06 W
	30	y = -266.22 + 7.76 W
70	12	y = -208.96 + 6.67 W
	18	y = -440.38 +11.38 W
	24	y = -272.13 + 9.19 W
	30	y = 102.01 + 2.39 W
110	12	y = -415.67 + 9.08 W
	18	y = 26.12 + 2.05 W
	24	y = 749.16 - 9.66 W
	30	y = 97.08 + 9.92 W
160	12	y = 300.21 - 3.30 W
	18	y = 123.22 + 0.51 W
	24	y = -237.87 + 6.27 W
	30	y = 113.78 + 1.31 W

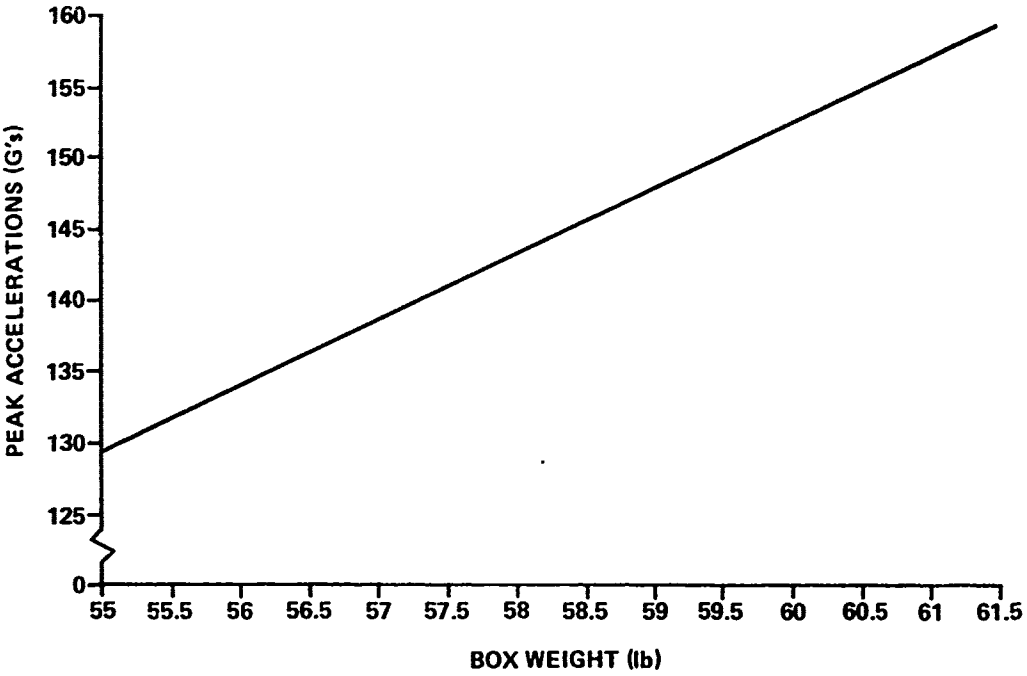

Figure 17. Individual total box prediction at -65°F and a 30-in. drop height.

resultant total box line to assure the proposed model is providing the hypothesized positive sloped line. The positive sloped line is based upon the concept that force is in direct proportion to weight. This leads to the selection of the following total box model:

$$G = -6.3548 + 0.0723\,\theta^{2}h^{1/2}W - 0.0092\,\theta^{3}h^{1/2}W \quad .$$

The confined total box model has a 0.772 correlation coefficient.

As can be seen, the previously mentioned model contains temperature θ, drop height h, and total box weight W as the parameters which vary. Consequently, it is possible to select a particular temperature, drop height, and total box weight, and predict the peak acceleration for those conditions.

Figure 18 is an example of the predictive ability of the total box general model.

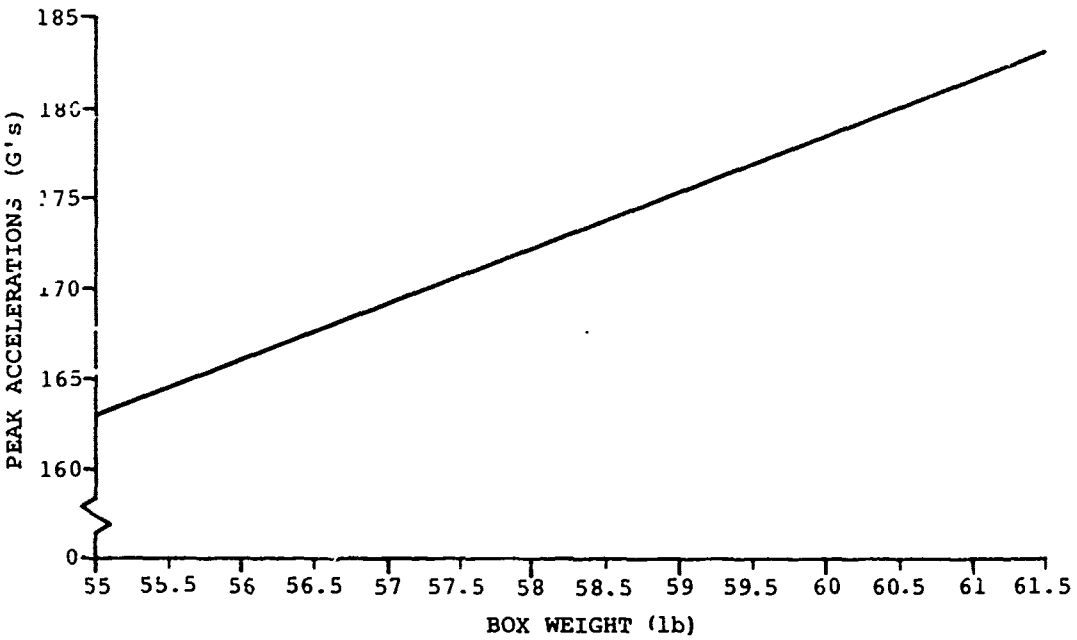

Figure 18. Total box general model prediction at -65°F and a 30-in. drop height.

The immediate task then is to validate the general models which have been developed in this chapter. This will be accomplished in Chapter VI.

CHAPTER VI. MODEL VALIDATION

In the previous chapter a basis for a general model was presented which approximates the peak acceleration upon an item within a cleated plywood container cushioned with corner void pads of 2-in. Minicel. This model had the general form:

$$G = C_0 + \sum_{\ell=0}^{1} h^{\ell/2} \sum_{k=0}^{1} \frac{1}{T^{(k+1/2)}} \sum_{j=1}^{3} \theta^j \sum_{i=0}^{2} C_{ijk\ell}(1 - \cos \sigma_s)^i$$

$$+ \sum_{n=1}^{3} \theta^n \sum_{m=0}^{2} C_{mn}(1 - \cos \sigma_s)^m \quad .$$

Out of the 45 terms generated by the previous equation, eight terms were retained using a stepwise regression procedure. Before the general model can be accepted as adequately predicting impact response, it must be validated.

To provide data for validation of the general model, additional drop tests were conducted in the same manner as the original drop tests. These tests were made at the same temperatures and static stress levels as previously, but at only one drop height, 21-in. Twenty-one inches was not one of the original drop heights. The 21-in. data were not utilized in the general model development but are unique data dropped at an intermediate drop height. These data are given in Appendix F.

Identification of Validation Approach

The ultimate test of validity for any model is to assess the ability of the model to predict some parameter, in this case, impact response. Natrella [19] states that "many statisticians, when analyzing an experiment for the purpose of testing a statistical hypothesis, find that they prefer to present results in terms of the appropriate prediction limit." The problem, of course, is that every statistical test cannot be put in the form of a prediction limit. In general, tests that are direct tests of the value of a parameter of the parent population can be expressed in terms of prediction limits.

The choice then is between a significance test which provides a go/no-go decision, or a prediction limit approach which provides much more information. The prediction limit procedure contains information similar to an OC curve, and is intuitively more appealing than a test of significance. If the model value is contained within the prediction limits, it is possible to state that the model has been validated. The width of the prediction interval is a good indication of the firmness of the yes/no conclusion. A great advantage of the prediction limit approach is that the width of the limit is in the same units as the parameter. Consequently, the information is easy to compare with other information already obtained. Thus, the prediction limit approach will be utilized in an attempt to validate both the interior box model and the total box model.

Interior Box Model Validation

The prediction limit method is based upon the premise that the general model is valid if, for selected values of static stress, the general model predicts values within the prediction limits. This method generates predicted peak accelerations for both the individual dynamic cushioning curve (IDCC) and the general model, using the IDCC to establish prediction limits.

Mendenhall and Scheaffer [20] outline an appropriate equation for the development of prediction limits for a second-order equation which can be modified for the interior box situation as follows:

$$PL_{IB} = \hat{y} \pm t_{\alpha/2}\, s \sqrt{1 + [\bar{a}]^T (x^T x)^{-1} [\bar{a}]}$$

where PL_{IB} = interior box prediction limit

$$y = b_0 + b_1 (1 - \cos \sigma_s) + b_2 (1 - \cos \sigma_s)^2$$

$$\bar{a} = \begin{bmatrix} 1 \\ (1 - \cos \sigma_s) \\ (1 - \cos \sigma_s)^2 \end{bmatrix}$$

$$x = \begin{bmatrix} 1 & \left(1 - \cos \sigma_{s_1}\right) & \left(1 - \cos \sigma_{s_1}\right)^2 \\ 1 & \left(1 - \cos \sigma_{s_2}\right) & \left(1 - \cos \sigma_{s_2}\right)^2 \\ \cdot & \cdot & \cdot \\ \cdot & \cdot & \cdot \\ \cdot & \cdot & \cdot \\ 1 & \left(1 - \cos \sigma_{s_n}\right) & \left(1 - \cos \sigma_{s_n}\right)^2 \end{bmatrix} .$$

Any alpha level can be utilized in the equation for the development of prediction limits. However, to be consistent with previous statistical tests, alpha is set at 0.10 for all prediction limit calculations in this work. Prediction limits are calculated at selected static stress levels for the usual combinations of temperature and a drop height of 21-in. The computer program for the interior box validation is given in Appendix G.

Table VI provides a typical example of the computer validation method for a temperature of 20°F. It should be noted that the static stress values are permitted to continue to 1.538 psi to indicate the general form of the curve beyond the upper data limit of 1.255. The column entitled IDCC represents the predicted peak acceleration based upon the experimental data for a particular temperature and a particular drop height. The upper and lower prediction limits are developed around the IDCC function and are shown in Columns Three and Five. The general model is then given the specific temperature and drop height under consideration, with the general model output given in Column Four. When the general model output is contained within the prediction limits, the general model is capable of predicting peak acceleration response with sufficient accuracy to be utilized in actual practice.

As can be seen from Table VI, the values calculated by the general model fall within the developed prediction limits. In fact, at the point of maximum cushioning (approximately 1.07 psi), the IDCC and the model predict within 2.65 G's of each other. Similar results are noted for the other five temperatures as shown in Table VII. In five of the six cases, the general

Table VI. Prediction Limit Validation for Interior Box at 20°F and a 21-in. Drop Height

Static Stress (psi)	Acceleration (G)			
	IDCC	Lower-P	Model	Upper-P
0.088	49.60	36.03	45.17	63.16
0.138	49.00	35.52	44.75	62.48
0.188	48.15	34.78	44.16	61.53
0.238	47.07	33.82	43.40	60.32
0.288	45.77	32.65	42.49	58.89
0.338	44.28	31.28	41.44	57.28
0.388	42.62	29.73	40.27	55.52
0.438	40.83	28.01	39.01	53.65
0.488	38.94	26.15	37.67	51.72
0.538	36.98	24.19	36.27	49.77
0.588	35.00	22.17	34.85	47.83
0.638	33.03	20.13	33.44	45.93
0.688	31.12	18.12	32.05	44.12
0.738	29.31	16.20	30.73	42.41
0.788	27.65	14.44	29.49	40.85
0.838	26.17	12.88	28.38	39.46
0.888	24.93	11.59	27.41	38.27
0.938	23.96	10.61	26.62	37.32
0.988	23.31	9.97	26.04	36.66
1.038	23.02	9.70	25.68	36.33
1.088	23.11	9.80	25.58	36.42
1.138	23.63	10.27	25.76	37.00
1.188	24.61	11.05	26.24	38.17
1.238	26.07	12.09	27.04	40.05
1.288	28.04	13.33	28.17	42.74
1.338	30.52	14.69	29.64	46.35
1.388	33.55	16.15	31.47	50.95
1.438	37.12	17.67	33.66	56.56
1.488	41.24	19.27	36.21	63.20
1.538	45.90	20.95	39.12	70.85

Table VII. Summary of Interior Box Prediction Limit Validation Results

Temperature (°F)	General Model Within Prediction Limits	Prediction Δ at Maximum Cushioning Level (G's)
-65	Yes	-0.05
-20	Yes	5.34
20	Yes	2.56
70	Yes	6.82
110	Yes	4.12
160	Yes	1.37

model predicted higher than the IDCC, providing for a conservative prediction of the cushioning ability of the particular material under the specified conditions. The remaining case (-. °F) indicated an optimistic prediction for the model. In cushion design it is desirable to predict in the conservative direction rather than in the optimistic direction. In general, the results presented in Table VII are very acceptable.

Total Box Model Validation

The total box model validation is somewhat less complicated than the interior box model validation. The primary difference between the two models is that the interior box model is quadratic while the total box model is linear. Consequently, the total box model prediction limits are acquired from the first-order equation modified as follows:

$$PL_{TB} = \hat{y} \pm t_{\alpha/2}\, s \sqrt{1 + [\bar{a}]^T (x^T x)^{-1} [\bar{a}]}$$

where PL_{TB} = total box prediction limit

$$\hat{y} = b_0 + b_1 W$$

$$\bar{a} = \begin{bmatrix} 1 \\ W \end{bmatrix}$$

$$x = \begin{bmatrix} 1 & W_1 \\ 1 & W_2 \\ \cdot & \cdot \\ \cdot & \cdot \\ \cdot & \cdot \\ 1 & W_n \end{bmatrix} .$$

The alpha level utilized for total box validation purposes is 0.10. The computer program for total box validation is given in Appendix H.

Table VIII provides a typical example of the prediction limits for a temperature of 20°F. The weight range for the total box is from 55.13 to 61.31 lb. Consequently, a weight range of 55 to 61.5 lb, by 0.5-lb increments, was selected for the development of prediction limits.

As can be seen in Table VIII, the individual total box line (ITBL) ranges from 144 G's at 55 lb to 164 G's at 61.5 lb. Over the same weight range, the total box model predicts values of 158 to 177 G's. The slope of both linear equations is noted to be positive which appears to be intuitively

Table VIII. Prediction Limit Validation for Total Box at 20°F and a 21-in. Drop Height

Weight (lb)	Acceleration (G)			
	ITBL	Lower	Model	Upper
55.00	143.95	29.68	157.99	258.23
55.50	145.44	34.08	159.48	256.80
56.00	146.93	38.16	160.98	255.71
56.50	148.42	41.89	162.47	254.96
57.00	149.92	45.24	163.96	254.59
57.50	151.41	48.20	165.46	254.62
58.00	152.90	50.74	166.95	255.05
58.50	154.39	52.86	168.45	255.91
59.00	155.88	54.55	169.94	257.21
59.50	157.37	55.80	171.44	258.93
60.00	158.86	56.82	172.93	261.09
60.50	160.35	57.02	174.42	263.68
61.00	161.84	57.01	175.92	266.67
61.50	163.33	56.60	177.41	270.06

correct, since a heavier falling item is expected to impact a rigid surface with more G's than a lighter falling item. It is also noted that the model values fall within the prediction limits associated with the ITBL for this particular case. In a similar fashion, the model values for the remaining five cases all fall within their respective prediction limits.

Table IX further substantiates the intuitive feeling expressed in the previous paragraph. The slope for all six ITBL equations is positive, indicating that G's increase as a function of increased weight. Table X presents the peak acceleration ranges for the ITBL and the model for the six different

Table IX. Regression Coefficients for ITBL for 21-in. Drop Height

Temperature (°F)	Coefficient	
	b_0	b_1
-65	-195.04	6.14
-20	-49.02	3.30
20	-20.00	2.98
70	-235.70	6.27
110	65.21	1.63
160	-51.44	3.46

Table X. Model and ITBL G-level Ranges for 21-in. Drop Height

Temperature (°F)	ITBL	Model
-65	142.85 — 185.85	135.60 — 153.66
-20	132.43 — 155.52	149.64 — 169.50
20	143.96 — 164.83	157.99 — 178.91
70	108.92 — 152.78	161.55 — 182.92
110	154.67 — 166.05	157.82 — 178.71
160	139.09 — 163.33	143.46 — 162.52

temperature levels. All six cases are noted to exhibit the expected near parallel line phenomenon, that is, the two lines are nearly parallel and do not intersect over the data range. Also, in five of the six cases, the model predicts higher peak accelerations than the ITBL, resulting in conservative designs. The only case in which this is not true is for -65°F. Since this case is at one

of the temperature extremes, it is possible that an unidentified physical phenomenon is taking place. However, a more plausible explanation is that erratic observations due to uneven drops have caused a distortion in the data for this one temperature. It should be noted that a similar situation exists for the interior box at -65°F, resulting in optimistic designs.

Thus, the validation for the total box model has shown that all model predictions are within the specified prediction limits. Hence, it is believed that the total box model is an adequate means to predict peak acceleration for intermediate temperature and drop height requirements for a total box possessing similar weight and size characteristics.

CHAPTER VII. RESEARCH FINDINGS

In Chapter V two general impact response models were developed, one for the interior box and one for the total box. Validation of these two general models was accomplished in Chapter VI. This Chapter will demonstrate the areas in which these two models may be utilized.

Integration of the Two General Models

As previously noted, the interior box general model prediction of peak acceleration is a function of static stress, temperature, drop height, and cushion thickness. The total box general model prediction of peak acceleration is a function of weight, temperature, and drop height. It is desirable to view the two general models as an integrated pair, in which the interior box general model is a subset of the total box general model. Then, it is possible to isolate the shock absorption capabilities of the cushioning material by taking the difference between the total box model results and the interior box model results for selected values of static stress.

Since the two models were developed with different (but related) parameters, to achieve compatibility it is necessary to utilize the basic equation:

$$\sigma_s = \frac{W}{A}$$

where

σ_s = an interior box static stress value

W = weight of the total box

A = footprint of the total box.

The footprint of the total box is the surface area of that portion which makes contact with the rigid surface. The experimental total boxes possessed surface areas of 172.5 $in.^2$. Since the weight range of the experimental boxes was from 55 to 61.5 lb, substitution of these values in the previous equation gives the range of static stress values for comparison purposes.

Utilizing the 21-in. validation data as an example (Tables XI through XVI), it is observed that the interior box has not reached the optimum loading point at any temperature level. The optimum point would be an inflection point on the curve plotted from the interior box column. In fact, the interior box peak accelerations are decreasing slightly with increases in total box weight. Furthermore, in each case the cushion still possesses sufficient ability to absorb most of the increase in peak acceleration which occurs as a function of increased weight. As expected, the total box peak accelerations continue to increase as a function of increased total box weight. The computer code utilized to develop Tables XI through XVI is contained in Appendix I.

Table XI. Integrated Confined Model Data for -65°F and a 21-in. Drop Height

Box Weight (lb)	Acceleration (G)		
	Total Box	Interior Box	Cushion
55.00	135.59	41.38	94.20
55.50	136.88	41.33	95.55
56.00	138.17	41.27	96.90
56.50	139.46	41.21	98.25
57.00	140.75	41.15	99.60
57.50	142.04	41.09	100.94
58.00	143.33	41.03	102.29
58.50	144.62	40.97	103.64
59.00	145.91	40.91	105.00
59.50	147.20	40.85	106.35
60.00	148.49	40.79	107.70
60.50	149.78	40.73	109.05
61.00	151.07	40.67	110.40
61.50	152.37	40.61	111.75

Table XII. Integrated Confined Model Data for -20°F and a 21-in. Drop Height

Box Weight (lb)	Acceleration (G)		
	Total Box	Interior Box	Cushion
55.00	149.64	42.27	107.37
55.50	151.06	42.20	108.85
56.00	152.47	42.14	110.33
56.50	153.89	42.08	111.81
57.00	155.31	42.02	113.29
57.50	156.73	41.96	114.77
58.00	158.15	41.89	116.25
58.50	159.57	41.83	117.73
59.00	160.98	41.77	119.21
59.50	162.40	40.70	120.70
60.00	163.82	41.64	122.18
60.50	165.24	41.57	123.66
61.00	166.66	41.51	125.15
61.50	168.07	41.44	126.63

Table XIII. Integrated Confined Model Data for 20°F and a 21-in. Drop Height

Box Weight (lb)	Acceleration (G)		
	Total Box	Interior Box	Cushion
55.00	157.99	41.85	116.13
55.50	159.48	41.79	117.69
56.00	160.98	41.73	119.24
56.50	162.47	41.67	120.80
57.00	163.96	41.60	122.36
57.50	165.46	41.54	123.92
58.00	166.95	41.47	125.47
58.50	168.45	41.41	127.03
59.00	169.94	41.35	128.59
59.50	171.44	41.28	130.15
60.00	172.93	41.21	131.71
60.50	174.42	41.15	133.27
61.00	175.92	41.08	134.83
61.50	177.41	41.02	136.39

Table XIV. Integrated Confined Model Data for 70°F and a 21-in. Drop Height

Box Weight (lb)	Acceleration (G)		
	Total Box	Interior Box	Cushion
55.00	161.55	39.65	121.89
55.50	163.07	39.59	123.48
56.00	164.60	39.54	125.06
56.50	166.13	39.48	126.65
57.00	167.65	39.42	128.23
57.50	169.18	39.36	129.82
58.00	170.71	39.30	131.41
58.50	172.23	39.23	132.99
59.00	173.76	39.17	134.58
59.50	175.29	39.11	136.17
60.00	176.81	39.05	137.76
60.50	178.34	38.99	139.35
61.00	179.86	38.92	140.94
61.50	181.39	38.86	142.52

Table XV. Integrated Confined Model Data for 110°F and a 21-in. Drop Height

Box Weight (lb)	Acceleration (G)		
	Total Box	Interior Box	Cushion
55.00	157.81	36.47	121.33
55.50	159.30	36.42	122.88
56.00	160.80	36.37	124.42
56.50	162.29	36.32	125.97
57.00	163.78	36.26	127.51
57.50	165.27	36.21	129.06
58.00	166.77	36.16	130.60
58.50	168.26	36.10	132.15
59.00	169.75	36.05	133.70
59.50	171.24	36.00	135.24
60.00	172.74	35.94	136.79
60.50	174.23	35.88	138.34
61.00	175.72	35.83	139.89
61.50	177.21	35.77	141.43

Table XVI. Integrated Confined Model Data for 160°F and a 21-in. Drop Height

Box Weight (lb)	Acceleration (G)		
	Total Box	Interior Box	Cushion
55.00	143.45	30.63	112.82
55.50	144.81	30.59	114.22
56.00	146.18	30.55	115.62
56.50	147.54	30.51	117.02
57.00	148.90	30.48	118.42
57.50	150.26	30.44	119.82
58.00	151.62	30.40	121.22
58.50	152.99	30.36	112.62
59.00	154.35	30.32	124.02
59.50	155.71	30.28	125.42
60.00	157.07	30.24	126.83
60.50	158.43	30.20	128.23
61.00	159.79	30.16	129.63
61.50	161.16	30.12	131.03

Temperature Effects

Perhaps the most significant finding of this research effort is the column entitled "Cushion" in Tables XI through XVI. Heretofore, the actual peak acceleration absorbed by a cushion as a function of weight and temperature has never been calculated. Consequently, Figure 19 illustrates the effect of temperature upon the interior box cushion as a function of total box weight. It should be noted that the Minicel cushion performs well at the lowest temperature, -65°F. This low temperature phenomenon is not common to all cushioning materials, but indicates some unique characteristics for the Minicel material. Further observation indicates that the Minicel material performs better, from a cushioning standpoint, at approximately 70°F.

This phenomenon may be due to the closed cell construction of the foam itself. Minicel is composed of tiny closed cells in which air is entrapped. Compressing the closed cell is comparable to compressing a balloon. Two factors in the construction of the cell which contribute to the cushioning ability of the foam material are the entrapped air and the walls of the cell. As the foam material is cooled, the air contracts and causes the cell to be compressed even though the cell walls are somewhat rigid from the cold temperature. At the higher temperatures, the walls of the cell become softer and are able to be compressed with less force than at lower temperatures. At the very low temperatures the contraction of air is a factor and at higher temperatures the flexibility of the cellular walls is a cushioning factor [21].

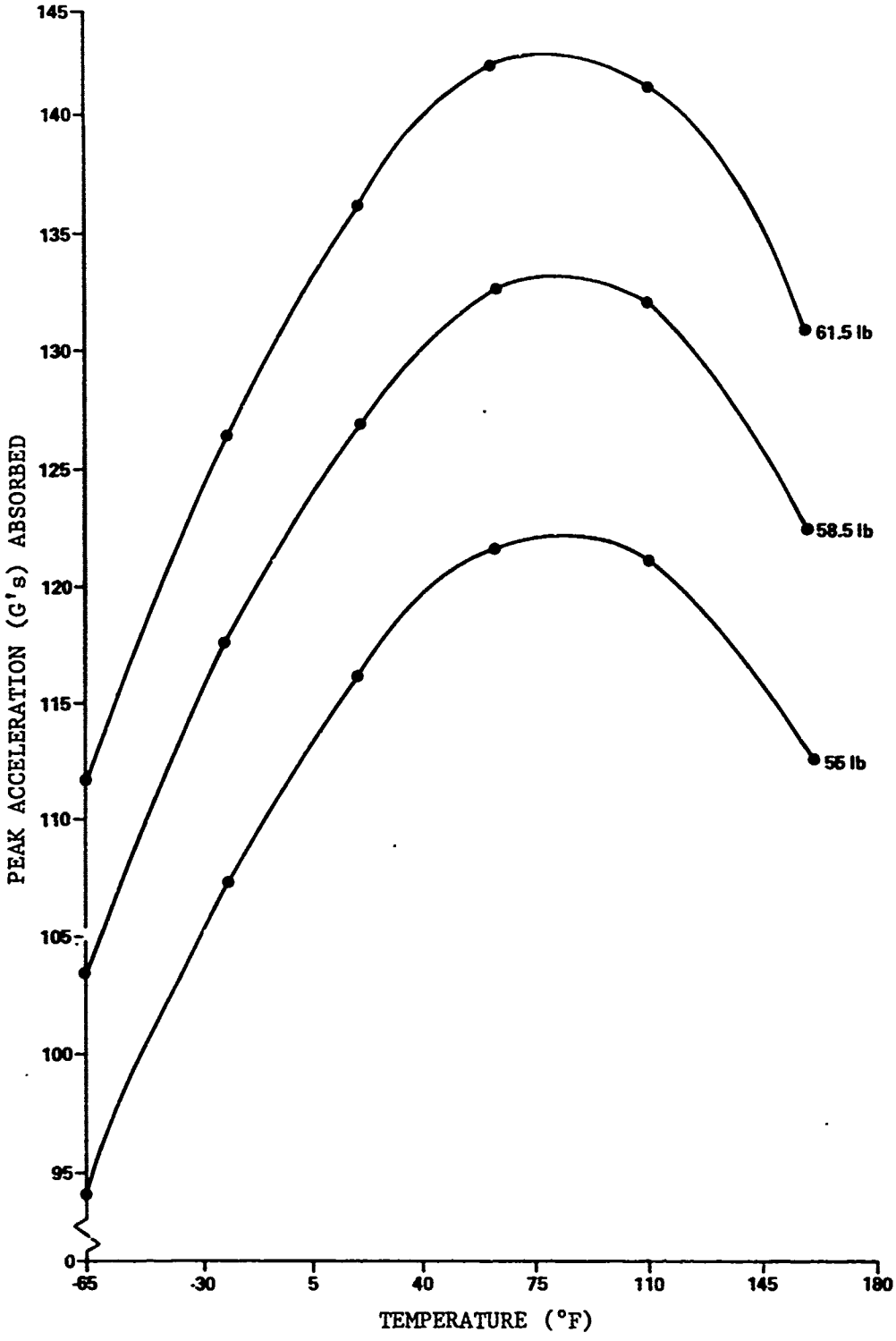

Figure 19. Cushion absorption as a function of temperature and total box weight for a 21-in. drop height.

Figure 20 illustrates the effect of temperature upon the interior box peak accelerations. It is evident that the total box weight has a much smaller effect than temperature. Furthermore, the interior box experiences the greatest peak acceleration near -20°F, and the smallest peak accelerations at the high temperature extreme, 160°F.

Figure 21 depicts the total box peak accelerations as a function of temperature. In this situation, the outside container is seen to be affected by the different temperature levels, which means the wooden construction serves as a better shock absorber at the cold and hot extremes than at ambient temperature. The wood is considered to be a closed cell composite [20]. As a closed cell material it undergoes changes as the temperature varies.

One additional effect of temperature is observed when the data for a particular item weight from Tables XI through XVI is selected. A summary of these data is provided in Table XVII for a 55-lb item. The development of an additional column in Table XVII which gives the percent of total box G's absorbed by the cushion reveals that the Minicel cushion performs best at the highest temperature, 160°F. It is noted that at the low temperature, -65°F, the cushion absorbs 69% of the total box G's available increasing slowly until a level of 79% is achieved at 160°F. Hence, the cushion absorbs considerably more of the available shock at the higher temperature than at the lower temperatures. Similar results in cushion absorption occur for varying item weights.

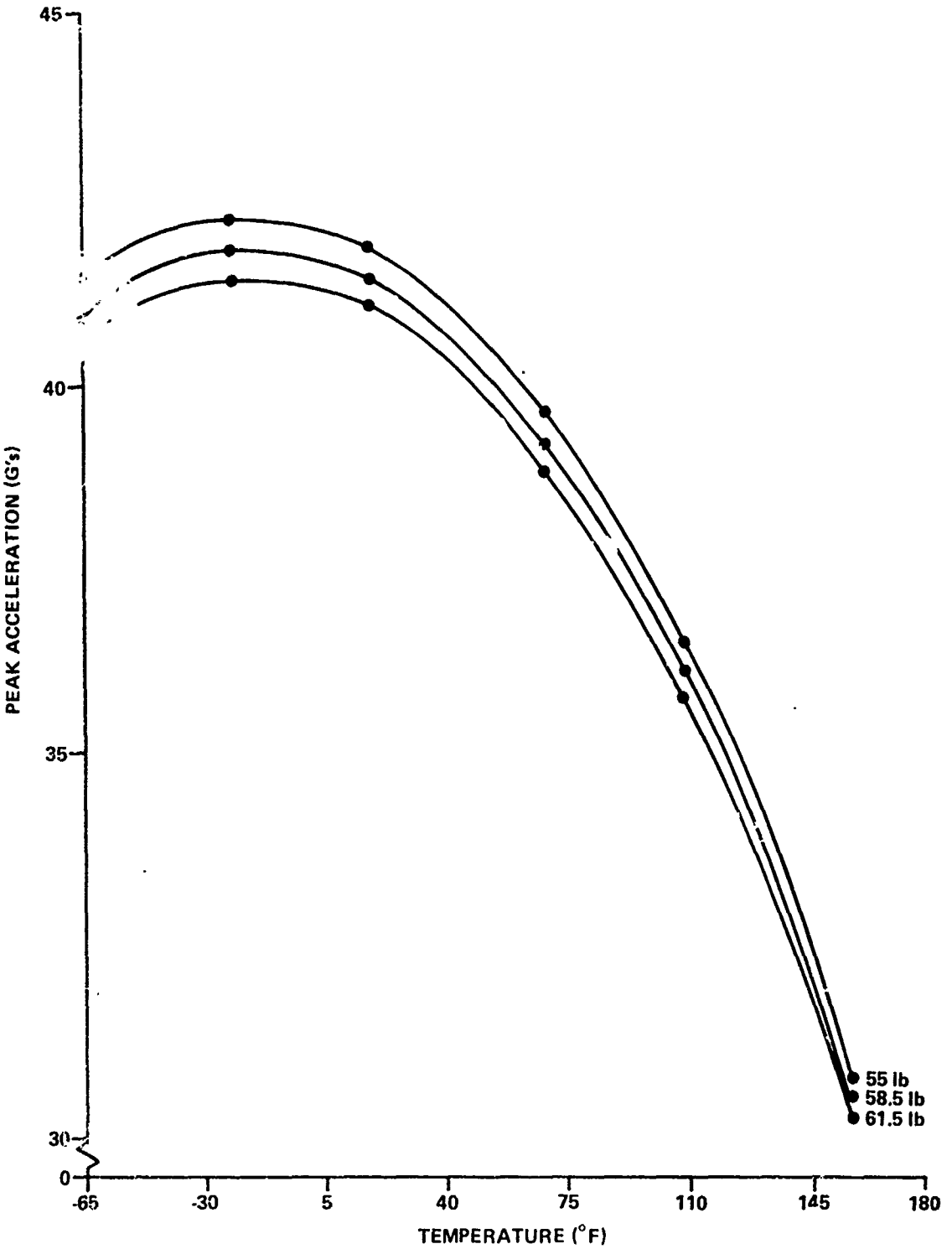

Figure 20. Interior box peak accelerations as a function of temperature and total box weight for a 21-in. drop height.

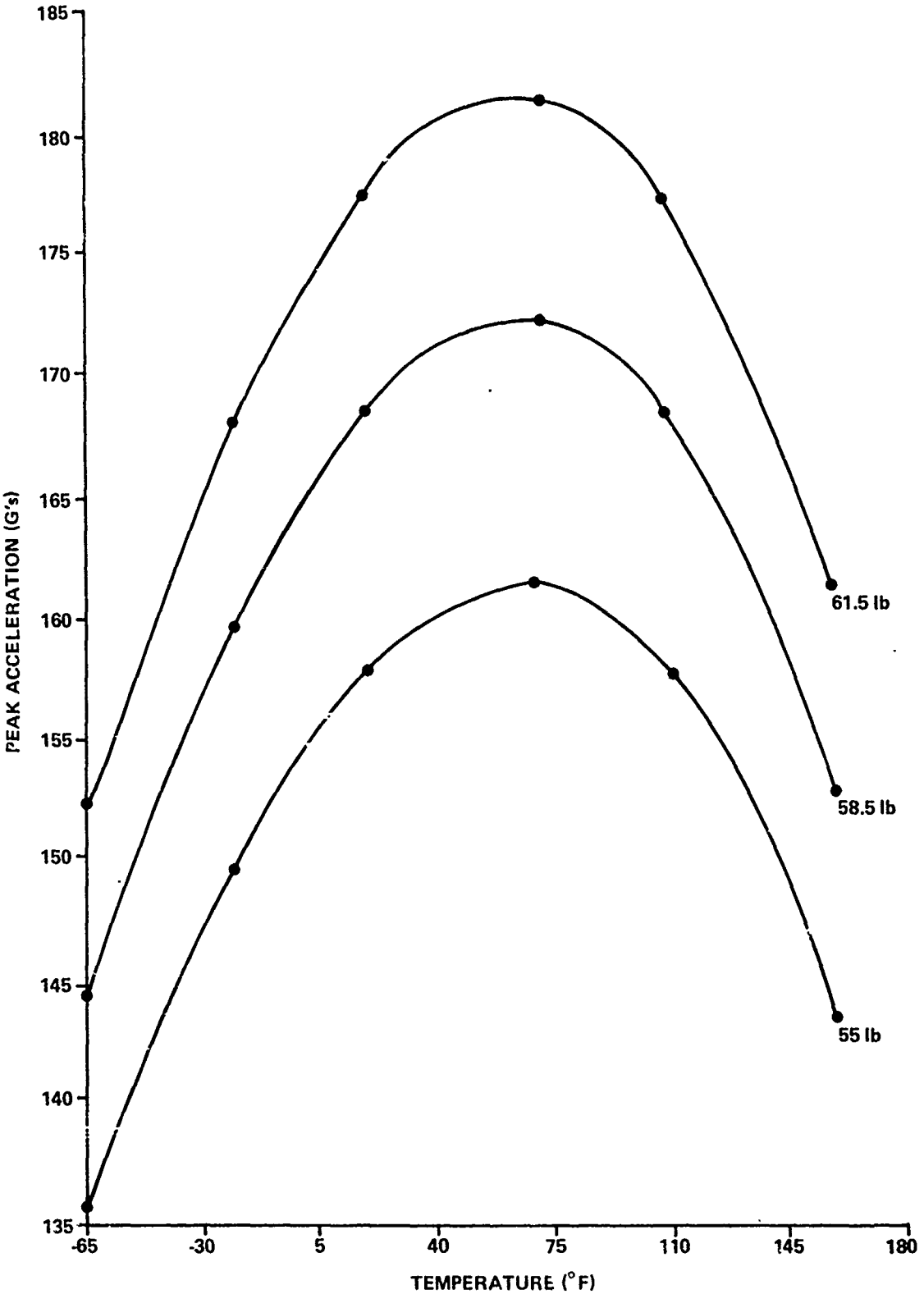

Figure 21. Total box peak accelerations as a function of temperature and total box weight at a 21-in. drop height.

Table XVII. Cushion Absorption Percentage as a Function of Temperature for a Selected Item Weight and a 21-in. Drop Height

Temperature	Acceleration (G)			Percent of G's Absorbed
	Total Box	Interior Box	Absorbed by Cushion	
-65	136	41	94	69
-20	150	42	107	71
20	158	42	116	73
70	162	40	122	75
110	158	36	121	77
160	143	31	113	79

Confined Versus Unconfined Comparisons

It is generally accepted that designing cushioning systems from unconfined (flat pad) drop tests will result in conservative (too much cushion) designs. The problem has been that the magnitude of conservatism which was experienced was unknown. Consequently, knowledgeable cushioning system designers continue to utilize the best source currently available (i.e., unconfined data).

The results of this research permit a comparison between confined and unconfined test results. As previously noted, McDaniel [10] developed a general Minicel cushioning model based upon unconfined data. Both this research and McDaniel's utilized Minicel cushioning material, with each including the 2-in. thickness. Since both models have generalized the

temperature and drop height parameters, it is possible to compare the unconfined interior box general model results with McDaniel's unconfined general model results.

Typical results are shown in Figures 22 through 24, where it is noted that the unconfined model predicts peak accelerations above the confined model

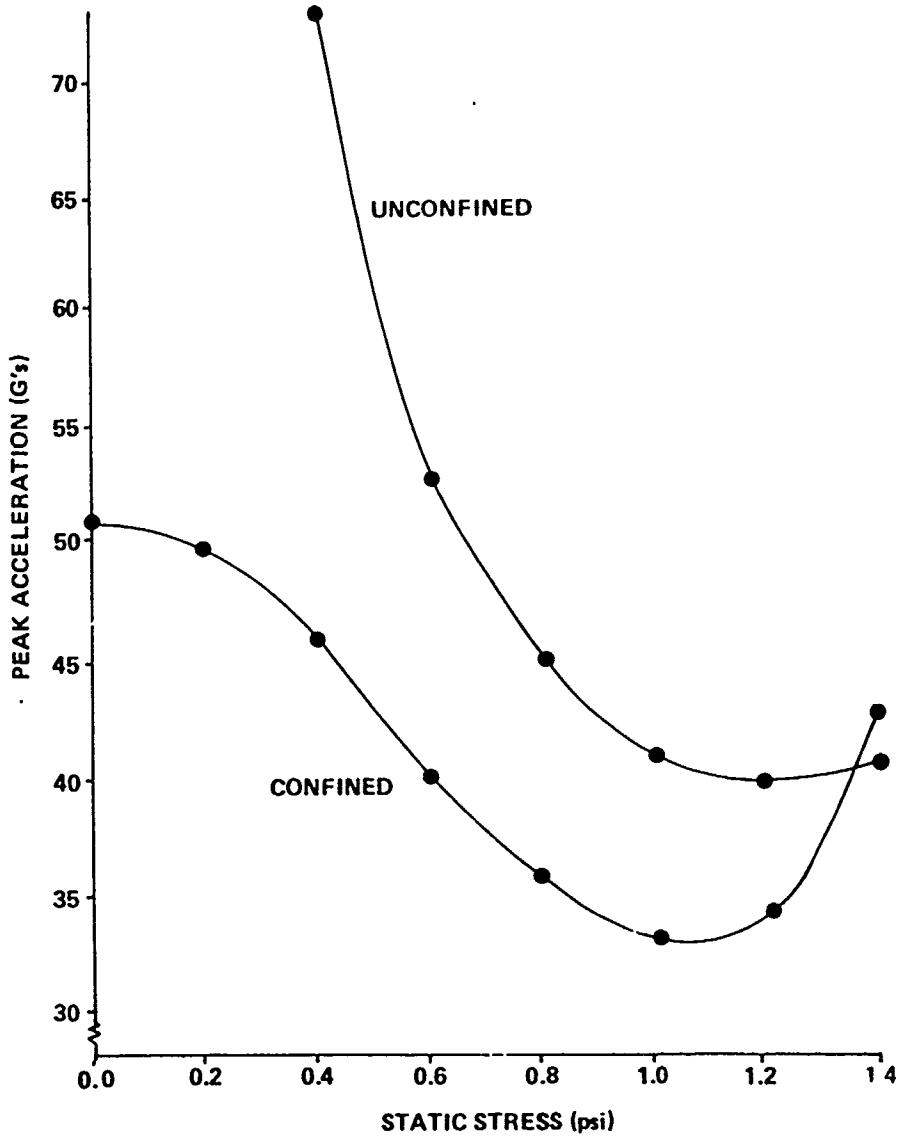

Figure 22. Comparison of confined and unconfined peak accelerations at -65°F with a 30-in. drop height.

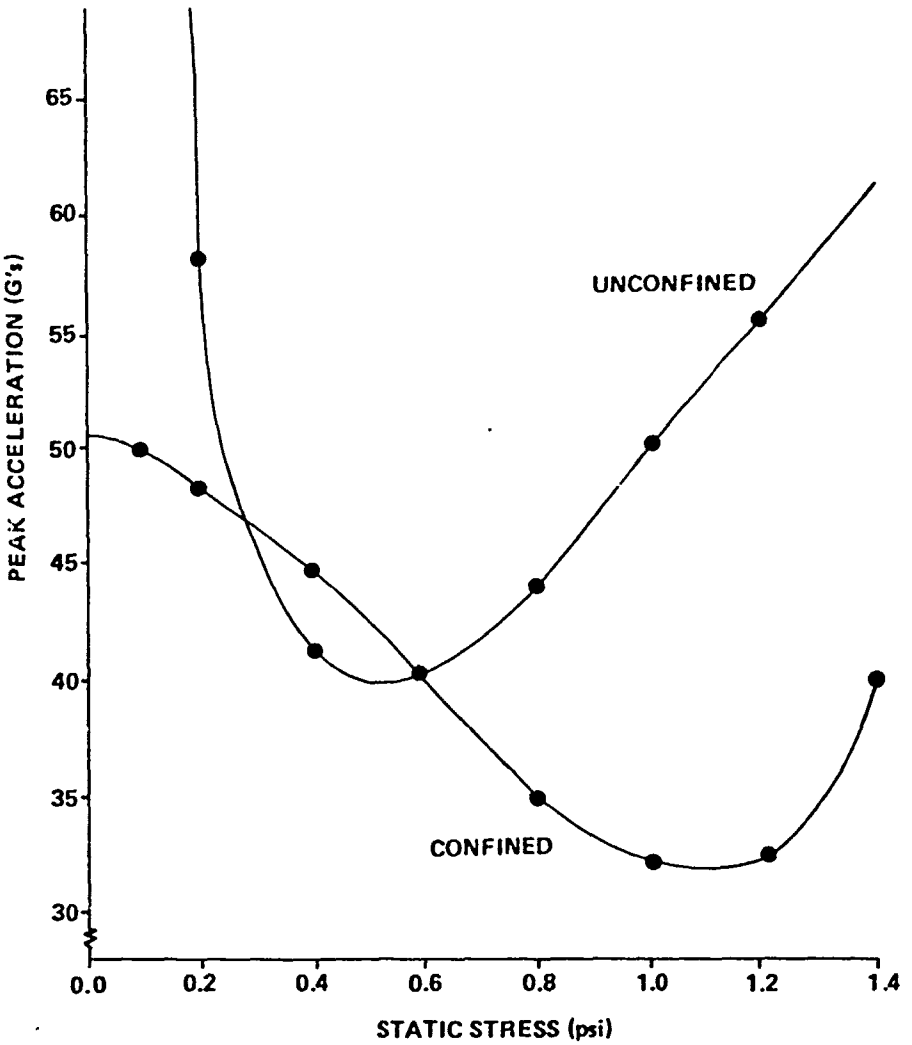

Figure 23. Comparison of confined and unconfined peak accelerations at 70°F with a 30-in. drop height.

when one considers the optimum cushioning point as the confined model minimum. This confirms the original hypothesis that unconfined drop tests result in conservative designs. It is further noted in Figures 22 through 24 that the optimum cushioning point (lowest peak acceleration) does not occur at the same static stress level for the unconfined and confined cases. In fact, when

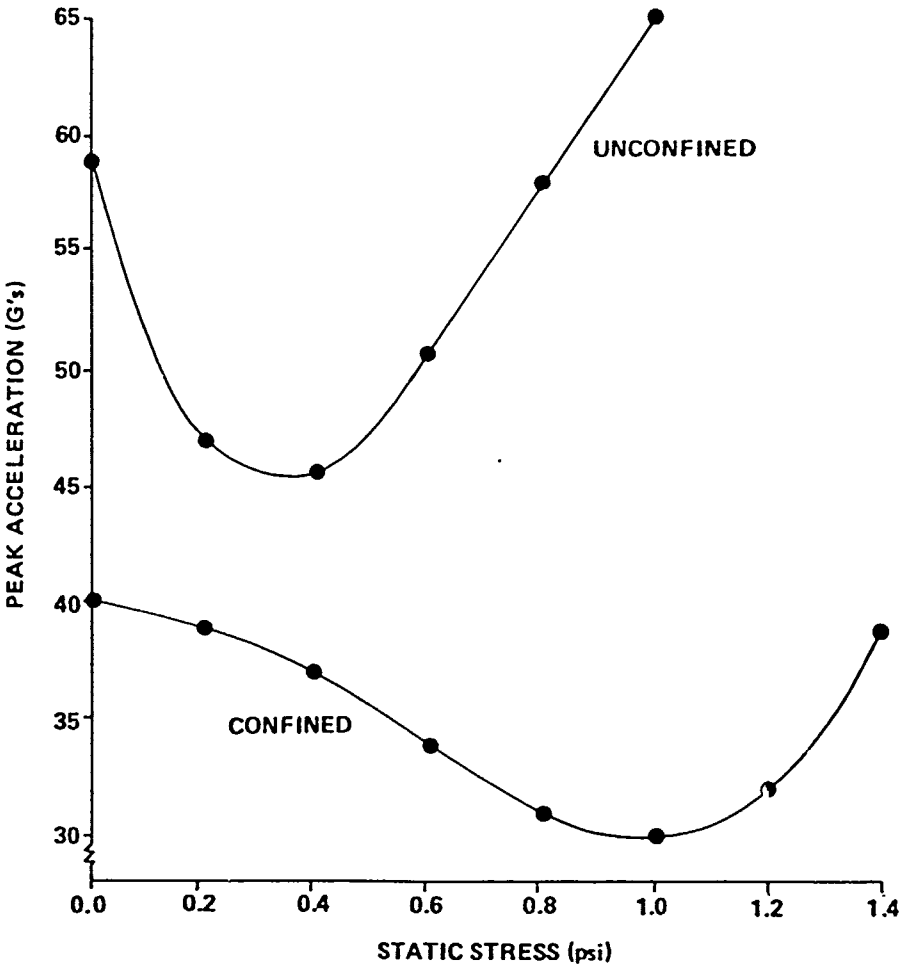

Figure 24. Comparison of confined and unconfined peak accelerations at 160°F with a 30-in. drop height.

the optimum cushioning point for the confined case is to the left of the unconfined point (Figure 22), the two curves intersect to the right of both optimum points. When the confined optimum cushioning point is to the right of the unconfined optimum point, the two curves intersect prior to the confined optimum point (Figure 23).

Table XVIII summarizes the optimum cushioning point at the six standard temperatures for the unconfined and confined cases for a 30-in.

Table XVIII. Summary of Unconfined Versus Confined Peak Acceleration Minimums for a 30-in. Drop Height

Temperature (°F)	Unconfined		Confined	
	Static Stress	G's	Static Stress	G's
-65	1.238	40	1.038	33
-20	0.938	43	0.988	33
20	0.688	42	1.088	32
70	0.538	40	1.088	31
110	0.388	39	1.038	31
160	0.338	44	0.938	30

drop height. For five of the six temperatures, the peak acceleration minimum for the confined case is at a larger static stress value than for the unconfined case. Only at -65°F is the peak acceleration minimum at a lower static stress value for the confined case. Furthermore, irrespective of the temperature or static stress value, the peak acceleration minimums for the confined case are always lower than those for the unconfined case. Hence, once again the conservative nature of the unconfined approach is identified.

One additional point concerning the confined and unconfined general models warrants mentioning. The general models available permit the cushion designer to acquire cushion design information at any desired intermediate drop height value between 12 and 30 in. Similar selections may be exercised for the range of temperature between -65 and 160°F.

Figure 25 is an illustration of the confined and unconfined general models' ability to predict at the drop height value of 20-in. for a temperature of 110°F. The usual phenomena between the two general models are noted.

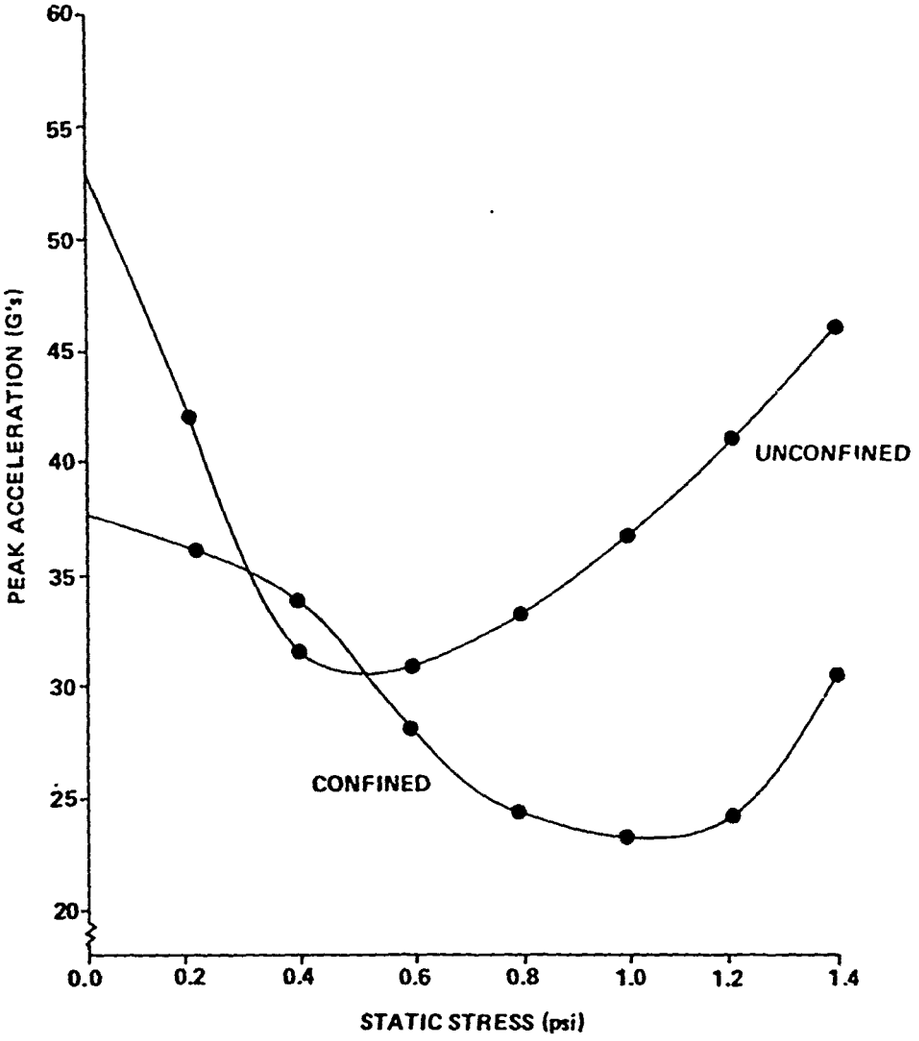

Figure 25. Comparison of unconfined and confined peak accelerations at 110°F with a 21-in. drop height.

CHAPTER VIII. CONCLUSIONS AND RECOMMENDATIONS

The scientific evolvement of cushioning design is beginning to reach fruition. Mindlin's [1] original scientific basis continues to serve as a framework for advances into understanding the phenomena of cushioning. The equations of motion first derived by Mindlin served as a basis for the work contained herein.

This research has resulted in the development of a general mathematical model for a confined cushioning system and a general mathematical model for the exterior container which surrounds the confined corner void configured cushions.

Conclusions

The objective of this research was to develop the methodology for modeling the impact response for the Minicel cushioning material in the unconfined state. This objective was satisfied through the development of an experimental drop test design, conducting an extensive drop test program, and then modeling the resultant test data.

The developed general model portraying the peak accelerations of the confined cushioning system utilizing 2 lb/ft^3 Minicel material is

$$G = C_0 + \sum_{\ell=0}^{1} h^{\ell/2} \sum_{k=0}^{1} \frac{1}{T^{(k+1/2)}} \sum_{j=0}^{1} \theta^j \sum_{i=0}^{1} C_{ijk\ell}(1 - \cos \sigma_s)^i$$

$$+ \sum_{n=1}^{3} \theta^m \sum_{m=0}^{1} C_{mn}(1 - \cos \sigma_s)^m \quad .$$

The model is predicated upon viscoelastic theory and incorporates the effect of drop height, static stress, thickness, and temperature of the cushion upon the peak acceleration of a confined cushioning system. This general model may provide the basic underlying structure of peak acceleration for any of the other bulk cushioning materials utilized in the confined configuration for shock isolation. Utilizing the developed confined Minicel model, it is possible to predict the peak accelerations which the protected item will experience. As expected, considerable disparity exists between the confined and unconfined (McDaniel's research) results for a protected item. It has been known for some time that the unconfined data result in conservative cushioning designs. These confined results provide a measure of this conservatism.

In addition, a general model was developed portraying the peak accelerations experienced by the total container. This model may be stated as

$$G = C_0 + \sum_{\ell=0}^{1} h^{\ell/2} \sum_{j=1}^{3} \theta^j \sum_{i=0}^{1} C_{ij\ell}(W)^i \quad .$$

This model incorporates the effects of drop height, temperature, and total box weight upon the peak acceleration of the total container.

The total container model places the temperature concept in perspective, since it is possible to identify the cushion absorption capability as a function of changing temperatures. Interestingly, the cushion is most effective at the high temperature extreme, which is a unique characteristic of polyethylene cushions.

It is believed that the combination of the two developed models provides the cushioning system designer with another measure of cushion performance to assist in the design of cushioning systems. In particular, the assessment of temperature controlled confined and unconfined cushions provides information unavailable until this time.

Recommendations

Based upon the consistent results obtained in this investigation, it is recommended that additional drop tests be performed to extend these results to other bulk cushioning materials. This would provide the cushioning system designer with a more valid indication of the materials' performance in the confined state.

It also appears reasonable to develop an expanded experimental design which includes containers from the 10-lb range up to 200 lb. This would permit the extension of the total box concept to the entire static stress range ordinarily desired. Perhaps the experimental design could emphasize data compaction between varying box sizes as a means to reduce the voluminous data problem.

The testing of containers in a controlled temperature environment is very costly. However, based upon the significant temperature results obtained by McDaniel, and the drop tests conducted in this research, it is recommended that any additional confined cushioning testing include the minimum six temperatures utilized in this work.

It is also possible that the general methodology provided in this research effort may be applicable to a relatively recent approach to cushioning, which involves a material in the form of bubbles in which air is entrapped. Since little is known about these bubbled cushioning materials' performance in the unconfined state, perhaps it would be best to progress to the confined state immediately. The methodology is now available to make this analysis, if the cushioning system designer desires.

REFERENCES

1. Mindlin, R. D., "Dynamics of Package Cushioning," Bell System Technical Journal, 25, pp. 353-67, July-October, 1945.

2. Masel, Marvin, "A Mathematical Approach to Cushioning," Modern Packaging, 26, No. 9, pp. 133-135, May, 1953.

3. Gretz, John L., "Engineering a Cushioned Package," Modern Packaging, 25, No. 8, pp. 129-133, April, 1952.

4. Janssen, R. R., A Method for the Proper Selection of a Package Cushion Material and its Dimensions, North American Aviation, Los Angeles, California, Report NA-51-1004, 1952.

5. Kerstner, O. S., General Principles of Package Design, Part I — Cushioning, Northrop Aircraft, Inc., Hawthrone, California, Report NAI-57-187, February, 1957.

6. Stern, R. K., "Selecting Package Cushioning," Modern Packaging, 33, No. 4, pp. 138-145, December, 1959.

7. Hilyard, N. C. and Djiauw, L. K., "Observations on the Impact Behavior of Polyurethane Foams; I. The Polymer Matrix," Journal of Cellular Plastics, pp. 33-42, January-February, 1971.

8. Humbert, W. G. and Hanlon, R. G., "Acceleration Versus Static-Stress Curves for Polyethylene Foam," Package Engineering, pp. 158-162, April, 1962.

9. McDaniel, D. M. and Wyskida, R. M., "The Development of a Generalized Impact Response Model for a Bulk Cushioning Material," The Shock and Vibration Bulletin, pp. 131-144, August, 1976.

10. McDaniel, D. M., Modeling the Impact Response of Bulk Cushioning Materials, US Army Missile Command, Redstone Arsenal, Alabama, Report No. RD-75-16, 1975.

11. Wyskida, R. M., Johannes, J. D. and Wilhelm, M. R., Container Cushioning Design Engineer Users Manual (HP-9810A Version), The University of Alabama in Huntsville, Huntsville, Alabama, UAH Research Report No. 187, II, October, 1976.

12. Grabowski, T. J., "Design and Evaluation of Packages Containing Cushioning Items, Using Peak Acceleration Versus Static Stress Data," The Shock and Vibration Bulletin, pp. 76-86, February, 1962.

13. Mazzei, J. H., A Comparison Study: Confined vs. Unconfined Test Data, Report FRL-TR-45, Picatinny Arsenal, Dover, New Jersey, September, 1961.

14. Flugge, W., Viscoelasticity, 2nd ed., Springer-Verlag, New York, 1975.

15. Fowles, G. R., Analytical Mechanics, Holt, Rinehart and Winston, New York, 1962.

16. Schapery, R. A., "Approximate Methods of Transform Inversion for Viscoelastic Stress Analysis," Proceedings of the 4th U. S. National Congress of Applied Mechanics, pp. 1075-85, 1962.

17. Cost, Thomas L., Dynamic Response of Container and Container Cushion Structures, Athena Engineering Company, Northport, Alabama, Technical Report No. 74-003, October 1974.

18. Draper, N. R. and Smith, H., Applied Regression Analysis, John Wiley & Sons, New York, 1966.

19. Natrella, M. G., Experimental Statistics, National Bureau of Standards Handbook 91, Washington, D. C., 1966.

20. Mendenhall, W., and Scheaffer, R. L., Mathematical Statistics with Applications, Duxbury Press, North Scituate, Massachusetts, 1973.

21. Otis, D. R., "Thermal Damping in Gas-filled Composite Materials During Impact Loading," American Society of Mechanical Engineers, Transactions, Series E, Journal of Applied-Mechanics, 37, pp. 38-43, March 1970.

APPENDIX A. INTERIOR BOX PEAK ACCELERATIONS

Table A-1. Original Peak Accelerations with Individual Static Stresses for Interior Box at -65°F

Box Surface	12-in. Drop Height		18-in. Drop Height		24-in. Drop Height		30-in. Drop Height		Replicate No.
	Static Stress	G's	Static Stress	G's	Static Stress	G's	Static Stress	G's	
A	0.08864	28.0	0.08444	35.0	0.08318	40.0	0.08318	36.0	1
	0.08570	31.0	0.08822	49.0	0.08360	56.0	0.08864	44.0	2
	0.08444	33.0	0.08906	31.0	0.08570	32.0	0.08549	52.0	3
B	0.24750	33.0	0.25500	44.0	0.24563	29.0	0.24750	45.0	1
	0.26375	33.0	0.26250	32.0	0.26375	28.0	0.24875	85.0	2
	0.25437	30.0	0.25125	55.0	0.23813	30.0	0.25500	55.0	3
C	0.51786	36.0	0.52041	42.0	0.50255	53.0	0.48597	31.0	1
	0.50765	34.0	0.48597	39.0	0.53571	33.0	0.50510	39.0	2
	0.53827	34.0	0.51276	39.0	0.51913	28.0	0.54082	35.0	3
D	0.68229	23.0	0.70486	39.0	0.69792	29.0	0.68750	42.0	1
	0.69097	29.0	0.66146	31.0	0.73264	34.0	0.68750	42.0	2
	0.73264	21.0	0.73611	32.0	0.70660	29.0	0.56146	29.0	3
E	0.81405	23.0	0.84298	30.0	0.81818	38.0	0.81198	26.0	1
	0.87190	24.0	0.86777	27.0	0.82231	31.0	0.81818	37.0	2
	0.84298	23.0	0.84091	32.0	0.83058	41.0	0.83058	35.0	3
F	1.25926	18.0	1.22222	27.0	1.24074	25.0	1.25309	36.0	1
	1.30247	18.0	1.29630	27.0	1.17593	36.0	1.17593	33.0	2
	1.30247	21.0	1.25926	25.0	1.25617	37.0	1.22222	33.0	3

Table A-2. Original Peak Accelerations with Individual Static Stresses for Interior Box at -20°F

Box Surface	12-in. Drop Height		18-in. Drop Height		24-in. Drop Height		30-in. Drop Height		Replicate No.
	Static Stress	G's	Static Stress	G's	Static Stress	G's	Static Stress	G's	
A	0.08759	47.0	0.08234	39.0	0.08843	89.0	0.08402	61.0	1
	0.08675	65.0	0.08906	42.0	0.08465	58.0	0.08801	68.0	2
	0.08549	31.0	0.08633	40.0	0.08780	64.0	0.08234	63.0	3
B	0.25000	41.0	0.26063	41.0	0.26250	57.0	0.26313	46.0	1
	0.26188	39.0	0.24750	40.0	0.25188	67.0	0.23813	45.0	2
	0.24563	44.0	0.25438	41.0	0.26125	69.0	0.26250	33.0	3
C	0.53189	32.0	0.51020	39.0	0.53699	40.0	0.50000	52.0	1
	0.51403	32.0	0.50510	37.0	0.54082	41.0	0.48597	56.0	2
	0.50510	30.0	0.52423	39.0	0.53571	37.0	0.51913	53.0	3
D	0.68056	24.0	0.69444	29.0	0.72917	32.0	0.73090	35.0	1
	0.68229	21.0	0.68750	29.0	0.71701	32.0	0.72743	37.0	2
	0.71354	23.0	0.68750	31.0	0.70660	34.0	0.72569	37.0	3
E	0.86983	17.0	0.81818	23.0	0.86157	31.0	0.78719	37.0	1
	0.87603	19.0	0.85331	23.0	0.86777	31.0	0.86570	35.0	2
	0.86364	18.0	0.84091	24.0	0.81818	30.0	0.84917	34.0	3
F	1.20988	22.0	1.23456	25.0	1.28704	25.0	1.17593	34.0	1
	1.29321	24.0	1.30864	26.0	1.27469	25.0	1.24383	33.0	2
	1.21296	21.0	1.22222	24.0	1.29630	27.0	1.25617	36.0	3

Table A-3. Original Peak Accelerations with Individual Static Stresses for Interior Box at 20°F

Box Surface	12-in. Drop Height		18-in. Drop Height		24-in. Drop Height		30-in. Drop Height		Replicate No.
	Static Stress	G's	Static Stress	G's	Static Stress	G's	Static Stress	G's	
A	0.08822	41.0	0.08003	31.0	0.08255	29.0	0.08318	54.0	1
	0.08360	27.0	0.08549	25.0	0.08528	79.0	0.08864	48.0	2
	0.08570	49.0	0.08003	36.0	0.08444	36.0	0.08276	69.0	3
B	0.24750	32.0	0.26250	44.0	0.25125	50.0	0.24563	60.0	1
	0.24875	30.0	0.26375	48.0	0.25375	49.0	0.25437	57.0	2
	0.26500	41.0	0.23813	29.0	0.25500	41.0	0.25125	46.0	3
C	0.53571	31.0	0.48597	26.0	0.48597	47.0	0.50128	51.0	1
	0.50765	66.0	0.51786	37.0	0.53827	43.0	0.51913	43.0	2
	0.51276	35.0	0.50255	33.0	0.54082	39.0	0.52041	43.0	3
D	0.68750	24.0	0.66146	30.0	0.68229	27.0	0.69792	31.0	1
	0.68750	24.0	0.69097	33.0	0.73264	35.0	0.70660	30.0	2
	0.73611	24.0	0.66146	25.0	0.69792	30.0	0.68403	39.0	3
E	0.81198	13.0	0.81818	24.0	0.86777	26.0	0.78719	29.0	1
	0.83884	18.0	0.87190	30.0	0.82231	33.0	0.83058	26.0	2
	0.82231	14.0	0.78719	25.0	0.87603	33.0	0.84298	31.0	3
F	1.21296	18.0	1.17593	26.0	1.22222	26.0	1.29630	41.0	1
	1.22840	18.0	1.25617	27.0	1.25309	23.0	1.30247	42.0	2
	1.25926	18.0	1.24074	25.0	1.30864	34.0	1.24074	23.0	3

Table A-4. Original Peak Accelerations with Individual Static Stresses for Interior Box at 70°F

Box Surface	12-in. Drop Height		18-in. Drop Height		24-in. Drop Height		30-in. Drop Height		Replicate No.
	Static Stress	G's	Static Stress	G's	Static Stress	G's	Static Stress	G's	
A	0.08402	52.0	0.08234	64.0	0.08843	70.0	0.08318	75.0	1
	0.08465	34.0	0.08906	45.0	0.08003	78.0	0.08801	55.0	2
	0.08633	26.0	0.08318	39.0	0.08549	37.0	0.08780	72.0	3
B	0.26063	23.0	0.24500	37.0	0.23813	41.0	0.26313	44.0	1
	0.26187	33.0	0.25187	33.0	0.26500	36.0	0.25813	38.0	2
	0.26375	34.0	0.25500	36.0	0.26125	39.0	0.24750	45.0	3
C	0.51020	26.0	0.50000	29.0	0.48597	32.0	0.53189	35.0	1
	0.54082	24.0	0.51403	26.0	0.53444	40.0	0.51276	38.0	2
	0.53827	25.0	0.52041	25.0	0.51913	36.0	0.50510	37.0	3
D	0.70833	19.0	0.68056	36.0	0.69444	35.0	0.69792	31.0	1
	0.71701	20.0	0.72743	36.0	0.73611	31.0	0.69965	32.0	2
	0.71354	21.0	0.72569	28.0	0.68750	33.0	0.70660	36.0	3
E	0.86983	22.0	0.82645	23.0	0.80992	29.0	0.81818	36.0	1
	0.87603	24.0	0.83264	25.0	0.86570	34.0	0.85331	36.0	2
	0.84917	19.0	0.84091	34.0	0.81818	33.0	0.86364	39.0	3
F	1.28704	21.0	1.23457	25.0	1.20988	29.0	1.29938	36.0	1
	1.30864	21.0	1.27469	20.0	1.24383	29.0	1.29321	38.0	2
	1.22222	21.0	1.30247	23.0	1.17593	28.0	1.29012	36.0	3

Table A-5. Original Peak Accelerations with Individual Static Stresses for Interior Box at 110°F

Box Surface	12-in. Drop Height		18-in. Drop Height		24-in. Drop Height		30-in. Drop Height		Replicate No.
	Static Stress	G's	Static Stress	G's	Static Stress	G's	Static Stress	G's	
A	0.08549	20.0	0.08003	28.0	0.08318	67.0	0.08906	38.0	1
	0.08864	21.0	0.08360	21.0	0.08528	58.0	0.08864	36.0	2
	0.08318	25.0	0.08444	26.0	0.08570	52.0	0.08576	35.0	3
B	0.23813	31.0	0.25437	31.0	0.24750	36.0	0.24750	37.0	1
	0.26375	29.0	0.25375	27.0	0.26250	35.0	0.24875	48.0	2
	0.24563	26.0	0.25500	31.0	0.24875	37.0	0.25125	33.0	3
C	0.48597	18.0	0.51913	26.0	0.50510	39.0	0.54082	23.0	1
	0.53571	28.0	0.53827	26.0	0.50765	34.0	0.53827	30.0	2
	0.50255	25.0	0.51276	29.0	0.50128	32.0	0.52041	28.0	3
D	0.66146	17.0	0.70660	29.0	0.73611	34.0	0.68750	20.0	1
	0.70486	12.0	0.72917	27.0	0.69097	25.0	0.73264	33.0	2
	0.68750	14.0	0.70833	16.0	0.68403	38.0	0.68229	26.0	3
E	0.78719	16.0	0.84091	27.0	0.81818	30.0	0.87190	28.0	1
	0.81818	14.0	0.83884	20.0	0.86777	28.0	0.87190	30.0	2
	0.81198	17.0	0.81405	22.0	0.83058	29.0	0.84298	32.0	3
F	1.22222	17.0	1.25617	25.0	1.30247	32.0	1.17593	35.0	1
	1.29630	14.0	1.25309	23.0	1.30247	24.0	1.22840	32.0	2
	1.22222	16.0	1.25926	21.0	1.24074	26.0	1.21296	35.0	3

Table A-6. Original Peak Accelerations with Individual Static Stresses for Interior Box at 160°F

Box Surface	12-in. Drop Height		18-in. Drop Height		24-in. Drop Height		30-in. Drop Height		Replicate No.
	Static Stress	G's	Static Stress	G's	Static Stress	G's	Static Stress	G's	
A	0.08234	39.0	0.08402	44.0	0.08759	39.0	0.08843	57.0	1
	0.08801	37.0	0.08906	39.0	0.08465	31.0	0.08675	48.0	2
	0.08549	28.0	0.08318	55.0	0.08633	24.0	0.08780	61.0	3
B	0.26313	26.0	0.26063	26.0	0.25125	25.0	0.25000	40.0	1
	0.26500	21.0	0.26187	21.0	0.25813	27.0	0.25187	30.0	2
	0.26125	26.0	0.25437	26.0	0.24750	34.0	0.26375	30.0	3
C	0.53699	16.0	0.51020	26.0	0.50000	32.0	0.53189	35.0	1
	0.54082	17.0	0.52679	26.0	0.51403	24.0	0.53444	39.0	2
	0.52041	18.0	0.51913	21.0	0.53827	20.0	0.51276	40.0	3
D	0.73090	19.0	0.72396	20.0	0.70833	22.0	0.68056	39.0	1
	0.69965	16.0	0.71701	25.0	0.73611	23.0	0.72743	36.0	2
	0.72569	15.0	0.70660	28.0	0.71354	25.0	0.68750	36.0	3
E	0.86157	19.0	0.86983	22.0	0.80992	19.0	0.87190	35.0	1
	0.84298	19.0	0.85331	22.0	0.83264	25.0	0.86570	39.0	2
	0.86364	16.0	0.81818	25.0	0.84917	26.0	0.84091	31.0	3
F	1.23457	16.0	1.28704	21.0	1.29938	27.0	1.30247	30.0	1
	1.30864	19.0	1.29321	24.0	1.24383	33.0	1.27469	36.0	2
	1.25617	17.0	1.29012	24.0	1.25926	28.0	1.22222	31.0	3

APPENDIX B. TOTAL BOX PEAK ACCELERATIONS

Table B-1. Individual Weights and Peak Accelerations of Total Boxes at -65°F

Box Surface	12-in. Drop Height		18-in. Drop Height		24-in. Drop Height		30-in. Drop Height		Replicate No.
	Box Weight (lb)	G's	Box Weight (lb)	G's	Box Weight (lb)	G's	Box Weight (lb)	G's	
A	58.7500	72.0	58.7500	170.0	59.2500	202.0	59.2500	144.0	1
	60.1875	130.0	60.7500	162.0	56.7500	159.0	60.1875	180.0	2
	58.1250	222.0*	61.3125	372.0*	58.7500	302.0	58.8750	161.0	3
B	59.2500	77.0	58.7500	128.0	55.1250	116.0	59.2500	122.0	1
	60.1875	99.0	60.7500	144.0	60.1875	126.0	56.7500	76.0	2
	58.8750	59.0	58.1250	94.0	61.3125	223.0	58.7500	99.0	3
C	56.8750	123.0	58.7500	155.0	57.0000	147.0	57.0000	96.0	1
	56.7500	93.0	58.1250	129.0	60.7500	162.0	60.1875	126.0	2
	58.7500	79.0	58.1250	187.0	58.8750	122.0	61.3125	83.0	3
D	60.1875	142.0	58.7500	107.0	58.1250	181.0	59.2500	272.0*	1
	56.7500	74.0	55.1250	142.0	60.1875	174.0	58.1250	201.0	2
	58.7500	79.0	58.7500	152.0	58.8750	247.0	56.8750	151.0	3
E	57.0000	114.0	58.7500	94.0	59.2500	160.0	58.1250	204.0	1
	60.1875	84.0	60.7500	210.0*	56.7500	174.0	61.3125	220.0	2
	58.7500	180.0*	58.8750	115.0	58.1250	168.0	56.8750	156.0	3
F	58.7500	147.0	59.2500	196.0	58.7500	112.0	59.2500	153.0	1
	60.1875	108.0	60.7500	203.0	55.1250	249.0	59.1250	173.0	2
	61.3125	144.0	58.7500	186.0	58.8750	144.0	59.2500	297.0*	3

*Indicates Outlier

Table B-2. Individual Weights and Peak Accelerations of Total Boxes at -20°F

Box Surface	12-in. Drop Height		18-in. Drop Height		24-in. Drop Height		30-in. Drop Height		Replicate No.
	Box Weight (lb)	G's	Box Weight (lb)	G's	Box Weight (lb)	G's	Box Weight (lb)	G's	
A	60.3125	151.0	56.7500	106.0	60.8750	170.0	57.8750	204.0	1
	59.7500	119.0	61.3125	166.0	56.7500	66.0*	60.6250	196.0	2
	58.8750	85.0	59.4375	192.0	60.5000	231.0	57.3125	114.0*	3
B	57.8750	66.0	60.3125	107.0	58.3150	136.0	59.4375	282.0*	1
	60.6250	65.0	58.7500	95.0	58.3150	103.0	55.1250	137.0	2
	58.1250	104.0	58.8750	143.0	60.1875	143.0	60.1875	116.0	3
C	60.3125	152.0	57.8750	197.0	60.8750	140.0	60.6250	157.0	1
	58.3150	72.0	58.7500	146.0	61.3125	175.0	55.1250	131.0	2
	58.1250	87.0	59.4375	100.0	58.8750	200.0	58.8750	145.0	3
D	56.7500	116.0	57.8750	225.0	60.1875	98.0	60.8750	165.0	1
	58.1250	75.0	58.7500	182.0	59.7500	107.0	56.7500	83.0*	2
	59.4375	102.0	57.3125	65.0*	60.1875	136.0	60.5000	244.0	3
E	60.8750	135.0	58.7500	147.0	60.3125	173.0	55.1250	234.0	1
	61.3125	147.0	59.7500	243.0	60.1875	98.0	60.6250	200.0	2
	60.5000	75.0	58.7500	147.0	57.3125	304.0*	60.8750	174.0	3
F	60.8750	135.0	57.8750	156.0	60.3125	106.0	55.1250	135.0	1
	61.3125	147.0	61.3125	154.0	59.7500	167.0	58.3150	120.0	2
	60.5000	75.0	58.7500	129.0	60.1875	124.0	58.8750	178.0	3

*Indicates outlier

Table B-3. Individual Weights and Peak Accelerations of Total Boxes at 20°F

Box Surface	12-in. Drop Height		18-in. Drop Height		24-in. Drop Height		30-in. Drop Height		Replicate No.
	Box Weight (lb)	G's	Box Weight (lb)	G's	Box Weight (lb)	G's	Box Weight (lb)	G's	
A	60.7500	106.0	55.1250	116.0	56.8750	198.0	59.2500	209.0	1
	56.7500	123.0	58.8750	158.0	58.7500	147.0	60.1875	224.0	2
	58.7500	74.0	58.1250	126.0	58.1250	126.0	57.0000	327.0*	3
B	59.2500	153.0	60.7500	131.0	58.1250	107.0	56.8750	126.0	1
	56.7500	99.0	58.1250	116.0	58.7500	88.0	58.8750	121.0	2
	61.3125	59.0	55.1250	98.0	58.7500	128.0	58.1250	163.0	3
C	60.7500	117.0	55.1250	104.0	55.1250	224.0	56.8750	148.0	1
	56.7500	65.0	58.7500	155.0	60.1875	148.0	58.8750	210.0	2
	58.1250	107.0	57.0000	187.0	61.3125	202.0	58.7500	171.0	3
D	59.2500	61.0	55.1250	100.0	56.8750	100.0	58.1250	185.0	1
	59.2500	144.0	56.7500	116.0	60.1875	136.0	58.8750	233.0	2
	61.3125	106.0	58.7500	160.0	58.1250	240.0*	57.0000	219.0	3
E	56.8750	78.0	59.2500	112.0	60.7500	137.0	58.1250	223.0	1
	58.7500	141.0	60.1875	143.0	56.7500	179.0	58.1250	246.0	2
	57.0000	80.0	55.1250	181.0	61.3125	150.0	58.7500	217.0	3
F	56.8750	72.0	55.1250	149.0	59.2500	162.0	60.7500	164.0	1
	56.7500	113.0	58.8750	232.0	58.7500	188.0	60.1875	185.0	2
	58.7500	80.0	60.1875	63.0*	61.3125	253.0	57.0000	150.0	3

*Indicates outlier

Table B-4. Individual Weights and Peak Accelerations of Total Boxes at 70°F

Box Surface	12-in. Drop Height		18-in. Drop Height		24-in. Drop Height		30-in. Drop Height		Replicate No.
	Box Weight (lb)	G's	Box Weight (lb)	G's	Box Weight (lb)	G's	Box Weight (lb)	G's	
A	57.8750	174.0	56.7500	402.0*	60.8750	340.0	59.2500	210.0	1
	58.3150	170.0	61.3125	264.0	55.1250	150.0	60.6250	428.0*	2
	59.4375	278.0	57.3125	128.0	58.8750	270.0	60.5000	254.0	3
B	60.3125	198.0	56.7500	212.0	55.1250	162.0	60.8750	310.0	1
	60.6250	222.0	58.3150	176.0	61.3125	220.0	59.7500	230.0	2
	60.1875	124.0	58.7500	278.0	60.5000	158.0	57.3125	198.0	3
C	57.8750	192.0	56.7500	134.0	55.1250	136.0	60.3125	284.0	1
	61.3150	140.0	60.5000	352.0*	60.6250	262.0	58.1250	286.0	2
	57.3125	142.0	58.7500	158.0	58.8750	280.0	57.3125	224.0	3
D	58.7500	188.0	56.7500	282.0	57.8750	394.0	58.1250	212.0	1
	59.7500	122.0	60.6250	230.0	61.3125	286.0	58.3150	312.0	2
	59.4375	224.0	58.3150	270.0	57.3125	308.0	58.8750	236.0	3
E	60.8750	176.0	57.8750	232.0	56.7500	232.0	59.2500	244.0	1
	61.3125	172.0	58.3150	226.0	60.6250	326.0	59.7500	294.0	2
	59.4375	198.0	58.8750	272.0	57.3125	220.0	60.5000	244.0	3
F	60.3125	212.0	57.8750	272.0	56.7500	264.0	60.8750	158.0	1
	61.3125	286.0	59.7500	216.0	58.3150	360.0	60.6250	520.0*	2
	60.1875	62.0*	58.7500	248.0	55.1250	366.0	60.5000	210.0	3

*Indicates outlier

Table B-5. Individual Weights and Peak Accelerations of Total Boxes at 110°F

Box Surface	12-in. Drop Height		18-in. Drop Height		24-in. Drop Height		30-in. Drop Height		Replicate No.
	Box Weight (lb)	G's	Box Weight (lb)	G's	Box Weight (lb)	G's	Box Weight (lb)	G's	
A	59.2500	138.0	55.1250	93.0	59.2500	130.0	55.1250	196.0	1
	56.7500	256.0*	60.7500	149.0	58.7500	138.0	60.1875	196.0	2
	56.8750	65.0	58.1250	155.0	58.7500	288.0	57.0000	222.0	3
B	55.1250	95.0	60.7500	141.0	56.7500	201.0	61.3125	276.0*	1
	60.1875	174.0	58.7500	102.0	59.2500	154.0	56.7500	79.0	2
	56.8750	82.0	58.7500	104.0	57.0000	133.0	58.1250	85.0	3
C	55.1250	139.0	58.8750	157.0	59.2500	109.0	61.3125	194.0	1
	60.7500	111.0	60.1875	117.0	56.7500	248.0	60.1875	238.0	2
	57.0000	126.0	58.1250	154.0	56.8750	225.0	58.7500	130.0	3
D	55.1250	217.0*	58.8750	213.0	61.3125	123.0	59.2500	181.0	1
	58.7500	116.0	58.8750	68.0*	56.7500	118.0	60.1875	120.0	2
	59.2500	80.0	58.7500	209.0	57.0000	233.0	56.8750	214.0	3
E	55.1250	61.0	58.8750	134.0	59.2500	198.0	60.1875	366.0*	1
	59.2500	140.0	58.7500	195.0	60.7500	122.0	60.1875	94.0	2
	56.8750	93.0	57.0000	195.0	58.1250	225.0	58.7500	150.0	3
F	59.2500	138.0	58.8750	121.0	60.1875	252.0	59.2500	119.0	1
	60.7500	139.0	58.7500	122.0	60.1875	205.0	56.7500	135.0	2
	57.0000	73.0	58.7500	130.0	58.1250	194.0	56.8750	128.0	3

*Indicates outlier

Table B-6. Individual Weights and Peak Accelerations of Total Boxes at 160°F

Box Surface	12-in. Drop Height		18-in. Drop Height		24-in. Drop Height		30-in. Drop Height		Replicate No.
	Box Weight (lb)	G's	Box Weight (lb)	G's	Box Weight (lb)	G's	Box Weight (lb)	G's	
A	56.7500	131.0	57.8750	157.0	60.3125	157.0	60.8750	212.0	1
	60.6250	46.0*	61.3125	126.0	58.3150	103.0	57.3125	193.0	2
	60.5000	184.0	57.3125	113.0	59.4375	211.0	60.5000	237.0	3
B	60.8750	58.0	60.3125	173.0	56.7500	93.0	57.8750	195.0	1
	61.3125	70.0	60.6250	109.0	59.7500	74.0	58.3150	66.0	2
	60.5000	54.0	58.8750	195.0	57.3125	103.0	59.4375	97.0	3
C	60.8750	63.0	57.8750	210.0	56.7500	92.0	60.3125	193.0	1
	61.3125	98.0	59.7500	197.0	58.3150	164.0	60.6250	235.0	2
	59.4375	61.0	58.8750	115.0	57.3125	141.0	60.5000	159.0	3
D	61.3125	95.0	60.3125	160.0	57.8750	308.0*	56.7500	315.0	1
	58.3150	76.0	59.7500	102.0	61.3125	137.0	60.6250	184.0	2
	60.5000	110.0	58.8750	187.0	59.4375	84.0	59.7500	117.0	3
E	60.3125	140.0	60.8750	203.0	56.7500	85.0	57.8750	191.0	1
	60.8750	150.0	59.7500	144.0	58.3150	197.0	60.6250	308.0	2
	60.5000	123.0	57.1325	126.0	59.4375	142.0	58.8750	119.0	3
F	57.8750	107.0	60.3125	104.0	60.8750	123.0	56.7500	198.0	1
	61.3125	101.0	60.6250	167.0	58.3150	196.0	59.7500	240.0	2
	58.8750	115.0	60.5000	179.0	59.4375	108.0	57.3125	188.0	3

*Indicates outlier

APPENDIX C. INTERIOR BOX ADJUSTED PEAK ACCELERATIONS

Table C-1. Peak Accelerations After Conversion to Common Static Stress for Interior Box at -65°F

Drop Height (in.)	Static Stress Levels (psi)						Replicate No.
	0.088	0.255	0.520	0.708	0.843	1.255	
12	27.7978*	34.00000	36.14877	23.86668	23.81795	17.93911	1
18	36.47560	44.00000	41.96691	39.1737*	30.00071	27.72414	1
24	42.31786	30.10626	54.8403*	29.41884	39.15275	25.2873*	1
30	38.08608	46.36364	33.17077	43.25236	26.99328	36.05487	1
12	31.83197	31.90521	34.82714	29.7147*	23.20450	17.34397	2
18	48.8778*	31.0857*	41.73097	33.18114	26.22930	26.13978	2
24	58.9474*	27.07109	32.03226	32.85652	31.7800*	38.42065	2
30	43.68231	87.1357*	40.15047	43.25236	38.12242	35.21893	2
12	34.39128	30.07430	32.84597	20.29373	23.00055	20.23463	3
18	30.63103	55.82090	39.55067	30.77801	32.07953	24.91543	3
24	32.85881	32.12531	28.04692	29.05746	41.61309	36.96554	3
30	53.52673	55.00000	33.65260	31.04043	35.52337	33.88506	3

*Indicates outlier

Table C-2. Peak Accelerations After Conversion to Common Static Stress for Interior Box at -20°F

Drop Height (in.)	Static Stress Levels (psi)						Replicate No.
	0.088	0.255	0.520	0.708	0.848	1.255	
12	47.22000	41.82000	31.28466	24.9677*	16.47563	22.82044	1
18	41.68084	40.11434	39.74912	29.56627	23.69772	25.41371	1
24	88.5672*	55.3714*	38.73443	31.07094	30.33184	24.37764	1
30	63.88955	44.57872	54.08000	33.90341	39.62322	36.28617	1
12	65.9366*	37.97541	32.37165	21.79132	18.28362	24.29088	2
18	41.50011	41.21212	38.09147	29.86473	22.72211	24.93428	2
24	60.29533	67.82992	39.42162	31.59789	30.11512	24.61383	2
30	67.99227	48.18796	59.92139	36.01171	34.08225	33.29635	2
12	31.91016	45.6785*	30.88497	22.82143	17.56982	21.72784	3
18	40.77377	41.09993	38.68531	31.9244*	24.05965	24.64368	3
24	64.14579	67.34928	35.91495	34.06736	30.91007	26.13978	3
30	67.33058	32.0571*	53.08882	36.09806	33.75296	35.96647	3

*Indicates outlier

Table C-3. Peak Accelerations After Conversion to Common Static Stress for Interior Box at 20°F

Drop Height (in.)	Static Stress Levels (psi)						Replicate No.
	0.088	0.255	0.520	0.708	0.848	1.255	
12	40.89776	32.96970	30.09091	24.71564	13.49664	18.62386	1
18	34.08722	42.74286	27.8206*	32.11079	24.72805	27.74825	1
24	30.91460	50.74627	50.29117	28.01741	25.25784	26.69732	1
30	57.12912	62.28881	52.90456	31.44773	31.05603	39.69374	1
12	28.4211*	30.75377	67.6056*	24.71564	18.0893*	18.38978	2
18	25.7340*	46.40758	37.15290	33.81333	20.0056*	26.97485	2
24	81.5197*	49.24138	41.54049	33.82289	33.83031	23.03506	2
30	47.65343	57.14117	43.07206	30.05944	26.38879	40.46926	2
12	50.31505	39.4528*	35.49419	23.08351	14.35225	17.93911	3
18	39.58516	31.0545*	34.14586	26.7590*	26.77244	25.28733	3
24	37.51776	41.0000	37.49861	30.43329	31.75576	32.60637	3
30	73.3688*	46.68657	42.96612	40.36665	31.00074	23.2643*	3

*Indicates outlier

Table C-4. Peak Accelerations After Conversion to Common Static Stress for Interior Box at 70°F

Drop Height (in.)	Static Stress Levels (psi)						Replicate No.
	0.088	0.255	0.520	0.708	0.848	1.255	
12	54.4632*	22.5032*	26.49941	18.99115	21.32141	20.47722	1
18	68.3993*	3.51020	30.16000	37.45151	23.46058	25.41371	1
24	69.6596	43.9046*	34.24080	35.68343	30.18446	30.08150	1
30	79.34600	42.64052	34.21760	31.44773	37.09208	34.77043	1
12	35.34554	32.13426	23.07607	19.74868	23.09510	20.13923	2
18	44.46441	33.41009	26.30197	35.03842	25.31106	19.69106	2
24	30.78845	34.64151	38.91934	29.81620	33.10847	29.26043	2
30	54.9938*	37.5392*	38.53655	32.38191	35.56503	36.87723	2
12	26.50295	32.87204	24.15145	20.83695	18.86195	21.56322	3
18	41.25992	36.00000	24.98030	27.31745	34.08450	22.16174	3
24	38.08633	38.06699	36.06033	33.98400	34.00108	29.88273	3
30	72.16401	46.36364	38.09147	36.07133	38.06794	35.02000	3

*Indicates outlier

Table C-5. Peak Accelerations After Conversion to Common Static Stress for Interior Box at 110°F

Drop Height (in.)	Static Stress Levels (psi)						Replicate No.
	0.088	0.255	0.520	0.708	0.848	1.255	
12	20.58720	33.19615	19.26045	18.19611	17.13436	17.45594	1
18	30.78845	31.07678	26.04357	29.05746	27.06711	24.97671	1
24	70.8824*	37.09091	40.15047	32.70163	30.91007	30.83372	1
30	37.54772	38.12121	22.1146*	29.5964*	27.07191	37.35341	1
12	20.84838	28.03791	27.17888	12.05346	14.42470	13.55396	2
18	22.10526	27.13300	25.11751	26.21611	20.09918	23.03506	2
24	59.84991	34.00000	34.82714	25.6162*	27.20076	23.12529	2
30	35.74007	49.2060*	28.98174	31.89015	29.00562	32.69293	2
12	26.44867	26.99182	25.86807	14.41745	17.64945	16.42912	3
18	27.09616	31.00000	29.40947	15.9925*	22.78238	20.92896	3
24	53.39557	37.92965	33.19502	39.33161	29.43365	26.29882	3
30	37.21605	33.49254	27.97794	26.97973	32.00076	36.21307	3

*Indicates outlier

Table C-6. Peak Accelerations After Conversion to Common Static Stress for Interior Box at 160°F

Drop Height (in.)	Static Stress Levels (psi)						Replicate No.
	0.088	0.255	0.520	0.708	0.848	1.255	
12	41.68084	25.19667	15.49377	18.40471	18.59048	16.26477	1
18	46.08427	25.43836	26.49941	19.55909	21.32141	20.47722	1
24	39.18256	25.37313	33.28000	21.98975	19.77603	26.07782	1
30	56.72283	40.80000	34.21760	40.57247	33.83989	28.90662	1
12	36.99580	20.2075*	16.34555	16.19095	19.00045	18.22121	2
18	38.53582	20.44908	25.66488	24.68585	21.73419	23.29088	2
24	32.22682	26.67261	24.27874	22.12169	25.31106	33.29635	2
30	48.69164	30.37281	37.94626	35.03842	37.97736	35.44391	2
12	28.8221*	25.37799	17.98582	14.63435	15.61762	16.98417	3
18	58.1871*	26.06439	21.03519	28.05548	25.75839	23.34667	3
24	24.46426	35.03030	19.32116	24.80590	25.81109	27.90528	3
30	61.13895	29.00474	40.56479	37.07345	31.07705	1.83142	3

*Indicates outlier

APPENDIX D. INTERIOR BOX DATA ANALYSIS CODE

```
C*************************************************************************
C
C                    INTERIOR BOX DATA ANALYSIS
C
C*************************************************************************
C
C
C     MAIN DRIVER READS THE CUSHION MATERIAL DATA RECORD CONSISTING OF
C     TEMPERATURE, DROP HEIGHT, THICKNESS, STRESS-LEVEL, G-VALUE,
C        REPLICATION AND MATERIAL TYPE     (IN THIS ORDER).
C     INITIALIZES ARRAYS CALL OUTLR (OUTLIER SUBPROGRAM), AND CALLS
C     CVREG (CURVILINEAR REGRESSION SUBPROGRAM).
C
C     THE OUTPUT IS IN THE FORM OF:
C     FOR A PARTICULAR
C        1.    DROP HEIGHT,TEMPERATURE,AND MATERIAL THICKNESS A
C              TABLE CONTAINING THE STRESS LEVELS AND G-VALUES,
C              AND ANY POINT THAT WAS REJECTED BY OUTLR IS ALSO LISTED.
C
C        2.    THE F - STATISTIC AND THE FIRST, SECOND, THIRD AND
C              FOURTH DEGREE POLYNOMIAL COEFFICIENTS ARE LISTED.
C
C
C*************************************************************************
      DIMENSION STR(75), G(75), ALPH(3), X(75)
      DIMENSION COEF(10), YI(75), SIGHAT(4)
      DIMENSION XNEW(75), YNEW(75)
      DIMENSION ST(18)
      DATA(ST(I),I=1,18) /.066,.086,.086,.255,.255,.255,.52,.52,.52,
     1     .708,.708,.708,.843,.843,.843,1.255,1.255,1.255   /
      READ(5,4020) N
      KNT=0
      IFLAG=0
      KFLAG=0
      J=1
      PRINT 2500
      GO TO 200
100   KNT=1
      J=1
      PRINT 2500
      GO TO 300
200   READ( 5,1700,END=400) A1,A2,A3,A4,A5,A6,(ALPH(I),I=1,3)
      IF(KNT.EQ.0)DTJ=A1
      IF (A1.NE. DTJ ) GO TO 500
      KNT=KNT+1
300   TEMP=A1
      PRINT 5500,A4,A5
      DHT=A2
      THCK=A3
      STR(KNT)=ST(J)
      G(KNT)=(ST(J)*A5)/A4
350   CONTINUE
```

```
      G=G+1
      REM=A6
      DTG=A1
      GO TO 200
400   IFLAG=1
500   NPTS=KNT
      DO 600 I=1,NPTS
      X(I)= 1.0-COS(STR(I))
600   CONTINUE
      WRITE (6,1800) ALPH,DHT,TEMP,THCK
      WRITE (6,1900)
      I=1
      ITEMP=NPTS
700   IF (I.GT.ITEMP) GO TO 1000
900   WRITE (6,2000) STR(I),STR(I+1),STR(I+2),X(I),X(I+1),X(I+2),G(I),G(
     1I+1),G(I+2)
      I=I+3
      GO TO 700
1000  CONTINUE
C*****************************************************************
      CALL OUTLR (NPTS,X,G,NEWPTS,XNEW,YNEW)
C*****************************************************************
      NI=0
1100  NI=NI+1
C*****************************************************************
      CALL CVREG (NI,NEWPTS,XNEW,YNEW,DEGREE,COEF)
C*****************************************************************
      SIGHAT(NI)=0.
C     POLYNOMIAL CALCULATION
      DO 1200 I=1,NEWPTS
      YI(I)=COEF(1)+COEF(2)*XNEW(I)
      IF(NI.EQ.2)YI(I)=YI(I)+COEF(3)*XNEW(I)**2
      IF(NI.EQ.3)YI(I)=YI(I)+COEF(4)*XNEW(I)**3
      IF(NI.EQ.4)YI(I)=YI(I)+COEF(5)*XNEW(I)**4
      SIGHAT(NI)=SIGHAT(NI)+(YNEW(I)-YI(I))**2
1200  CONTINUE
      DF=NEWPTS-NI-1
      SIGHAT(NI)=SIGHAT(NI)/DF
      IF (NI.GT.1) GO TO 1300
      GO TO 1100
1300  IF(NI .NE. 2) GOTO 1350
      WRITE(N,4000) THCK,DHT,TEMP,NEWPTS,(COEF(I),I=1,3)
      WRITE(N,4010) (XNEW(I),I=1,NEWPTS)
      WRITE(N,4010) (YNEW(I),I=1,NEWPTS)
1350  CONTINUE
      IF (NI.LT.4) GO TO 1100
1400  IF (IFLAG.EQ.1) GO TO 1500
      GO TO 100
1500  STOP
C
1600  FORMAT (///2X,'F =',E15.8,5X,'SIG',I1,'SQ =',E15.8,5X,'SIG',I1,'SQ
     1 =',E15.8)
```

```
1700  FORMAT (3F10.0,2F10.5,F10.0,6X,3A4)
1800  FORMAT(//1X,3A4,' DROP HEIGHT OF',F5.1,2H'',', TEMPERATURE ',F6.1
     1,'F, THICKNESS',F4.1,2H'',/)
1900  FORMAT (1H ,8X,'STRESS LEVELS',21X,'1.0-COS(STRESS LEVEL)',25X,3HG
     1'S)
2000  FORMAT (1H ,3(5F10.4,5X))
2100  FORMAT (1H ,3(F10.4,25X))
2200  FORMAT (1H ,3(2F10.4,15X))
2300  FORMAT(1H1,15X,'ORIGINAL DATA',//)
4000  FORMAT(5F5.1,15, 5F12.7)
4010  FORMAT(10F8.4,/,10F8.4)
4020  FORMAT(I1)
5500  FORMAT(5X,F12.5,F15.5)
      END
```

```
      SUBROUTINE OUTLR (NPTS,X,Y,NEWPTS,XNEW,YNEW)
C*****************************************************************
C
C                  OUTLIER POINT REJECTION SUBPROGRAM.
C
C*****************************************************************
C     METHOD BASED ON THE NAIR CRITERION (AN EXTENSION OF THE
C     EXTREME STUDENTIZED DEVIATE FROM THE SAMPLE MEAN).
C
C     FOR THE SET OF OBSERVATIONS HAVING THE LARGEST VARIANCE
C     EACH OBSERVATION OF THE SET IS TESTED INDIVIDUALLY AS A
C     CANDIDATE FOR REJECTION AS AN OUTLIER.
C
C*****************************************************************
      DIMENSION X(1), Y(1), XNEW(1), YNEW(1), XA(25), XB(25), XC(25), YA
     1(25), YB(25), YC(25), YMEAN(25), S2N(25), KEY(25)
      TESTV = 1./34
      DO 100 I=1,25
100   KEY(I)=0
      NTEMP=NPTS-2
      L=1
      I=1
200   CONTINUE
      J=I+1
      K=I+2
      IF (I.GT.NTEMP) GO TO 500
       GOTO 250
      IF (X(J).NE.X(K)) GO TO 400
      IF (X(I).NE.X(J)) GO TO 300
250    CONTINUE
      XA(L)=X(I)
      XB(L)=X(J)
      XC(L)=X(K)
      YA(L)=Y(I)
      YB(L)=Y(J)
      YC(L)=Y(K)
      KEY(L)=0
      L=L+1
      I=I+3
      GO TO 200
300   CONTINUE
      I=I+1
      GO TO 200
400   CONTINUE
      I=I+2
      GO TO 200
500   CONTINUE
      L=L-1
      NP=L
      NPTS=(L*3)-1
C     CALCULATE MEANS & VARIANCES
      DO 700 I=1,NP
```

```
      IF (YA(I).NE.YB(I).OR.YA(I).NE.YC(I)) GO TO 600
      YMEAN(I)=YA(I)
      S2N(I)=0.0
      WRITE (6,2500) YMEAN(I),S2N(I)
      GO TO 700
600   CONTINUE
      YMEAN(I)=(YA(I)+YB(I)+YC(I))/3.
      S2N(I)=((YA(I)-YMEAN(I))**2+(YB(I)-YMEAN(I))**2+(YC(I)-YMEAN(I))**
     1 2)/2.
700   CONTINUE
C*****************************************************************
C     SORT IN ORDER OF DECREASING VARIANCE
      CALL SORT (NP,S2N,YMEAN,YA,YB,YC,XA,XB,XC)
C*****************************************************************
C     CALCULATE SNU
      L=1
C     SUM VARIANCES
800   KNT=0
      SUMV=0.
      DO 900 I=1,NP
      IF (KEY(I).EQ.1) GO TO 900
      IF (I.EQ.L) GO TO 900
      SUMV=SUMV+S2N(I)
      KNT=KNT+1
900   CONTINUE
      SNU=SQRT(SUMV/(KNT-1))
C     TEST
      TA=ABS((YA(L)-YMEAN(L))/SNU)
      TB=ABS((YB(L)-YMEAN(L))/SNU)
      TC=ABS((YC(L)-YMEAN(L))/SNU)
      IF (TA.EQ.TB.OR.TA.EQ.TC.OR.TB.EQ.TC) GO TO 1300
      TE=MAX(TA,TB,TC)
      IF (TE.LE.TESTV) GO TO 1300
      IF (TE.EQ.TA) GO TO 1000
      IF (TE.EQ.TB) GO TO 1100
      IF (TE.EQ.TC) GO TO 1200
      GO TO 1300
1000  WRITE (6,2400) L,XA(L),YA(L),TE,SNU
      XA(L)=999.
      KEY(L)=1
      GO TO 1300
1100  WRITE (6,2400) L,XB(L),YB(L),TE,SNU
      XB(L)=999.
      KEY(L)=1
      GO TO 1300
1200  WRITE (6,2400) L,XC(L),YC(L),TE,SNU
      XC(L)=999.
      KEY(L)=1
C     CHECK TO SEE IF ALL VALUES
1300  IF (L.EQ.NP) GO TO 1400
      L=L+1
      GO TO 800
```

```
C     PUT IN NEW ARRAYS
1400  L=0
      NEWPTS=0
1500  L=L+1
      IF (XA(L)-999.) 1600,1700,1600
C     POINT ACCEPTED
1600  NEWPTS=NEWPTS+1
      XNEW(NEWPTS)=XA(L)
      YNEW(NEWPTS)=YA(L)
1700  IF (XB(L)-999.) 1800,1900,1800
1800  NEWPTS=NEWPTS+1
      XNEW(NEWPTS)=XB(L)
      YNEW(NEWPTS)=YB(L)
1900  IF (XC(L)-999.) 2000,2100,2000
2000  NEWPTS=NEWPTS+1
      XNEW(NEWPTS)=XC(L)
      YNEW(NEWPTS)=YC(L)
2100  IF (L.GE.NP) GO TO 2200
      GO TO 1500
2200  RETURN
C
2300  FORMAT (1H0,12A,'SAME VALUES   ',2F6.0)
2400  FORMAT ('0REJECT POINT',I3,', X =',F8.4,', Y =',F6.2,',T =',F6.2,'
     1,SNO =',F6.2)
      END
```

```
      SUBROUTINE CVREG (N1,NPT,X,Y,DEGRE,COEF)
C*****************************************************************
C
C     CURVILINEAR REGRESSION
C     CURVILINEAR REGRESSION DETERMINES THE EQUATIONS
C     OF THE STATISTICALLY BEST FITTING POLYNOMIALS OF FIRST,
C     SECOND, THIRD AND FOURTH ORDER.
C
C*****************************************************************
      DIMENSION A(10,11), X(1), Y(1), COEF(1), KON(10)
      N=N1+1
      M=N+1
      ANPT=NPT
      DO 100 I=1,N
      DO 100 J=1,M
  100 A(I,J)=0.
      A(1,1)=NPT
      DO 400 K=1,NPT
      DO 300 I=1,N
      DO 300 J=1,N
      IPJ2=I+J-2
      IF (IPJ2) 300,300,200
  200 A(I,J)=A(I,J)+X(K)**IPJ2
  300 CONTINUE
      DO 400 I=2,N
  400 A(I,M)=A(I,M)+X(K)**(I-1)*Y(K)
      DO 500 J=1,NPT
  500 A(1,M)=A(1,M)+Y(J)
      DO 600 J=1,M
      DO 600 I=1,N
  600 A(I,J)=A(I,J)/ANPT
      IERR=0
      M=N+1
      DO 1300 I=1,N
      IF (A(I,1)) 800,700,800
  700 IERR=1
      GO TO 1400
  800 TEMP=1.0/A(I,I)
      IP1=I+1
      DO 900 J=IP1,M
  900 A(I,J)=A(I,J)*TEMP
      DO 1200 K=1,N
      IF (I-K) 1000,1200,1000
 1000 DO 1100 J=IP1,M
 1100 A(K,J)=A(K,J)-A(K,I)*A(I,J)
 1200 CONTINUE
 1300 CONTINUE
      N=N1+1
      M=N+1
 1400 IF (IERR) 1500,1600,1500
 1500 WRITE (6,3100)
      GO TO 2500
```

```
1600  CONTINUE
      DO 1700 K=1,N
1700  COEF(K)=A(K,M)
      SUMR2=0.0
      DO 1900 I=1,NPT
      YC=COEF(1)
      DO 1800 K=2,N
1800  YC=YC+COEF(K)*X(I)**(K-1)
      R=Y(I)-YC
1900  SUMR2=SUMR2+R*R
      SIGMA=SQRT(SUMR2/ANPT)
      SSERR=SUMR2
      SUMR2=Y(1)
      DO 2000 I=2,NPT
2000  SUMR2=SUMR2+Y(I)
      BARY1=SUMR2/NPT
      SUMR2=0.0
      DO 2100 I=1,NPT
      R=Y(I)-BARY1
2100  SUMR2=SUMR2+R*R
      SSTOT=SUMR2
      SSREG=SSTOT-SSERR
      DSREG=SSREG/N1
      DSERR=SSERR/(NPT-(N1+1))
      FRATO=DSREG/DSERR
      DEGFT=N1
      DEGFB=NPT-(N1+1)
      DEGRE=NPT-1
      ETS=SSERR/SSTOT
      IF(ETS.GE.1.0)ETS=1.0
      CORR=SQRT(1.0-ETS)
      WRITE (6,3000) N1
      WRITE (6,2600)
      WRITE (6,2700) SSREG,DEGFT,DSREG,FRATO,CORR
      WRITE (6,2800) SSERR,DEGFB,DSERR
      WRITE (6,2900) SSTOT,DEGRE
      WRITE (6,2400)
      MM=N1+1
      DO 2200 I=1,10
2200  KON(I)=I-1
      WRITE (6,2500) (KON(I),COEF(I),I=1,MM)
2300  RETURN
C
2400  FORMAT (//,2X,'CURVE COEFFICIENTS')
2500  FORMAT (//2X,2HB(,I1,1H),3X,E15.7)
2600  FORMAT(//,2X,'SOURCE',9X,'S.S',9X,'D.F',9X,'M.S',9X,'F',12X,'R')
2700  FORMAT (//,2X,'DUE TO',5(4X,E10.4))
2800  FORMAT (//,2X,'ABOUT',3(4X,E10.4))
2900  FORMAT (//,2X,'TOTAL',2(4X,E10.4))
3000  FORMAT (1H1,2X,'ANOVA FOR CURVE OF ORDER',I3)
3100  FORMAT (//,4X,'SINGULAR MATRIX ',/,4X,'CURVE FIT IMPOSSIBLE')
      END
```

```
      SUBROUTINE SORT(N,VAL,X1,X2,X3,X4,X5,X6,X7)
C*****************************************************************
C
C     SUBROUTINE FOR SORTING N NUMBERS IN DESCENDING ORDER
C
C*****************************************************************
      DIMENSION VAL(1),X1(1),X2(1),X3(1),X4(1),X5(1),X6(1),X7(1)
      M=N-1
      DO 100 I=1,M
      L=I+1
      DO 100 II=L,N
      IF(VAL(I) .GE. VAL(II)) GOTO 100
      F = VAL(I)
      VAL(I) = VAL(II)
      VAL(II) = F
      F=X1(I)
      X1(I)=X1(II)
      X1(II)=F
      F=X2(I)
      X2(I)=X2(II)
      X2(II)=F
      F=X3(I)
      X3(I)=X3(II)
      X3(II)=F
      F=X4(I)
      X4(I)=X4(II)
      X4(II)=F
      F=X5(I)
      X5(I)=X5(II)
      X5(II)=F
      F=X6(I)
      X6(I)=X6(II)
      X6(II)=F
      F=X7(I)
      X7(I)=X7(II)
      X7(II)=F
100   CONTINUE
      RETURN
      END
```

APPENDIX E. TOTAL BOX DATA ANALYSIS CODE

```
C*****************************************************************************
C
C                    TOTAL BOX DATA ANALYSIS
C
C*****************************************************************************
C
C
C     MAIN DRIVER READS THE CUSHION MATERIAL DATA RECORD CONSISTING OF
C     TEMPERATURE, DROP HEIGHT, THICKNESS, BOX WEIGHTS , G-VALUE
C     BOX NUMBER AND MATERIAL TYPE     (IN THIS ORDER) .
C     INITIALIZES ARRAYS CALL OUTLR (OUTLIER SUBPROGRAM), AND CALLS
C     CVREG (CURVILINEAR REGRESSION SUBPROGRAM).
C
C
C             THE F - STATISTIC AND THE FIRST, SECOND, THIRD AND
C             FOURTH DEGREE POLYNOMIAL COEFFICIENTS ARE LISTED.
C
C
C*****************************************************************************
C
      DIMENSION  WT(75), G(75), ALPH(3), X(75),BOX(75)
      DIMENSION COEF(10), YI(75), SIGHAT(4)
      DIMENSION XNEW(75), YNEW(75)
      KNT=0
      IFLAG=0
      KFLAG=0
      GO TO 200
100   KNT=1
      GO TO 300
200   READ( 5,1700,END=400) A1,A2,A3,A4,A5,A6,(ALPH(I),I=1,3)
      IF(KNT.EQ.0)DTO=A2
      IF (A2.NE. DTO ) GO TO 500
      KNT=KNT+1
500   TEMP=A1
      DHT=A2
      THCK=A3
      DTO=A2
      WT(KNT) = A4
      BOX(KNT)=A6
      G(KNT)=A5
      GO TO 200
400   IFLAG=1
500   NPTS=KNT
      DO 600 I=1,NPTS
      X(I) = WT(I)
600   CONTINUE
      WRITE (6,1600) ALPH,DHT,TEMP,THCK
      WRITE (6,1900)
      I=1
      ITEMP=NPTS
700   IF (I.GT.ITEMP) GO TO 1000
      WRITE (6,2100) WT(I), G(I) ,BOX(I)
```

```
      KFLAG=1
      I=I+1
      GO TO 700
1000  CONTINUE
C*************************************************************************
      CALL OUTLR (NPTS,X,G,NEWPTS,XNEW,YNEW)
C*************************************************************************
      NI=0
1100  NI=NI+1
C*************************************************************************
      CALL CVREG (NI,NEWPTS,XNEW,YNEW,DEGRE,COEF)
C*************************************************************************
      SIGHAT(NI)=0.
C     POLYNOMIAL CALCULATION
      DO 1200 I=1,NEWPTS
      YI(I)=COEF(1)+COEF(2)*XNEW(I)
      IF(NI.EQ.2)YI(I)=YI(I)+COEF(3)*XNEW(I)**2
      IF(NI.EQ.3)YI(I)=YI(I)+COEF(4)*XNEW(I)**3
      IF(NI.EQ.4)YI(I)=YI(I)+COEF(5)*XNEW(I)**4
      SIGHAT(NI)=SIGHAT(NI)+(YNEW(I)-YI(I))**2
1200  CONTINUE
      DF=NEWPTS-NI-1
      SIGHAT(NI)=SIGHAT(NI)/DF
      IF (NI.GT.1) GO TO 1300
      GO TO 1100
1300  F=ABS((SIGHAT(NI-1)-SIGHAT(NI))/SIGHAT(NI))
      IF(NI.EQ.4)F=ABS((SIGHAT(2)-SIGHAT(4))/SIGHAT(4))
      NII=NI-1
      WRITE (6,1600) F,NII,SIGHAT(NII),NI,SIGHAT(NI)
      IF (NI.LT.4) GO TO 1100
1400  IF (IFLAG.EQ.1) GO TO 1500
      GO TO 100
1500  STOP
C
1600  FORMAT (///2X,'F =',E15.8,5X,'SIG',I1,'SQ =',E15.8,5X,'SIG',I1,'SQ
     1 =',E15.8)
1700  FORMAT (3F10.0,F10.2,2F10.0,8X,3A4)
1800  FORMAT (1H1,3A4,'' DROP HEIGHT OF',F5.1,2H'',', TEMPERATURE ',F6.1
     1,'F, THICKNESS',F4.1,2H'')
1900  FORMAT (1H ,2X,' BOX WEIGHTS ', 12X,3H6'S, 23X,'BOX NUMBER')
2100  FORMAT (1H ,4(F10.4,15X))
      END
```

```
      SUBROUTINE OUTLR (NPTS,X,Y,NEWPTS,XNEW,YNEW)
C*****************************************************************
C
C                  OUTLIER POINT REJECTION SUBPROGRAM
C
C*****************************************************************
C     METHOD BASED ON THE NAIR CRITERION (AN EXTENSION OF THE
C     EXTREME STUDENTIZED DEVIATE FROM THE SAMPLE MEAN).
C
C
C*****************************************************************
      DIMENSION X(1), Y(1), XNEW(1), YNEW(1), XA(25), XB(25), XC(25), YA
     1(25), YB(25), YC(25), YMEAN(25), S2N(25), KEY(25)
      TESTV = 1.734
      DO 100 I=1,25
100   KEY(I)=0
      NTEMP=NPTS-2
      L=1
      I=1
200   CONTINUE
      J=I+1
      K=I+2
      IF (I.GT.NTEMP) GO TO 500
250    CONTINUE
      XA(L)=X(I)
      XB(L)=X(J)
      XC(L)=X(K)
      YA(L)=Y(I)
      YB(L)=Y(J)
      YC(L)=Y(K)
      KEY(L)=0
      L=L+1
      I=I+3
      GO TO 200
300   CONTINUE
      I=I+1
      GO TO 200
400   CONTINUE
      I=I+2
      GO TO 200
500   CONTINUE
      L=L-1
      NP=L
      NPTS=(L*3)-1
C     CALCULATE MEANS & VARIANCES
      DO 700 I=1,NP
      IF (YA(I).NE.YB(I).OR.YA(I).NE.YC(I)) GO TO 600
      YMEAN(I)=YA(I)
      S2N(I)=0.0
      WRITE (6,2300) YMEAN(I),S2N(I)
      GO TO 700
600   CONTINUE
```

```
      YMEAN(I)=(YA(I)+YB(I)+YC(I))/3.
      S2N(I)=((YA(I)-YMEAN(I))**2+(YB(I)-YMEAN(I))**2+(YC(I)-YMEAN(I))**
     12)/2.
700   CONTINUE
C*****************************************************************************
C     SORT IN ORDER OF DECREASING VARIANCE
      CALL SORT (NP,S2N,YMEAN,YA,YB,YC,XA,XB,XC)
C*****************************************************************************
C     CALCULATE SNU
      L=1
C     SUM VARIANCES
800   KNT=0
      SUMV=0.
      DO 900 I=1,NP
      IF (KEY(I).EQ.1) GO TO 900
      IF (I.EQ.L) GO TO 900
      SUMV=SUMV+S2N(I)
      KNT=KNT+1
900   CONTINUE
      SNU=SQRT(SUMV/(KNT-1))
C     TEST
      TA=ABS((YA(L)-YMEAN(L))/SNU)
      TB=ABS((YB(L)-YMEAN(L))/SNU)
      TC=ABS((YC(L)-YMEAN(L))/SNU)
      IF (TA.EQ.TB.OR.TA.EQ.TC.OR.TB.EQ.TC) GO TO 1300
      TE=MAX(TA,TB,TC)
      IF (TE.LE.TESTV) GO TO 1300
      IF (TE.EQ.TA) GO TO 1000
      IF (TE.EQ.TB) GO TO 1100
      IF (TE.EQ.TC) GO TO 1200
      GO TO 1300
1000  WRITE (6,2400) L,XA(L),YA(L),TE,SNU
      XA(L)=999.
      KEY(L)=1
      GO TO 1300
1100  WRITE (6,2400) L,XB(L),YB(L),TE,SNU
      XB(L)=999.
      KEY(L)=1
      GO TO 1300
1200  WRITE (6,2400) L,XC(L),YC(L),TE,SNU
      XC(L)=999.
      KEY(L)=1
C     CHECK TO SEE IF ALL VALUES
1300  IF (L.EQ.NP) GO TO 1400
      L=L+1
      GO TO 800
C     PUT IN NEW ARRAYS
1400  L=0
      NEWPTS=0
1500  L=L+1
      IF (XA(L)-999.) 1600,1700,1600
C     POINT ACCEPTED
```

```
1600  NEWPTS=NEWPTS+1
      XNEW(NEWPTS)=XA(L)
      YNEW(NEWPTS)=YA(L)
1700  IF (XB(L)-999.) 1800,1900,1800
1800  NEWPTS=NEWPTS+1
      XNEW(NEWPTS)=XB(L)
      YNEW(NEWPTS)=YB(L)
1900  IF (XC(L)-999.) 2000,2100,2000
2000  NEWPTS=NEWPTS+1
      XNEW(NEWPTS)=XC(L)
      YNEW(NEWPTS)=YC(L)
2100  IF (L.GE.NP) GO TO 2200
      GO TO 1500
2200  RETURN
C
2300  FORMAT (1H0,12X,'SAME VALUES   ',2F6.0)
2400  FORMAT ('0REJECT POINT',I3,', X =',F8.4,', Y =',F6.2,',T =',F6.2,'
     1,SNU =',F6.2)
      END
```

```
      SUBROUTINE CVREG (N1,NPT,X,Y,DEGRE,COEF)
C*****************************************************************************
C
C     CURVILINEAR REGRESSION
C     CURVILINEAR REGRESSION DETERMINES THE EQUATIONS
C     OF THE STATISTICALLY BEST FITTING POLYNOMIALS OF FIRST,
C     SECOND, THIRD AND FOURTH ORDER.
C
C*****************************************************************************
      DIMENSION A(10,11), X(1), Y(1), COEF(1), KON(10)
      N=N1+1
      M=N+1
      ANPT=NPT
      DO 100 I=1,N
      DO 100 J=1,M
100   A(I,J)=0.
      A(1,1)=NPT
      DO 400 K=1,NPT
      DO 300 I=1,N
      DO 300 J=1,N
      IPJ2=I+J-2
      IF (IPJ2) 300,300,200
200   A(I,J)=A(I,J)+X(K)**IPJ2
300   CONTINUE
      DO 400 I=2,N
400   A(I,M)=A(I,M)+X(K)**(I-1)*Y(K)
      DO 500 J=1,NPT
500   A(1,M)=A(1,M)+Y(J)
      DO 600 J=1,M
      DO 600 I=1,N
600   A(I,J)=A(I,J)/ANPT
      IERR=0
      M=N+1
      DO 1300 I=1,N
      IF (A(I,I)) 800,700,800
700   IERR=1
      GO TO 1400
800   TEMP=1.0/A(I,I)
      IP1=I+1
      DO 900 J=IP1,M
900   A(I,J)=A(I,J)*TEMP
      DO 1200 K=1,N
      IF (I-K) 1000,1200,1000
1000  DO 1100 J=IP1,M
1100  A(K,J)=A(K,J)-A(K,I)*A(I,J)
1200  CONTINUE
1300  CONTINUE
      N=N1+1
      M=N+1
1400  IF (IERR) 1500,1600,1500
1500  WRITE (6,3100)
      GO TO 2300
```

```
 1600  CONTINUE
       DO 1700 K=1,N
 1700  COEF(K)=A(K,M)
       SUMR2=0.0
       DO 1900 I=1,NPT
       YC=COEF(1)
       DO 1800 K=2,N
 1800  YC=YC+COEF(K)*X(I)**(K-1)
       R=Y(I)-YC
 1900  SUMR2=SUMR2+R*R
       SIGMA=SQRT(SUMR2/ANPT)
       SSERR=SUMR2
       SUMR2=Y(1)
       DO 2000 I=2,NPT
 2000  SUMR2=SUMR2+Y(I)
       BARY1=SUMR2/NPT
       SUMR2=0.0
       DO 2100 I=1,NPT
       R=Y(I)-BARY1
 2100  SUMR2=SUMR2+R*R
       SSTOT=SUMR2
       SSREG=SSTOT-SSERR
       DSREG=SSREG/N1
       DSERR=SSERR/(NPT-(N1+1))
       FRATO=DSREG/DSERR
       DEGFT=N1
       DEGFB=NPT-(N1+1)
       DEGRE=NPT-1
       ETS=SSERR/SSTOT
       IF(ETS.GE.1.0)ETS=1.0
       CORR=SQRT(1.0-ETS)
       WRITE (6,3000) N1
       WRITE (6,2600)
       WRITE (6,2700) SSREG,DEGFT,DSREG,FRATO,CORR
       WRITE (6,2800) SSERR,DEGFB,DSERR
       WRITE (6,2900) SSTOT,DEGRE
       WRITE (6,2400)
       MM=N1+1
       DO 2200 I=1,10
 2200  KON(I)=I-1
       WRITE (6,2500) (KON(I),COEF(I),I=1,MM)
 2300  RETURN
C
 2400  FORMAT (//,2X,'CURVE COEFFICIENTS')
 2500  FORMAT (//2X,2HB(,I1,1H),3X,E15.7)
 2600  FORMAT(//,2X,'SOURCE',9X,'S.S',9X,'D.F',9X,'M.S',9X,'F', 2X,'R')
 2700  FORMAT (//,2X,'DUE TO',5(4X,E10.4))
 2800  FORMAT (//,2X,'ABOUT',3(4X,E10.4))
 2900  FORMAT (//,2X,'TOTAL',2(4X,E10.4))
 3000  FORMAT (1H1,2X,'ANOVA FOR CURVE OF ORDER',I3)
 3100  FORMAT (//,4X,'SINGULAR MATRIX ',//,4X,'CURVE FIT IMPOSSIBLE')
       END
```

```
      SUBROUTINE SORT(N,VAL,X1,X2,X3,X4,X5,X6,X7)
C*****************************************************************
C
C     SUBROUTINE FOR SORTING N NUMBERS IN DESCENDING ORDER
C
C*****************************************************************
      DIMENSION VAL(1),X1(1),X2(1),X3(1),X4(1),X5(1),X6(1),X7(1)
      M=N-1
      DO 100 I=1,M
      L=I+1
      DO 100 II=L,N
      IF(VAL(I) .GE. VAL(II)) GOTO 100
      F = VAL(I)
      VAL(I) = VAL(II)
      VAL(II) = F
      F=X1(I)
      X1(I)=X1(II)
      X1(II)=F
      F=X2(I)
      X2(I)=X2(II)
      X2(II)=F
      F=X3(I)
      X3(I)=X3(II)
      X3(II)=F
      F=X4(I)
      X4(I)=X4(II)
      X4(II)=F
      F=X5(I)
      X5(I)=X5(II)
      X5(II)=F
      F=X6(I)
      X6(I)=X6(II)
      X6(II)=F
      F=X7(I)
      X7(I)=X7(II)
      X7(II)=F
  100 CONTINUE
      RETURN
      END
```

APPENDIX F. PEAK ACCELERATIONS AT 21-INCH DROP HEIGHT

Table F-1. Data Obtained from 21-in. Drop Tests at -65°F

Static Stress	Interior Box Peak Accelerations (G's)	Total Box Weight (lb)	Total Box Peak Accelerations (G's)	Replicate No.
0.08318	46.0	59.2500	206.0	1
0.08864	50.0	60.1875	214.0	2
0.08360	45.0	56.7500	135.0	3
0.24750	35.0	59.2500	126.0	1
0.26375	44.0*	60.1875	119.0	2
0.24875	37.0	56.7500	160.0	3
0.50510	37.0	59.2500	157.0	1
0.53827	41.0	60.1875	160.0	2
0.50765	35.0	56.7500	198.0	3
0.68750	35.0	59.2500	144.0	1
0.73264	29.0*	60.1875	202.0	2
0.69097	34.0	56.7500	142.0	3
0.81818	34.0	59.2500	126.0	1
0.87190	35.0	60.1875	168.0	2
0.82231	36.0	56.7500	264.0*	3
1.22222	38.0*	59.2500	196.0	1
1.30247	31.0	60.1875	228.0	2
1.22840	24.0	56.7500	149.0	3

*Indicates Outlier

Table F-2. Data Obtained from 21-in. Drop Tests at -20°F

Static Stress	Interior Box Peak Accelerations (G's)	Total Box Weight (lb)	Total Box Peak Accelerations (G's)	Replicate No.
0.08318	59.0	59.2500	185.0	1
0.08864	32.0*	60.1875	184.0	2
0.08360	72.0	56.7500	68.0*	3
0.24750	43.0	59.2500	157.0	1
0.26375	44.0	60.1875	125.0	2
0.24875	45.0	56.7500	115.0	3
0.50510	28.0	59.2500	163.0	1
0.53827	40.0	60.1875	79.0*	2
0.50765	40.0	56.7500	161.0	3
0.68750	44.0	59.2500	137.0	1
0.73264	32.0	60.1875	136.0	2
0.69097	28.0	56.7500	114.0	3
0.81818	43.0	59.2500	138.0	1
0.87190	29.0	60.1875	113.0	2
0.82231	36.0	56.7500	103.0	3
1.22222	17.0	59.2500	41.0*	1
1.30247	22.0	60.1875	155.0	2
1.22840	21.0	56.7500	185.0	3

*Indicates Outlier

Table F-3. Data Obtained from 21-in. Drop Tests at 20°F

Static Stress	Interior Box Peak Accelerations (G's)	Total Box Weight (lb)	Total Box Peak Accelerations (G's)	Replicate No.
0.08318	56.0	59.2500	210.0	1
0.08864	34.0*	60.1875	212.0	2
0.08360	57.0	56.7500	75.0*	3
0.24750	45.0	59.2500	112.0	1
0.26375	34.0	60.1875	188.0	2
0.24875	45.0	56.7500	130.0	3
0.50510	36.0	59.2500	93.0	1
0.53827	28.0	60.1875	136.0	2
0.50765	32.0	56.7500	176.0	3
0.68750	22.0	59.2500	136.0	1
0.73264	37.0	60.1875	151.0	2
0.69097	36.0	56.7500	195.0	3
0.81818	22.0	59.2500	140.0	1
0.87190	30.0	60.1875	100.0	2
0.82231	34.0	56.7500	109.0	3
1.22222	23.0	59.2500	200.0	1
1.30247	28.0	60.1875	205.0	2
1.22840	27.0	56.7500	84.0*	3

*Indicates Outlier

Table F-4. Data Obtained from 21-in. Drop Tests at 70°F

Static Stress	Interior Box Peak Accelerations (G's)	Total Box Weight (lb)	Total Box Peak Accelerations (G's)	Replicate No.
0.08318	50.0	59.2500	112.0	1
0.08864	60.0	60.1875	92.0	2
0.08360	77.0*	56.7500	244.0*	3
0.24750	37.0	59.2500	187.0	1
0.26375	37.0	60.1875	176.0	2
0.24875	41.0	56.7500	129.0	3
0.50510	30.0	59.2500	145.0	1
0.53827	36.0	60.1875	242.0*	2
0.50765	32.0	56.7500	107.0	3
0.68750	28.0	59.2500	124.0	1
0.73264	28.0	60.1875	144.0	2
0.69097	27.0	56.7500	143.0	3
0.81818	20.0	59.2500	103.0	1
0.87190	27.0	60.1875	146.0	2
0.82231	33.0*	56.7500	229.0*	3
1.22222	20.0	59.2500	137.0	1
1.30247	28.0*	60.1875	153.0	2
1.22840	19.0	56.7500	102.0	3

*Indicates Outlier

Table F-5. Data Obtained from 21-in. Drop Tests at 110°F

Static Stress	Interior Box Peak Accelerations (G's)	Total Box Weight (lb)	Total Box Peak Accelerations (G's)	Replicate No.
0.08318	47.0	59.2500	111.0	1
0.08864	53.0	60.1875	116.0	2
0.08360	60.0*	56.7500	133.0	3
0.24750	68.0*	59.2500	122.0	1
0.26375	39.0	60.1875	180.0	2
0.24875	32.0	56.7500	104.0	3
0.50510	30.0	59.2500	138.0	1
0.53827	29.0	60.1875	189.0	2
0.50765	24.0*	56.7500	165.0	3
0.68750	26.0	59.2500	238.0	1
0.73264	28.0	60.1875	86.0*	2
0.69097	26.0	56.7500	233.0	3
0.81818	26.0	59.2500	179.0	1
0.87190	28.0	60.1875	205.0	2
0.82231	27.0*	56.7500	80.0*	3
1.22222	18.0*	59.2500	244.0*	1
1.30247	21.0	60.1875	140.0	2
1.22840	21.0	56.7500	158.0	3

*Indicates Outlier

Table F-6. Data Obtained from 21-in. Drop Te ·· at 160°F

Static Stress	Interior Box Peak Accelerations (G's)	Total Box Weight (lb)	Total Box Peak Accelerations (G's)	Replicate No.
0.08318	41.0	59.2500	103.0	1
0.08864	48.0	60.1875	125.0	2
0.08360	45.0	56.7500	140.0	3
0.24750	28.0	59.2500	145.0	1
0.26375	38.0*	60.1875	138.0	2
0.24875	24.0	56.7500	114.0	3
0.50510	25.0	59.2500	155.0	1
0.53827	34.0	60.1875	122.0	2
0.50765	26.0	56.7500	303.0*	3
0.68750	27.0	59.2500	164.0	1
0.73264	33.0	60.1875	180.0	2
0.69097	23.0	56.7500	169.0	3
0.81818	23.0	59.2500	196.0	1
0.87190	28.0	60.1875	190.0	2
0.82231	21.0	56.7500	160.0	3
1.22222	24.0	59.2500	170.0	1
1.30247	24.0	60.1875	180.0	2
1.22840	25.0	56.7500	140.0	3

*Indicates Outlier

APPENDIX G. INTERIOR BOX VALIDATION CODE

```
C*********************************************************************
C
C                    INTERIOR BOX VALIDATION
C
C*********************************************************************
C
      INTEGER TYPEM
      COMMON TYPEM(3),NV,CONST,COEF(45)
      COMMON TP,DH,TC,SS,GL,NVR,V(45)
      DIMENSION X(500), Y(500), YM(500),  YPL(500),
     1 YPU(500),B(3),YL(500),YU(500)
      DATA (TYPEM(I),I=1,3) / 'MINI','CEL ','BOX '/
      DATA (COEF(I),I=1,45) /0.0,0.0,0.0,7.1865626,8*0.0,-0.57911897,
     A     7*0.0,-0.53894447,6*0.0,30.088255,  0.0,66.557902,4*0.0,
     B     4.1031526,5*0.0,10.219992,0.0,-0.22965288,2*0.0/
C
      RANGE=1.0
      CONST = -14.475703
C
C            PRINT CUSHION MATERIAL TERMS AND COEFFICIENTS.
      PRINT 3999,CONST
      PRINT 4000,(I,COEF(I),I=1,45)
C
C     NUMBER OF COEFFICIENTS FOR THE MODEL
C
      NV =45
      NA =45
C
400   PRINT 1700
C
      READ (5,1600,END=1500) TC,DH,TP,NPTS,(B(K),K=1,3)
      NPTA=NPTS+1
      READ(5,3000) (X(LL),LL=2,NPTA)
      READ(5,3000) (Y(LL),LL=2,NPTA)
500   PRINT 2300, TYPEM(1),TYPEM(2),TYPEM(3), DH,TC,TP
      X(1)=NPTS
      Y(1)=NPTS
      CALL CONFIG(X,Y,NPTS,YL,YU,B)
      DELTA=0.05
      X(2)=0.088
      I=2
600   CONTINUE
      IF(X(I) .GT. 2.5) GOTO 700
C
C     SECOND ORDER POLYNOMIAL
C
      Y(I)=B(1)+B(2)*(1.0 - COS(X(I)))
      I=I+1
      X(I) =X(I-1)+DELTA
      GOTO 600
700   CONTINUE
      X(1)=I-2
```

```
      Y(1)=I-2
800   CONTINUE
      K=I-1
      DO 900 L=2,K
      Y(L)=Y(L)+B(3)*(1.0 - COS(X(L)))**2
C
C     GENERAL CUSHION MATERIAL MODEL
C
      SS = X(L)
C*****************************************************************************
      CALL MODEL
C*****************************************************************************
      YM(L) =GL
900   CONTINUE
C
C     CALCULATE PREDICTION LIMITS
C
      NPTA=X(1)
C*****************************************************************************
      CALL PREDIC(X,Y,NPTA,YL,YU,B,YPL,YPU)
C*****************************************************************************
C
C     FIND MINIMUM IDCC G-LEVEL
C
      YMIN=1000.0
      DO 1200 I=2,K
      IF (YMIN.LE.Y(I)) GO TO 1200
      YMIN=Y(I)
      M=I
1200  CONTINUE
C
C     DETERMINE VALID MODEL RANGE FROM BOUNDED IDCC
C       AND PREDICTION LIMITS.
C
      XMIN=X(M)
      XL=XMIN-RANGE
      XU=XMIN+RANGE
      WRITE (6,2500)
      WRITE (6,2600)
      DO 1400 I=2,K
      N=3H
      IB=3H
      IF(X(I).GE.XL.AND.X(I).LE.XU)IB=3H **
      IF(YPL(I).GT.YM(I).OR.YPU(I).LT.YM(I))N=3H  *
      IF (YPL(I).LE.0.0) GO TO 1300
      WRITE (6,2700) X(I),Y(I),YPL(I),IB,YM(I),N,YPU(I)
      GO TO 1400
C     NEGATIVE G-VALUES SET TO - - .
1300  WRITE (6,2800) X(I),Y(I),IB,YM(I),N,YPU(I)
1400  CONTINUE
C
C     PRINT 5000,B(1),B(2),B(3)
```

```
3300  FORMAT(5X,'B(1) =',F12.7,3X,'B(2)= ',F12.7,3X,'B(3'= ',F12.7)
C     NEXT CASE
      GOTO 400
C
C     END OF JOB
1500  WRITE (6,2900)
      CALL EXIT
C
C
1600  FORMAT(3F5.2,I3,3F12.7)
1700  FORMAT(1H1)
2100  FORMAT (///,22X,'0',F15.8)
2200  FORMAT (18X,I5,F15.8,5X,15A4)
2300  FORMAT (1H1,13X,3A4,4X,F4.1,' IN. D.H. ',F7.1,' IN. THICK',F8.1,'
     1TEMPERATURE')
2500  FORMAT (///16X,'STATIC STRESS',17X,'ACCELERATION  (G)')
2600  FORMAT (21X,'PSI',13X,'IDCC',4X,'LOWER-P',9X,'MODEL',6X,'UPPER-P')
2700  FORMAT(18X,F7.4,9X,F7.2,4X,F7.2,4X,A3,F7.2,A3,3X,F7.2)
2800  FORMAT(18X,F7.4,9X,F7.2,7X,'- -',5X,A3,F7.2,A3,3X,F7.2)
2900  FORMAT (1H1,'    END OF JOB')
3000  FORMAT(10F8.4)
3999  FORMAT(1H1,5X,'CONST',F15.7)
4000  FORMAT(45(5X,I3,F15.8,/))
      END
```

```
      SUBROUTINE CONFID(X,Y,NPTS,YL,YU,B)
C*****************************************************************************
C
C       COMPUTE THE PREDICTION LIMITS OF THE CURVES
C
C*****************************************************************************
      COMMON TYPEM(3),NV,CONST,COEF(45)
      COMMON TP,UH,TC,SS,GL,NVR,V(45)
      DIMENSION X(1), Y(1), YPU(1), YPL(1), B(1),YL(1),YU(1)
      DIMENSION XAR(500,3), YAR(500), C(3), A(3,3), XIN(3,3), E(3)
      TAH= 1.734
      BX=0.0
      YS=0.0
      NPTS=X(1)
      DO 300 I=1,3
      C(I)=0.0
      E(I)=0.0
      DO 100 L=1,3
      XIN(I,L)=0.0
      A(I,L)=0.0
100   CONTINUE
      DO 200 J=1,NPTS
      XAR(J,I)=0.0
      YAR(J)=0.0
200   CONTINUE
300   CONTINUE
      F=0.0
      S=0.0
      SSQ=0.0
      DO 400 I=1,NPTS
      J=I+1
      XAR(I,1)=1.0
      XAR(I,2) = X(J)
      XAR(I,3)=XAR(I,2)**2
      YAR(I)=Y(J)
400   CONTINUE
      DO 600 I=1,3
      DO 500 J=1,NPTS
      C(I)=C(I)+XAR(J,I)*YAR(J)
500   CONTINUE
      BX= BX+C(I)*B(I)
600   CONTINUE
      DO 700 J=1,NPTS
      YS=YS+YAR(J)**2
700   CONTINUE
      SSQ=(YS-BX)/(X(1)-3.0)
      S=SQRT(SSQ)
      DO 800 J=1,NPTS
      A(1,1)=A(1,1)+XAR(J,1)*XAR(J,1)
      A(1,2)=A(1,2)+XAR(J,1)*XAR(J,2)
      A(1,3)=A(1,3)+XAR(J,1)*XAR(J,3)
      A(2,1)=A(2,1)+XAR(J,2)*XAR(J,1)
```

```
      A(2,2)=A(2,2)+XAR(J,2)*XAR(J,2)
      A(2,3)=A(2,3)+XAR(J,2)*XAR(J,3)
      A(3,1)=A(3,1)+XAR(J,3)*XAR(J,1)
      A(3,2)=A(3,2)+XAR(J,3)*XAR(J,2)
      A(3,3)=A(3,3)+XAR(J,3)*XAR(J,3)
500   CONTINUE
      D=A(1,1)*(A(2,2)*A(3,3)-A(3,2)*A(2,3))+A(1,2)*(A(3,1)*A(2,3)-A(2,1
     1)*A(3,3))+A(1,3)*(A(2,1)*A(3,2)-A(3,1)*A(2,2))
      XIN(1,1)=(A(2,2)*A(3,3)-A(3,2)*A(2,3))/D
      XIN(1,2)=(A(3,2)*A(1,3)-A(1,2)*A(3,3))/D
      XIN(1,3)=(A(1,2)*A(2,3)-A(2,2)*A(1,3))/D
      XIN(2,1)=(A(3,1)*A(2,3)-A(2,1)*A(3,3))/D
      XIN(2,2)=(A(1,1)*A(3,3)-A(3,1)*A(1,3))/D
      XIN(2,3)=(A(2,1)*A(1,3)-A(1,1)*A(2,3))/D
      XIN(3,1)=(A(2,1)*A(3,2)-A(3,1)*A(2,2))/D
      XIN(3,2)=(A(3,1)*A(1,2)-A(1,1)*A(3,2))/D
      XIN(3,3)=(A(1,1)*A(2,2)-A(2,1)*A(1,2))/D
      RETURN
C
C
      ENTRY PREDIC(X,Y,NPTS,YL,YU,B,YPL,YPU)
```

```
      DO 900 I=1,NPTS
      XAR(I,1)=1.
      J=I+1
      XAR(I,2) = 1.0-COS(X(J))
      XAR(I,3)=XAR(I,2)**2
  900 CONTINUE
      YPL(1)=NPTS
      YPU(1)=NPTS
      DO 1400 J=1,NPTS
      DO 1100 I=1,3
      DO 1000 K=1,3
      E(I)=E(I)+XAR(J,K)*XIN(K,I)
 1000 CONTINUE
 1100 CONTINUE
      DO 1200 I=1,3
      F=F+E(I)*XAR(J,I)
 1200 CONTINUE
      F2=1.0+F
      F2=SQRT(F2)
      F=SQRT(F)
      N=J+1
      YU(N)=Y(N)+TAH*S*F
      YL(N)=Y(N)-TAH*S*F
      YPU(N)=Y(N)+TAH*S*F2
      YPL(N)=Y(N)-TAH*S*F2
      F=0.0
      DO 1300 I=1,3
      E(I)=0.0
 1300 CONTINUE
 1400 CONTINUE
      RETURN
      END
```

```
      SUBROUTINE MODEL
C*************************************************************************
C********* DYNAMIC CUSHIONING MODEL ***************************************
C*************************************************************************
      INTEGER TYPEM
      COMMON TYPEM(3),NV,CONST,COEF(45)
      COMMON TP,DH,TC,SS,GL,NVR,V(45)
C
      AL = 1.0-COS(SS)
      AL2 = AL * AL
      SRDH = SQRT( DH )
      TR  =(TP + 460.0)/100.
      TR2 = TR * TR
      TR3 = TR * TR2
      TR4 = TR3 * TR
      TCOH = TC ** (-0.5)
      TCTH = TC ** (-1.5)
C
      V(01) = TR    * TCOH
      V(02) = TR    * TCOH                  * AL
      V(03) = TR    * TCOH                  * AL2
      V(04) = TR    * TCTH    * SRDH
      V(05) = TR    * TCTH    * SRDH        * AL
      V(06) = TR    * TCTH    * SRDH        * AL2
      V(07) = TR    * TCOH    * SRDH
      V(08) = TR    * TCOH    * SRDH        * AL
      V(09) = TR    * TCOH    * SRDH        * AL2
      V(10) = TR2   * TCOH
      V(11) = TR2   * TCOH                  * AL
      V(12) = TR2   * TCOH                  * AL2
      V(13) = TR2   * TCTH    * SRDH
      V(14) = TR2   * TCTH    * SRDH        * AL
      V(15) = TR2   * TCTH    * SRDH        * AL2
      V(16) = TR2   * TCOH    * SRDH
      V(17) = TR2   * TCOH    * SRDH        * AL
      V(18) = TR2   * TCOH    * SRDH        * AL2
      V(19) = TR3   * TCOH
      V(20) = TR3   * TCOH                  * AL
      V(21) = TR3   * TCOH                  * AL2
      V(22) = TR3   * TCTH    * SRDH
      V(23) = TR3   * TCTH    * SRDH        * AL
      V(24) = TR3   * TCTH    * SRDH        * AL2
      V(25) = TR3   * TCOH    * SRDH
      V(26) = TR3   * TCOH    * SRDH        * AL
      V(27) = TR3   * TCOH    * SRDH        * AL2
      V(28) = TR    * TCTH
      V(29) = TR    * TCTH                  * AL
      V(30) = TR    * TCTH                  * AL2
      V(31) = TR2   * TCTH
      V(32) = TR2   * TCTH                  * AL
      V(33) = TR2   * TCTH                  * AL2
      V(34) = TR3   * TCTH
```

```
      V(35) = TR3   * TCTH              * AL
      V(36) = TR3   * TCTH              * AL2
      V(37) = TR
      V(38) = TR * AL
      V(39) = TR * AL2
      V(40) = TR2
      V(41) = TR2 * AL
      V(42) = TR2 * AL2
      V(43) = TR3
      V(44) = TR3 * AL
      V(45) = TR3 * AL2
C
C         COMPUTE DYNAMIC CUSHIONING FUNCTION
C
      GL = CONST
      DO 100 J=1,NV
100   GL =GL +COEF(J) * V(J)
      RETURN
      END
```

APPENDIX H. TOTAL BOX VALIDATION CODE

```
C*****************************************************************
C
C                    TOTAL BOX VALIDATION
C
C*****************************************************************
      COMMON A(2,3),COEF(2),KON(2),N1,NPT,ILYA(72)
      COMMONSSREG,DSERR,T,UL(51),DL(51),AL(119),BARX
      COMMON Y(150),X(2,150),IERR,TC,DH,TP
      N1 = 1
      T = 1.734
      READ(5,99) ILYA
10     READ(5,1600,END = 999) DH,TC,TP,NPT
      DO 30 I = 1,NPT
      READ(5,1700) X(1,I),Y(I)
30    CONTINUE
      WRITE(6,89)ILYA
      WRITE(6,1800) DH,TC,TP
      DO 40 J = 1,NPT
40    WRITE(6,79) X(1,J),Y(J)
      CALL LREG
      IF(IERR .EQ. 1) GOTO 10
       WRITE(6,89) ILYA
      WRITE(6,1600) DH,TC,TP
      CALL LIMIT
      GOTO 10
999   WRITE(6,1900)
      CALL EXIT
C
79    FORMAT(10X,F10.4,F10.4)
89    FORMAT(1H1,12X,72A1)
99    FORMAT(72A1)
1600   FORMAT(3F5.2,I3)
1700  FORMAT(32X,F8.4,5X,F8.4)
1800  FORMAT(13X,                4X,F4.1,' IN. D.H. ',F7.1,' IN. THICK',
     A     F8.1,' TEMPERATURE',//)
1900  FORMAT(1H1,10X,'END OF JOB')
      END
```

```
      SUBROUTINE LREG
C*****************************************************************
C
C                    LINEAR REGRESSION
C
C*****************************************************************
      COMMON A(2,3),COEF(2),KON(2),N1,NPT,ILYA(72)
      COMMON/SSREG/USERR,T,UL(51),DL(51),AL(119),BARX
      COMMON Y(150),X(2,150),IERR,TC,DH,TP
      N=N1+1
      M=N+1
      ANPT=NPT
      DO 100 I=1,N
      DO 100 J=1,M
  100 A(I,J)=0.
      A(1,1)=NPT
      DO 400 K=1,NPT
      DO 300 I=1,N
      DO 300 J=1,N
      IPJ2=I+J-2
      IF (IPJ2) 300,300,200
  200 A(I,J)=A(I,J)+X(1,K)**IPJ2
  300 CONTINUE
      BARX = A(1,N)/ANPT
      DO 400 I=2,N
  400 A(I,M) = A(I,M)+X(1,K)**(I-1)*Y(K)
      DO 500 J=1,NPT
  500 A(1,M)=A(1,M)+Y(J)
      DO 600 J=1,M
      DO 600 I=1,N
  600 A(I,J)=A(I,J)/ANPT
      IERR=0
      M=N+1
      DO 1300 I=1,N
      IF (A(I,I)) 800,700,800
  700 IERR=1
      GO TO 1400
  800 TEMP=1.0/A(I,I)
      IP1=I+1
      DO 900 J=IP1,M
  900 A(I,J)=A(I,J)*TEMP
      DO 1200 K=1,N
      IF (I-K) 1000,1200,1000
 1000 DO 1100 J=IP1,M
 1100 A(K,J)=A(K,J)-A(K,I)*A(I,J)
 1200 CONTINUE
 1300 CONTINUE
      N=N1+1
      M=N+1
 1400 IF (IERR) 1500,1600,1500
 1500 WRITE (6,3100)
      GO TO 2500
```

```
1600  CONTINUE
      DO 1700 K=1,N
1700  COEF(K)=A(K,M)
      SUMR2=0.0
      DO 1900 I=1,NPT
      YC=COEF(1)
      DO 1800 K=2,N
1800  YC = YC+COEF(K)*X(1,I)**(K-1)
      R=Y(1)-YC
1900  SUMR2=SUMR2+R*R
      SIGMA=SQRT(SUMR2/ANPT)
      SSERR=SUMR2
      SUMR2=Y(1)
      DO 2000 I=2,NPT
2000  SUMR2=SUMR2+Y(I)
      BARY1=SUMR2/NPT
      SUMR2=0.0
      DO 2100 I=1,NPT
      R=Y(I)-BARY1
2100  SUMR2=SUMR2+R*R
      SSTOT=SUMR2
      SSREG=SSTOT-SSERR
      DSREG=SSREG/N1
      DSERR=SSERR/(NPT-(N1+1))
      FRATO=DSREG/DSERR
      DEGFT=N1
      DEGFB=NPT-(N1+1)
      DEGRE=NPT-1
      ETS=SSERR/SSTOT
      IF(ETS.GE.1.0)ETS=1.0
      CORR=SQRT(1.0-ETS)
      WRITE (6,3000) N1
      WRITE (6,2600)
      WRITE (6,2700) SSREG,DEGFT,DSREG,FRATO,CORR
      WRITE (6,2800) SSERR,DEGFB,DSERR
      WRITE (6,2900) SSTOT,DEGRE
      WRITE (6,2400)
      MM=N1+1
      DO 2200 I=1,2
2200  KON(I)=I-1
      WRITE (6,2500) (KON(I),COEF(I),I=1,MM)
2300  RETURN
C
2400  FORMAT (//,2X,'CURVE COEFFICIENTS')
2500  FORMAT (//2X,2H$(,I1,1H),3X,E15.7)
2600  FORMAT(//,2X,'SOURCE',9X,'S.S',9X,'D.F',9X,'M.S',9X,'F',12X,'R')
2700  FORMAT (//,2X,'DUE TO',5(4X,E10.4))
2800  FORMAT (//,2X,'ABOUT',3(4X,E10.4))
2900  FORMAT (//,2X,'TOTAL',2(4X,E10.4))
3000  FORMAT (1H1,2X,'ANOVA FOR CURVE OF ORDER',I3)
3100  FORMAT (//,4X,'SINGULAR MATRIX '/,4X,'CURVE FIT IMPOSSIBLE')
      END
```

```
      SUBROUTINE LIMIT
C*****************************************************************  *******
C
C                    CONFIDENCE LIMITS
C
C*****************************************************************************
      COMMON A(2,3),COEF(2),KON(2),N1,NPT,ILYA(72)
      COMMONSSREG,DSERR,T,UL(51),DL(51),AL(119),BARX
      COMMON Y(150),X(2,150),IERR,TC,DH,TP
      DIMENSION CM(5),YM(51)
      DATA (CM(I),I=1,5) /-6.3487467,0.0,0.07231763,-0.0091702196,0.0 /
     1=1
      DSERR=SQRT(DSERR)
      SUMK=SSREG/(COEF(2)**2)
      DELTA = 0.5
          X(1,1)=55.0
10        I=I+1
          X(1,I)=X(1,I-1)+DELTA
          IF(X(1,I) .LE. 62.0) GOTO 10
      NX = I-1
      H2=SQRT(DH)
      TH=(TP+460.0)/100.0
      TH2= TH*TH
      TH3=TH2*TH
      DO 20 I= 1,NX
      Y(I)=COEF(1)+COEF(2)*X(1,I)
      TER = H2*X(1,I)
      YM(I) = CM(1)+CM(2)*TH*TER+CM(3)*TH2*TER+CM(4)*TH3*TER
     1   +CM(5)*TH2*H2
20    CONTINUE
      DO 30 I = 1,NX
      SHERI = SQRT(1.0+1.0/ANPT+(((X(1,I)-BARX)**2)/SUMK))
      SHERI=T*DSERR*SHERI
      UL(I)=Y(I)+SHERI
30    DL(I)=Y(I)-SHERI
      WRITE(6,50)
      DO 40 I = 1,NX
      WRITE(6,51) X(1,I),Y(I),DL(I),YM(I),UL(I)
40    CONTINUE
      RETURN
50    FORMAT(14X,4HWI. ,16X,4HIEBL,16X,5HLOWER,15X,5HMODEL,15X,
     A     5HUPPER,/)
51    FORMAT(5(10X,F10.4)/)
      END
```

APPENDIX I. TOTAL BOX VS. INTERIOR BOX CODE

```
C*************************************************************
C
C                TOTAL BOX VS. INTERIOR BOX
C
C*************************************************************
      INTEGER TYPEM
      COMMON TYPEM(3),NV,CONST,COEF(45)
      COMMON TP,DH,TC,SS,GL,NVR,V(45)
      DIMENSION Z(6),CM(5),X(100),Y(100),YM(100),YC(100)
      DATA (TYPEM(I),I=1,3) / 'MINI','CEL ','BOX '/
      DATA (COEF(I),I=1,45) /0.0,0.0,0.0,0.0,7.1865626,8*0.0,-0.57911897,
     A     7*0.0,-0.53894447,6*0.0,30.098255,  0.0.66.5579U2,4*0.0,
     B     4.1031526,5*0.0,-10.219992,0.0,-0.22965288,2*0.0/
      DATA (CM(I),I=1,5) /-6.3487467,0.0,0.07231763,-0.0091702196,0.0 /
      DATA (Z(I),I=1,6) /0.088,0.255,0.520,0.708,0.843,1.255  /
C
      CONST = -14.57570
C
C               PRINT CUSHION MATERIAL TERMS AND COEFFICIENTS.
      PRINT 3999,CONST
      PRINT 4000,(I,COEF(I),I=1,45)
C
C
C     NUMBER OF COEFFICIENTS FOR THE MODEL
C
      NV =45
C
400   PRINT 1700
C
      DELTA = 0.5
      X(1) = 55.0
      I=1
500   CONTINUE
      IF(X(I) .GE. 62.0) GOTO 700
C
      I=I+1
      X(I) =X(I-1)+DELTA
      GOTO 600
700   CONTINUE
      K=I-1
800   CONTINUE
      READ (5,1600,END=1500) TC,DH,TP
      H2=SQRT(DH)
      TH=(TP+460.0)/100.0
      TH2= TH*TH
      TH3=TH2*TH
      DO 900 L=1,K
      TER = H2*X(L)
C     EXTERIOR BOX MODEL
      YM(L) = CM(1)+CM(2)*TH*TER+CM(3)*TH2*TER+CM(4)*
C
C     GENERAL CUSHION MATERIAL MODEL
```

```
C
      SS = X(L)/172.5
C*****************************************************************
      CALL MODEL
C*****************************************************************
       Y(L) =SL
900   CONTINUE
C
      WRITE(6,2500) (TYPEM(I),I=1,3),DH,TC,TP
      WRITE(6,2600)
      DO 1040 I=1,K
C     CUSHION
      YC(I) = YM(I) - Y(I)
      WRITE(6,51) X(I),YM(I),Y(I),YC(I)
1040  CONTINUE
      GOTO 800
1500  WRITE(6,1700)
      CALL EXIT
2500  FORMAT (1H1,15X,3A4,4X,F4.1,' IN. D.H. ',F7.1,' IN. THICK',F8.1,'
     1TEMPERATURE',//)
2600  FORMAT(15X,'BOX WEIGHT   ',2X,'   TOTAL BOX',5X,'INTERIOR BOX',
     1        5X,'CUSHION',/)
51    FORMAT(10X,F13.4,5X,F12.4,5X,F12.4,5X,F9.4,/)
1600  FORMAT(3F5.2)
1700  FORMAT(1H1)
4999  FORMAT(1H1,5X,'CONST',F15.7)
4000  FORMAT(45(5X,I5,F15.8,/))
      END
```

```
      SUBROUTINE MODEL
C*********************************************************************
C
C*********************************************************************
C
C*********************************************************************
      INTEGER TYPEM
      COMMON TYPEM(3),NV,CONST,COEF(45)
      COMMON TP,DH,TC,SS,GL,NVR,V(45)

C
      AL = 1.0-COS(SS)
      AL2 = AL * AL
      SRDH = SQRT( DH )
      TR  =(TP + 460.0)/100.
      TR2 = TR * TR
      TR3 = TR * TR2
      TR4 = TR3 * TR
      TCOH = TC ** (-0.5)
      TCTH = TC ** (-1.5)

C
      V(01) = TR    * TCOH
      V(02) = TR    * TCOH
      V(03) = TR    * TCOH
      V(04) = TR    * TCTH    * SRDH
      V(05) = TR    * TCTH    * SRDH    * AL
      V(06) = TR    * TCTH    * SRDH    * AL2
      V(07) = TR    * TCOH    * SRDH
      V(08) = TR    * TCOH    * SRDH    * AL
      V(09) = TR    * TCOH    * SRDH    * AL2
      V(10) = TR2   * TCOH
      V(11) = TR2   * TCOH
      V(12) = TR2   * TCOH
      V(13) = TR2   * TCTH    * SRDH
      V(14) = TR2   * TCTH    * SRDH    * AL
      V(15) = TR2   * TCTH    * SRDH    * AL2
      V(16) = TR2   * TCOH    * SRDH
      V(17) = TR2   * TCOH    * SRDH    * AL
      V(18) = TR2   * TCOH    * SRDH    * AL2
      V(19) = TR3   * TCOH
      V(20) = TR3   * TCOH
      V(21) = TR3   * TCOH
      V(22) = TR3   * TCTH    * SRDH
      V(23) = TR3   * TCTH    * SRDH    * AL
      V(24) = TR3   * TCTH    * SRDH    * AL2
      V(25) = TR3   * TCOH    * SRDH
      V(26) = TR3   * TCOH    * SRDH    * AL
      V(27) = TR3   * TCOH    * SRDH    * AL2
      V(28) = TR    * TCTH
      V(29) = TR    * TCTH
      V(30) = TR    * TCTH
      V(31) = TR2   * TCTH
      V(32) = TR2   * TCTH    * AL
```

```
      V(33) = TR2   * TCTH              * AL2
      V(34) = TR3   * TCTH
      V(35) = TR3   * TCTH              * AL
      V(36) = TR3   * TCTH              * AL2
      V(37) = TR
      V(38) = TR * AL
      V(39) = TR * AL2
      V(40) = TR2
      V(41) = TR2 * AL
      V(42) = TR2 * AL2
      V(43) = TR3
      V(44) = TR3 * AL
      V(45) = TR3 * AL2
C
C          COMPUTE DYNAMIC CUSHIONING FUNCTION
C
      GL = CONST
      DO 100 J=1,NV
100   GL =GL +COEF(J) * V(J)
      RETURN
      END
```

DISTRIBUTION

	No. of Copies
Defense Technical Information Center Cameron Station Alexandria, VA 22314	12
IIT Research Institute Attn: GACIAC 10 West 35th Street Chicago, IL 60616	1
US Army Materiel Systems Analysis Activity Attn: DRXSY-MP Aberdeen Proving Ground, MD 21005	1
DRSMI-LP, Mr. Voigt	1
-EX, Mr. Owen	1
-R, Dr. Kobler	1
-RLD	25
-RPR	3
-RPT (Record Copy)	1
(Reference Copy)	1
BMDATC-T, Dr. V. Kobler	25